Doctoral Thesis

Performance Studies for Mobile Ad Hoc Networks with Erasure Coding and f-cast Relay

by

Bin Yang

Graduate School of Systems Information Science

Future University Hakodate

September 2015

Abstract

The mobile ad hoc networks (MANETs) are a class of infrastructure-less self-organizing networks consisting of mobile devices communicating with each other over peer-to-peer wireless links. Due to their distinctive features of robustness, self-organization, quick deployment and reconfiguration, MANETs hold great promises for many important application scenarios, like disaster relief, battle field communications, and wide area sensing, and are thus increasingly becoming an indispensable component for the next generation (5G) networks. To efficiently support these critical applications with stringent performance requirements, it is of great importance to thoroughly understand the fundamental performance of such networks, like the delivery delay and throughput capacity.

This work focuses on the performance studies of an important class of MANETs with erasure coding and packet redundancy (f-cast), i.e., each coded packet at source node is transmitted to at most f distinct relay nodes. The erasure coding and packet redundancy are two promising techniques that have been extensively studied in the literature for improving the packet delivery performance in MANETs. On one hand, previous studies showed that erasure coding technique can considerably reduce the delay variance in MANETs, while it may lead to a relatively large packet delivery delay, since the early arrived coded packets in destination node have to wait a long time for the arrivals of other coded packets from distinct relay nodes. On the other hand, packet redundancy technique can efficiently reduce the packet delivery delay due to the fact that multiple relays will carry redundant copies of a packet, increasing the chance of the packet being received by its destination; however, it usually incurs high variance of packet delivery delay. Thus, we consider a combination of erasure coding and packet redundancy in MANETs to have a flexible trade-off between packet delivery delay and delay variance.

We combine these two techniques together and study the packet delivery delay and throughput capacity in MANETs, under a general two-hop relay routing algorithm with unicast traffic pattern, i.e., a source node has only a destination node, which covers available routing algorithms with pure erasure coding or pure packet redundancy as special cases. To analyze the packet delivery delay, we propose a Markov chain model to depict the packet delivery process under this routing algorithm, with which we derive the analytical expressions for the mean value and variance of packet delivery delay. To analyze the throughput capacity, we propose two Markov chain models to depict the fastest packet distributing process and fastest packet receiving process at source and destination nodes, respectively, with which we derive the analytical expression for the throughput capacity. Extensive simulation and theoretical results are provided to validate the accuracy of our theoretical performance analysis as well as our findings.

Then, we study packet delivery delay of MANETs adopting a two-hop relay routing algorithm with packet redundancy, and multicast traffic pattern, where a source node has multiple destination nodes. To this end, we propose a Markov chain model to capture the packet delivery process under the routing algorithm, with which we derive the analytical expressions for the mean value and variance of packet deliv-

ery delay. Extensive simulations demonstrate the efficiency of our theoretical delay results.

Acknowledgments

I would like to express my deepest gratitude to all those who gave me the opportunity to complete this thesis. First and foremost, I am deeply indebted, grateful to my supervisor, Professor Xiaohong Jiang for giving me copious amounts of insightful guidance, constant support, and expertise on every subject that arose throughout all these three years. He is more than a supervisor and a teacher but a role model and a friend. Working with him is proven to be an enjoyable and rewarding experience. I would also like to give my special thanks to Dr. Yin Chen for giving me a lot of help in my academic research. This thesis would not have been possible without their guidance.

I would like to acknowledge my thesis committee members, Professor Osamu Takahashi, Professor Yuichi Fujino, Professor Nobuyuki Takahashi and Professor Hideki Satoh, for their interests and for their constructive comments that help to improve this thesis.

I would like to give my sincere thanks to Professor Osamu Takahashi for his generous support. I am also very grateful to all the people I have interacted with at Future University Hakodate, specifically everyone affiliated with Jiang's Laboratory. My graduate study at the Future University Hakodate has been a really rewarding experience.

This work is dedicated to my family, whose love and unconditional support provide a constant inspiration in my life. In particular, I would like to thank my wife for her understanding, encouragement, and support in these three years.

THIS PAGE INTENTIONALLY LEFT BLANK

Contents

List of Figures

Chapter 1

Introduction

In this chapter, we first introduce the background of mobile ad hoc networks (MANETs) [1]. We then describe our motivations of this thesis.

1.1 Background

In the last decade, wireless networks, including cellular network, Wi-Fi (or hotspot) network, etc, have become an indispensable part of our daily lives for meeting the need of fast and convenient Internet access. However, these wireless networks rely heavily on centralized control such as cellular network, in which information is relayed by the base stations. Upon the base stations are destroyed in nature disasters and artificial attacks, this will result in the complete loss of all the information in such network. Motivated by this, many researchers from both academia and industry have been making efforts to develop a novel class of wireless networks termed as mobile ad hoc networks without fixed infrastructure or centralized control.

Mobile ad hoc networks consist of a collection of movement nodes that can directly communicate with each other through wireless links without a pre-established networking infrastructure or centralized control. Compared with those traditional wireless networks, MANETs have the following distinctive features. First, they can be rapidly deployed and flexibly reconfigured even in those geographically tough areas, since they are built without the support of infrastructure or base station. Second,

they are highly robust such that node failure can be tolerated, since when any node carrying a packet leaves the networks, other nodes carrying copies of the packet can forward the packet to desired nodes which move into their transmission range. Finally, they can provide low-cost Internet service for these users residing in remote areas.

Due to these attractive features of MANETs, these networks are highly appealing for a lot of future applications, such as the disaster relief, daily information exchange, military communication, environment monitoring, etc. It is believed that the MANET will become one of the most important and indispensable component among the next generation (5G) networks.

1.2 Motivations

Motivated by these promising application potentials of MANETs, extensive studies have been dedicated towards deeper understanding of the fundamental MANET performance, such as delivery delay [2–12] and throughput capacity [1, 13–21], which serve as the instruction guideline for the design, development and commercialization of such networks. Delivery delay is the time it takes a packet to reach its destination node(s) after source node starts to transmit the packet. Throughput capacity is defined as the maximum packet input rate that the considered MANET can stably support.

The available studies indicated that the erasure coding and packet redundancy are two promising techniques for improving the packet delivery performance in MANETs, where these two techniques are usually adopted separately. Specially, previous studies showed that erasure coding technique can considerably reduce the delay variance in MANETs, while it may lead to a relatively large packet delivery delay, since the early arrived coded packets in destination node have to wait a long time for the arrivals of other coded packets from distinct relay nodes. Packet redundancy technique (i.e. simple packet duplication) can efficiently reduce the packet delivery delay due to the fact that multiple relays will carry redundant copies of a packet, increasing the chance

of the packet being received by its destination; however, it usually incurs high variance of packet delivery delay. Thus, we consider a combination of erasure coding and packet redundancy in MANETs to have a flexible trade-off between packet delivery delay and delay variance. Remarkably, we propose theoretical models to analyze packet delivery performance in terms of delivery delay, delay variance and throughput capacity under such combinational technique in MANETs. Notice that these studies adopt simple unicast traffic pattern, where a source node has a unique destination node. We further extend unicast traffic pattern to more challenging multicast traffic pattern, where a source node has multiple destination nodes. Under multicast traffic pattern, we analytically study the delivery delay performance in MANETs.

1.3 Thesis Outline

In this thesis, the overall aim is to provide a comprehensive study on the fundamental delay and throughput performance in mobile ad hoc networks with unicast/muticast traffic patterns. The main contents of this thesis are summarized as follows:

Chapter 2 Related work. In this chapter, we introduce previous work related to unicast delivery delay, multicast delivery delay and throughput capacity.

Chapter 3 Preliminaries. This chapter introduces system models and transmission scheduling scheme involved in our study. Specifically, the following issues are included: the network model, the node mobility model, the communication model and the equivalent-class based transmission scheduling scheme.

Chapter 4 Unicast delivery delay Study for MANETs with Erasure Coding and f-cast Relay. In this chapter, we focus on the study of packet delivery delay in MANETs under unicast traffic pattern, which measures the time that a source node takes to deliver a packet to its destination node. We first introduce traffic pattern and definition of the delay performance metric. To explore the delay performance in MANETs with erasure coding [3] and packet redundancy [22], we develop a Markov chain model to capture the packet delivery process under a general two-hop relay routing algorithm. Based on the Markov chain model, the analytic expressions

are derived for the mean value and variance of the packet delivery delay. Finally, extensive simulation and theoretical results are provided to validate our theoretical delay analysis and to illustrate how system parameters impact on the packet delivery delay performance.

Chapter 5 Throughput Capacity Study for MANETs with Erasure Coding and f-cast Relay. In this chapter, we study the throughput capacity in MANETs under unicast traffic pattern. We first introduce the traffic pattern in our throughput capacity analysis. We then develop two Markov chain models to depict the fastest packet distributing process at source node and the fastest packet receiving process at destination node based on the routing algorithm introduced in chapter 4. With the help of these two Markov chain models, the analytic expression is derived for the throughput capacity. Simulation and numerical results are further provided to illustrate the accuracy of theoretical throughput capacity analysis as well as our theoretical findings.

Chapter 6 Multicast delivery Delay Study for MANETs with f-cast Relay. In this chapter, we focus on the study of packet delivery delay under multicast traffic pattern, which measures the time that a source node takes to deliver a packet to multiple destination nodes. We first introduce traffic pattern, multicast routing algorithm with packet redundancy, and definition of packet delivery delay. We then develop a Markov chain model to depict the packet delivery process under the multicast routing algorithm. Based the Markov chain model, the analytic expressions are derived for both mean value and variance of packet multicast delivery delay. Finally, extensive simulation and theoretical results are provided to validate our theoretical multicast delay analysis and to illustrate the impact of system parameters on multicast delay performance.

Chapter 7 Conclusion. We conclude the whole thesis by summarizing the main contributions of this thesis, and discuss the future work.

Chapter 2

Related Work

In this chapter, we present a survey of related work on the studies of unicast delivery delay, multicast delivery delay and throughput capacity.

2.1 Unicast delivery delay

A lot of work has been dedicated to the study of packet delivery delay under unicast traffic pattern by employing either erasure coding or packet redundancy technique in MANETs. It was first demonstrated through simulation study in [2, 3] that erasure coding technique can reduce variance of packet delivery delay and worst-case delay in MANETs with opportunistic routing. By combining probabilistic routing and erasure coding, a novel routing algorithm was proposed in [6] to improve packet delivery delay performance in opportunistic MANETs. Hanbali *et al.* [5] developed a simple theoretical model to analyze delay performance under two-hop relay and erasure coding in a very simple network scenario, where there is only one source-destination pair and the source node has only one single packet to be delivered. Also, a simple coding technique was considered [5], in which a single packet (message) is first divided into multiple blocks and these blocks are then encoded into code blocks for transmission. Later, Liu *et al.* [7] extended the work in [5] to a more general network scenario with multiple source-destination pairs. Recently, Chen *et al.* [4] tried to combine erasure coding and packet redundancy techniques for improving delay performance in special

MANETs, where interference among simultaneous transmissions is neglected. Also, only simulation results are provided in [4] for performance evaluation.

Applying packet redundancy technique for the study of packet delivery delay in MANETs has been explored under various mobility models, like under the i.i.d. mobility model in [8], under the Brownian mobility in [23], as well as under the hybrid random walk model and discrete random direction model in [24]. Delay performance modeling under packet redundancy technique has also been extensively studied recently. The work [9, 25, 26] conducted delay modeling under a simple network scenario, where only one source-destination pair is available in the network. Later, Liu *et al.* [11, 12] explored delay modeling under more general network scenarios with multiple source-destination pairs.

Recently, a lot of research efforts have been devoted to the study of packet delivery delay adopting packet redundancy technique in DTNs (delay tolerant networks), a special class of sparse MANETs where interference among transmissions can be neglected. Spyropoulos *et al.* [27] proposed a single period routing algorithm (called spray and wait) for the study of delay performance in DTNs, and Bulut *et al.* [10] extended the algorithm in [27] and further proposed a more general multi-period spraying algorithm in DTNs. Panagakis *et al.* [9] developed a theoretical framework for delay modeling in DTNs with packet redundancy.

The aforementioned work on the study of packet delivery delay in MANETs mainly adopts erasure coding and packet redundancy techniques separately. Different from existing work, we propose a Markov chain-based theoretical model to analytically study packet delivery performance in MANETs with a combination of erasure coding and packet redundancy, which has a flexible trade-off between packet delivery delay and delay variance. Here, we adopt a general two-hop relay routing algorithm for packet routing. It is notable that the general routing algorithm covers available routing algorithms with pure erasure coding , e.g., [28, 29], or pure packet redundancy, e.g., [8, 22], as special cases.

2.2 Multicast delivery delay

Multicast in MANETs is a fundamental routing service for supporting many practical applications with one-to-many communication pattern [30–39], like the information exchanges among a group of soldiers in battlefield communication, emergency communications among the rescuers in disaster relief, video conferencing, real-time monitoring, VoIP, etc. For an efficient support of these critical multicast-intensive applications in the future MANETs, multicast delivery delay analysis in such networks has been a critical research issue, where multicast delay is defined as the time it takes for a packet to be delivered out to all its destination nodes. However, the multicast delay analysis is extremely complicated because of dynamic network topology and multiple destination nodes associated with each node. By now, the multicast delay performance still remains largely unexplored in MANETs.

Recently, some work has reported the asymptotic bounds on the multicast delay in MANETs. Wang *et al* showed in [40, 41] that by adopting packet redundancy technique in MANETs, a multicast delay of $\Theta(\sqrt{n\log k})$ is achievable under a two-hop relay algorithm, which is better than the $\Theta(n\log k)$ delay reported without packet redundancy, where n represents the number of nodes in the considered networks and k is the number of destination nodes associated with each source node. Wang *et al* also showed in [42] packet redundancy technique can improve the multicast delay performance in MANETs under two different mobility models, where nodes move either in a local region or in a global region. Later, Wang *et al* found in [43] that under the two-hop relay algorithm with packet redundancy, cooperation among destination nodes can achieve the multicast delay smaller than $\Theta(\sqrt{n})$ in MANETs. More recently, Liu *et al* studied in [44] the asymptotic multicast delay in sparse MANETs and showed that the multicast delay can achieve $\Omega(\log k \cdot n^{2(\gamma+\omega)})$, $\Omega(\log k \cdot n^{2(\gamma+\omega)})$ and $O\big(\max\big\{\log\frac{n-k}{n-k-f}, \frac{\log k}{f}\big\} \cdot n^{2(\gamma+\omega)}\big)$ under three packet delivery algorithms: one-hop relay, two-hop relay without packet redundancy and two-hop relay with packet redundancy, respectively, where the network area is first evenly divided into $n^{2\gamma}$ cells and each cell is then divided into $n^{2\omega}$ equal subcells ($\gamma, \omega \geq 0, \gamma + \omega > 1/2$).

We note that although asymptotic results can help us understand how the multicast delay varies with network size and the number of destination nodes associated with each source node, they can not be used to estimate the actually achievable delay performance, which provides more meaningful insights for network designers. Recently, Li *et al* in [45] studied the exact multicast delay with the help of a Makov chain model and showed how the selfish behaviors of nodes affect the delay performance in DTNs, i.e., a class of very sparse MANETs where the interference is neglected.

It is notable that the available work on MANET multicast delay investigated either the asymptotic multicast delay or the exact multicast delay in special MANETs where the interference and medium access contention are largely neglected, therefore these results can not be used to estimate the actual multicast delay performance in general MANETs. In this thesis, we study the exact multicast delay performance in a general MANET where both the interference and medium access control are taken into account.

2.3 Throughput capacity

Throughput capacity of MANETs (i.e., the maximum throughput that the networks can stably support) serves as a fundamental guideline for the development and commercialization of such networks [1, 14, 15, 20], and still remains largely unknown by now [46].

To study the important yet challenging research problem on throughput capacity, a lot of efforts have been conducted since the breakthrough work of Gupta and Kumar [13]. The work of [13] showed that the per node throughput capacity scales as $\Theta(1/\sqrt{nlogn})$ in wireless ad hoc network without node mobility, where n is the number of nodes in the network.[1] The result suggests that the per node throughput capacity diminishes with increase of n. Later, some work [16–18] indicated similarly

[1]Recall the following notation [47]: $f(n) = \Theta(g(n))$ means that $f(n) = O(g(n))$ and $g(n) = O(f(n))$, where $f(n) = O(g(n))$ means that there exists a constant c and integer N such that $f(n) \leq cg(n)$ for $n > N$.

pessimistic results that the per node throughput capacity tends to 0 as n goes to infinity in the network. Many studies tried to improve the throughput capacity by introducing node mobility in wireless ad hoc network. In the seminal work [48], Grossglauser and Tse investigated the throughput capacity of MANETs and showed that the per node throughput capacity can achieve $\Theta(1)$ under a two-hop relay routing when nodes follow independently and identically distributed (i.i.d.) mobility model. Following [48], the per node throughput capacity of $\Theta(1)$ has also been proved to be achievable under various mobility models, like the Brownian mobility model [49], the random walk model [50] and the restricted mobility model [51]. In addition, there also exist some work that explored the trade-off between throughput capacity and delay in MANETs [19–21].

The research discussed above mainly focus on deriving order sense results on throughput capacity. Although the scaling law results can help us to understand the general trends of throughput capacity as network size scales, it tells little information on the actually achievable throughput capacity of a network, which would greatly facilitate the design and optimization in practical MANET applications. To this end, some initial work has been conducted for the exact throughput capacity. Neely *et al.* [8, 52] derived the exact throughput capacity of cell-partitioned MANETs under i.i.d. mobility model and Markovian mobility model, respectively. Gao *et al.* [53] later extended the above work to that with a group-based scheduling scheme and proved the exact throughput capacity there by adopting Lyapunov drift technique. Also, Liu *et al.* [22] investigated the exact throughput capacity under a two-hop relay routing with packet redundancy in MANETs.

Recently, erasure coding technique has been playing an increasingly important role in improving the performance of MANETs such as delivery ratio, delivery delay and throughput capacity [2, 3, 6, 28, 29, 54–58]. Specifically, Ying *et al.* [58] employed joint coding-scheduling algorithms to achieve optimal order sense trade-off between throughput capacity and delay in MANETs using erasure coding technique. Later, Kong *et al.* [29] proposed an erasure coding based two-hop relay routing and showed that it not only provides a significant improvement in order sense trade-off between

throughput capacity and delay in MANETs, but also offers potential benefits on robustness and security.

It is notable that all the aforementioned erasure coding based work on throughput capacity in MANETs assume that the number of coded packets can be arbitrarily large. However, a large number of coded packets will cause high computational complexity in encoding and decoding operations and thus consume a lot of limited resources of MANETs. Hence, an interesting issue raised naturally in this context is how to improve the throughput capacity in MANETs under an erasure coding based routing with a limited number of coded packets. Answering this question would provide helpful fundamental insights into the understanding and design of MANETs. To the best of our knowledge, this issue remains an unexplored area in the literature.

In order to address the above issue, this thesis studies the exact throughput capacity in MANETs under the general two-hop relay routing algorithm which combines both erasure coding and packet redundancy [8, 22] techniques, which is introduced in chapter 3. Under the routing algorithm, a source node first employs erasure coding technique to encode a group of x packets into g ($g \geq x$) distinct coded packets, and then dispatches at most f copies of each coded packet to different relay nodes that help to forward them to the destination node. All packets can be recovered once the destination node receives any x distinct coded packets of the group.

Chapter 3

Preliminaries

In this chapter, we first introduce system models of this thesis, regarding network model, mobility model and communication model in MANETs, and then present transmission scheduling scheme to support as many simultaneous transmissions as possible without interfering with each other over a shared channel.

3.1 System Models

3.1.1 Network and Mobility Models

As shown in Fig. 3-1, the considered MANET consists of n mobile nodes moving over a unit square region where the opposite edges are wrap-around, i.e., when a node reaches an edge, it will move across and appear in the opposite side of the network area. Time is slotted into non-overlapping time slots of unit duration and the network area is evenly partitioned into $m \times m$ squares (cells) with the same side length $1/m$ [8, 20, 29, 52, 58, 59]. The nodes in the network move among these cells following the widely used independently and identically distributed (i.i.d.) mobility model [8, 20, 40, 52, 58, 59]. According to the i.i.d. mobility model, each node independently and randomly selects one from m^2 cells with the probability of $1/m^2$ at the beginning of each time slot, then moves to the selected cell and resides in it for the time slot.

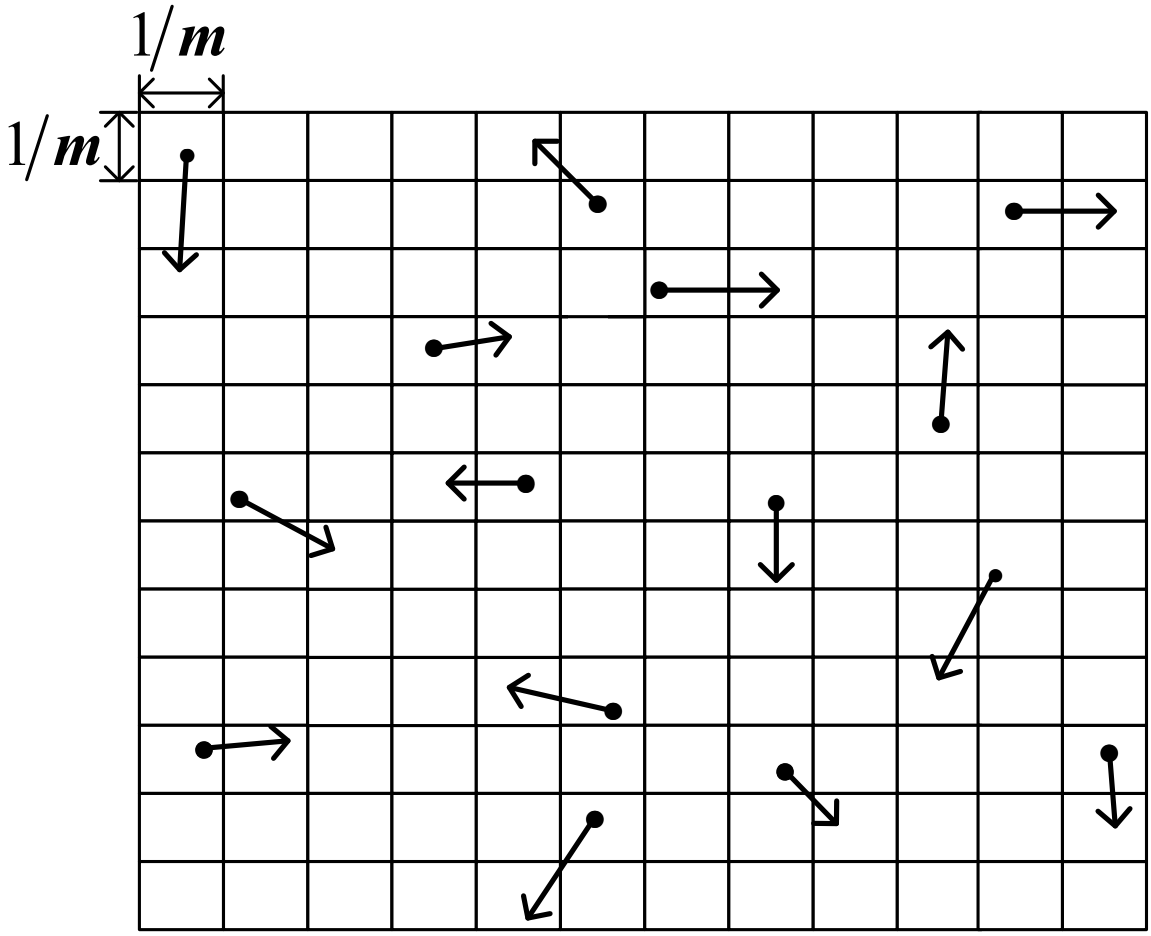

Figure 3-1: A snapshot of a cell-partitioned MANET with $m = 12$.

3.1.2 Communication Model

Similar to previous studies [18, 20, 53, 60], we consider a local transmission scenario where a transmitting node (transmitter) can only transmit to those nodes (receivers) in the same cell or in its eight neighboring cells. Two cells are called neighboring cells if they share a common point.

We adopt the widely used protocol model [13] here to ensure that each transmission will not be interrupted by interference from other concurrent transmissions. In particular, for three nodes i, j and k in time slot t, we use $X_i(t)$, $X_j(t)$ and $X_k(t)$ to denote their locations, respectively and use $|X_i(t) - X_j(t)|$ (resp. $|X_k(t) - X_j(t)|$) to denote the Euclidean distance between i and j (resp. k and j). Suppose that in time slot t, node j is in the same cell of i or its eight neighboring cells and that node i is

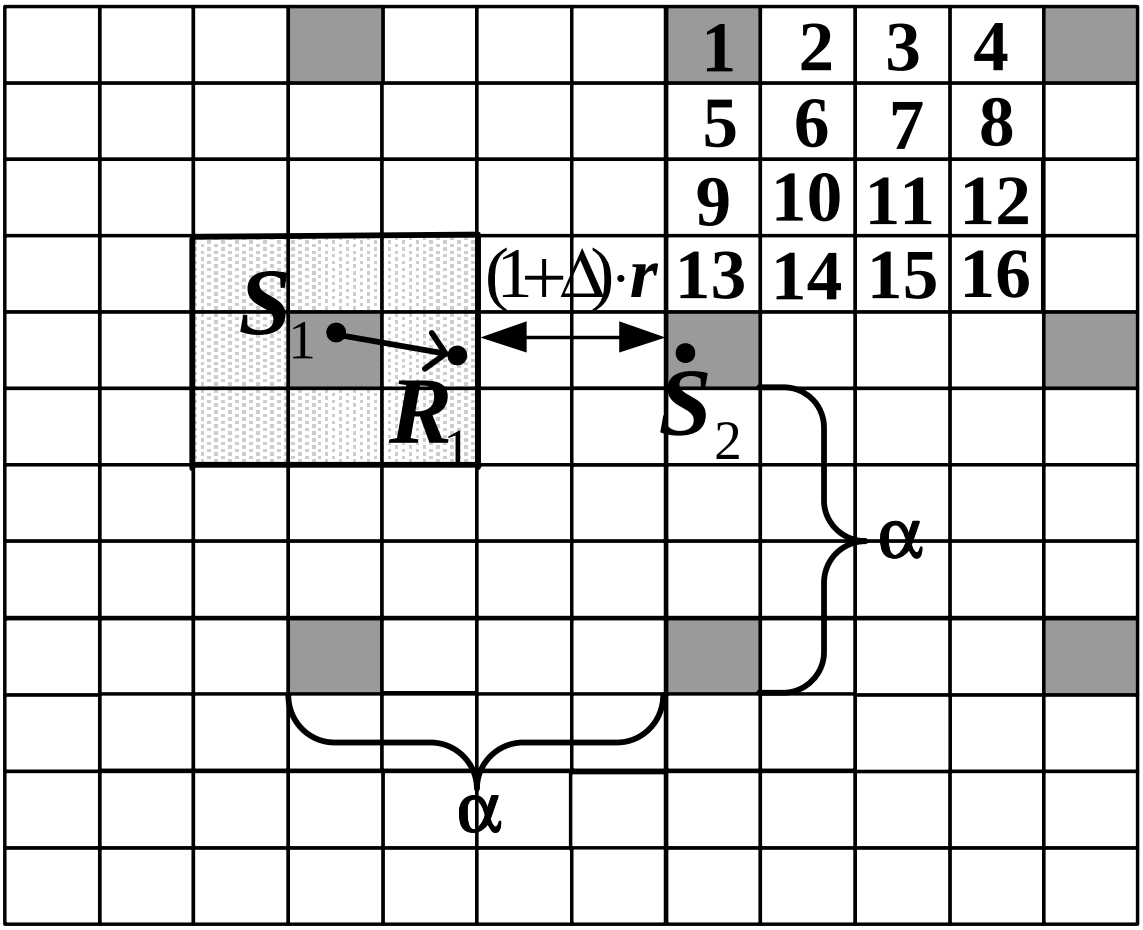

Figure 3-2: Illustration of equivalent-class based scheduling model with $m = 12$ and $\alpha = 4$.

transmitting a packet to node j in this time slot, then node j can receive this packet successfully if and only if for any other transmitting node k in the network,

$$|X_k(t) - X_j(t)| \geq (1 + \Delta)|X_i(t) - X_j(t)|, \tag{3.1}$$

where $\Delta > 0$ is a guard factor that represents a guard zone around each receiver.

We adopt the widely used assumption of communication model in this thesis mainly due to the following two reasons. First, it provides necessary mathematical tractability. Second, the analysis based on the assumption still provides meaningful theoretical performance results.

3.2 Transmission Scheduling Scheme

In order to support simultaneous transmissions as many as possible, we adopt an equivalent-class based transmission scheduling scheme to coordinate these transmissions without interfering with each other [60, 61]. According to this scheme, all cells in the network are divided into α^2 distinct equivalent-classes. In each equivalent-class, a cell is separated from another cell by a distance of some multiples of α cells in horizontal and vertical directions, respectively (e.g., in Fig. 3-2 all dark gray cells of the equivalent-class denoted by 1). To fairly use the shared channel, these equivalent-classes will become active in turn. The cells in an active equivalent-class are called active cells, each of which only allows a node randomly selected from all nodes in this cell to execute a transmission in this time slot.

To prevent concurrent transmissions from being interfered with each other in an equivalent-class, we must determine the parameter α appropriately. As shown in Fig. 3-2, suppose that a transmitter S_1 is transmitting to a receiver R_1. Since each transmitter can only transmit to the receivers in the same cell or in its eight neighboring cells, the maximum distance r between S_1 and R_1 is $2\sqrt{2}/m$. We can see from Fig. 3-2 that the minimum distance between R_1 and the most possibly closest concurrent transmitter S_2 is $(\alpha - 2)/m$. For the transmission between transmitter S_1 and its receiver R_1 to be successful, the following condition should be satisfied according to the protocol model [13]:

$$(\alpha - 2)/m \geq (1 + \Delta)2\sqrt{2}/m. \tag{3.2}$$

Notice that $\alpha \leq m$. Therefore, to maximize the number of active cells (m^2/α^2) in one active equivalent-class, the parameter α can be calculated as

$$\alpha = \min\{\lceil 2\sqrt{2}\Delta + 2(1 + \sqrt{2})\rceil, m\}, \tag{3.3}$$

where ceiling function $\lceil \cdot \rceil$ returns an integer number rounded up.

3.3 Summary

In this chapter, we introduced the considered MANETs, including the cell-partitioned network model, the i.i.d. mobility model, the communication model. In order to to schedule as many simultaneous transmissions as possible in a cell-partitioned network, we defined the equivalent-class based scheduling scheme, where the transmission scheduling is introduced.

THIS PAGE INTENTIONALLY LEFT BLANK

Chapter 4

Unicast Delivery Delay Study for MANETs with Erasure Coding and f-cast Relay

Packet delivery delay in MANETs is critical to support unicast-intensive applications in such networks. To study the packet delivery delay in MANTEs with erasure coding and packet redundancy, this chapter proposes a discrete time multi-dimensional Markov chain model to depict the packet delivery process under a general routing algorithm adopted in our study, where a group of x packets at source node are first encoded into g $(x \cdot \tau)$ encoded packets using erasure coding, and each encoded packet is then delivered to at most f distinct relay nodes, which is called f-cast relay here. Based on this Markov chain model, analytical expressions are further derived for the mean and variance of packet delivery delay.

4.1 System Assumptions and Performance Metric

In this section, we first introduce the traffic pattern, then introduces a two-hop relay algorithm with erasure coding and packet redundancy, and finally provide the definition of packet delivery delay adopted in our study.

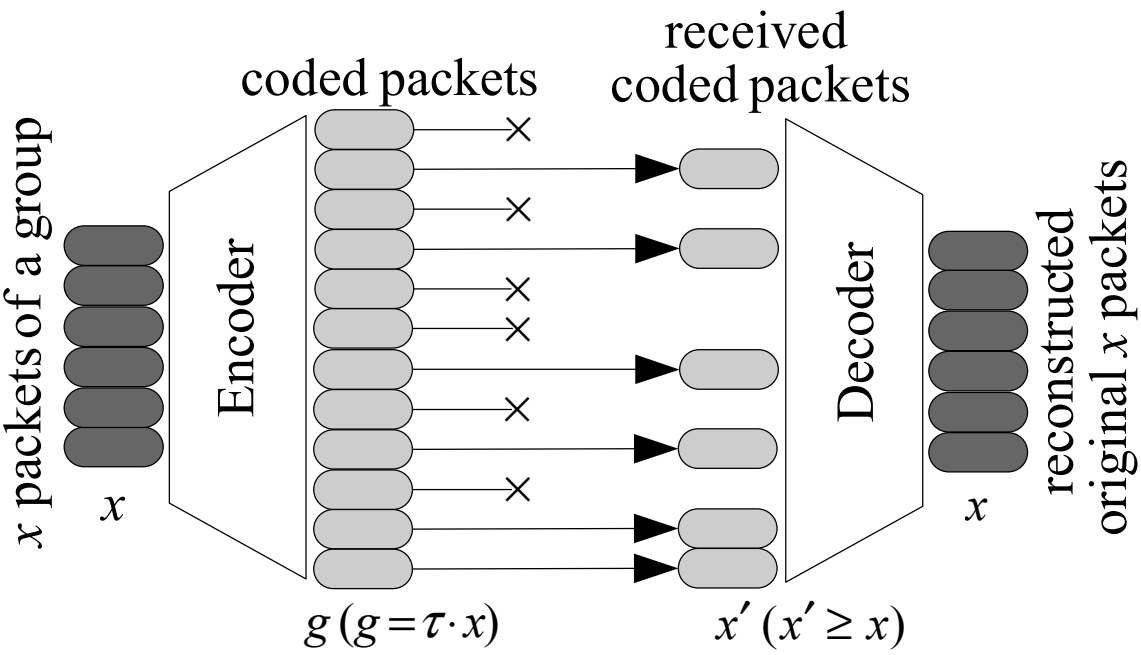

Figure 4-1: Illustration of erasure coding with replication factor $\tau \geq 1$.

4.1.1 Traffic Pattern

We consider the widely used permutation traffic pattern [7, 62, 63], where each node is the source of one flow and the destination of another flow. Here, one flow corresponds to one source-destination (S-D) pair. Without loss of generality, we assume n source-destination pairs are as follows: $1 \to 2, \cdots, i \to i+1, \cdots, n \to 1$, where the destination of node i is node $i+1$, and the destination of node n is node 1. We assume that the total number of bits that can be transmitted between a node pair is normalized as one packet per time slot. We further assume that there are no constraints of nodes' buffer size and packet loss.

4.1.2 Two-hop relay routing algorithm with erasure coding and packet redundancy

To better understand the considered routing algorithm, we first introduce erasure coding technique. The main idea of erasure coding with replication factor $\tau \geq 1$ is shown in Fig. 4-1, where a coding group of x packets at source node are first encoded into g ($g = \tau \cdot x$) equal-sized coded packets, and these x packets can then be decoded

at destination node when $x' \geq x$ distinct coded packets are received [2].

We use one simple example here to illustrate the basic encoding and decoding processes in erasure coding. For a coding group $(s_1, s_2, s_3)^T$ of three packets s_1, s_2 and s_3, we encode them into six coded packets $(c_1, c_2, \cdots, c_6)^T$ with replication factor $\tau = 2$ as

$$(c_1, c_2, \cdots, c_6)^T = \mathbf{G} \cdot (s_1, s_2, s_3)^T, \tag{4.1}$$

here $\mathbf{G}$ is a 6-by-3 generator matrix of the erasure coding. Suppose that coded packets c_2, c_3 and c_5 have been received at destination node, then we have

$$(c_2, c_3, c_5)^T = \mathbf{G}' \cdot (s_1, s_2, s_3)^T, \tag{4.2}$$

where $\mathbf{G}'$ is a 3-by-3 submatrix composed of the 2th, 3th and 5th rows of matrix $\mathbf{G}$. Based on the property of $\mathbf{G}$ that a submatrix composed of any of its 3 rows will be an invertible matrix [64], we know that $\mathbf{G}'$ is invertible. Thus, the original packets s_1, s_2 and s_3 can then be decoded as

$$(s_1, s_2, s_3)^T = (\mathbf{G}')^{-1} \cdot (c_2, c_3, c_5)^T. \tag{4.3}$$

Without loss of generality, we focus on one source-destination pair with source node S and destination node D in our discussion. Fig. 4-2 shows the mechanism of the routing algorithm, including the processes of erasure coding, packet delivery and decoding. For a specified coding group, the source node S first encodes x packets into multiple distinct coded packets, and then S will distribute redundant copies for each coded packet (e.g., coded packet P) to at most f distinct relay nodes, and these relay nodes (also source node S) will finally deliver each coded packet to the destination node D. After receiving x distinct coded packets of the coding group, D can finally decoded the packets group. To simplify the analysis, we assume that each relay node will carry at most one coded packet for any particular coding group.

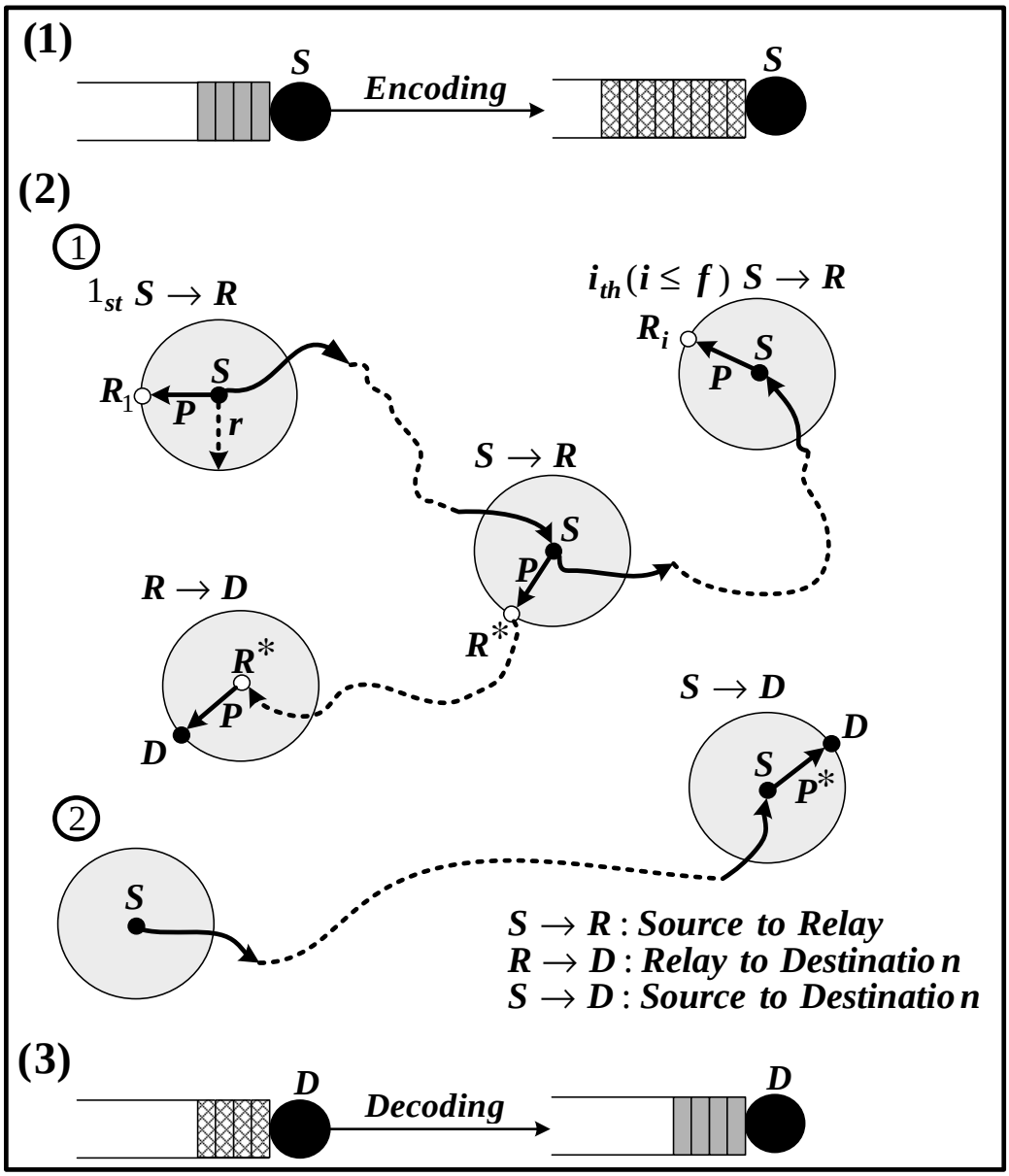

Figure 4-2: Illustration of the routing algorithm for a tagged source-destination pair. (1) and (3) denote the encoding and decoding processes at S and D, respectively. (2) denotes the packet delivery process, where ① illustrates that S is transmitting coded packet P to D with the help of relay nodes; ② illustrates that S is directly transmitting coded packet P^* to D.

Before introducing the routing algorithm, we first define the following terms.

- **New coded packet and non-new coded packet:** A coded packet is called

a new coded packet if it has not been received yet by its destination; otherwise, it is a non-new coded packet.

- **Utilized relay node and unutilized relay node:** A relay node is called a utilized relay node of a specified coding group if it carries a new coded packet of the coding group; otherwise, it is called an unutilized relay node.

- **Local-queue:** S maintains a local-queue to store coded packets of the packets generated at S, which will be replicated to relay nodes later.

- **Backup-queue:** S maintains a backup-queue to store its coded packets whose f copies have been sent out but their reception at D has not been confirmed yet.

- **Relay-queue:** S (as a relay node) also maintains $n-2$ relay-queues for other $n-2$ source-destination pairs to store their coded packets (one queue per source-destination pair).

Based on above definitions, the considered routing algorithm is summarized in Algorithm 1.

Notice that in the above relay-to-destination transmission, node S acts as a relay that helps to forward coded packets to destinations for other $n-2$ source-destination pairs. Regarding the traffic model in the routing algorithm, there exist in total n flows, each of which corresponds to one source-destination pair, since there are n mobile nodes in the network and each node is the source of one flow and the destination of another flow. Each node can be a potential relay for other $n-2$ flows (except the two flows originated from and destined for itself).

4.1.3 Performance Metric

Delivery Delay: For a specified coding group, the delivery delay of a packet in it is defined as the time duration starting from the time slot when source S starts to replicate the first coded packet of the group to the time slot when destination D has received x distinct coded packets of the group.

Algorithm 1 Routing Algorithm:

Encoding:

Source S encodes a group of x packets into $\tau \cdot x$ coded packets that are stored into its local-queue.

Delivery:

if S gets a transmission opportunity at a time slot **then**
    if D is within the transmission range of S **then**
        S executes Procedure 1;
    else
        S selects to perform source-to-relay transmission or relay-to-destination transmission with equal probability;
        if S schedules a source-to-relay transmission **then**
            S executes Procedure 2;
        else if S schedules a relay-to-destination **then**
            S executes Procedure 3;
        end if
    end if
end if

Decoding:

Destination D will decode the group of x packets when it receives x distinct coded packets of the group;

Procedure 1 Source-to-destination transmission:

S initiates a handshake to check which coded packets of the coding group have been received by D.
if the head-of-line coded packet P_h in local-queue is a new coded packet **then**
    S transmits P_h to D;
else if there exists a new coded packet waiting behind P_h in local-queue **then**
    S transmits the coded packet to D;
else if there exists a new coded packet in backup-queue of S **then**
    S transmits the coded packet to D;
end if

S deletes all the non-new coded packets in its local-queue and backup-queue;

It is notable that with routing algorithm, packets of a coding group are first encoded together as encoded packets, so essentially they are dispatched from S at the same time and also they are received by D at the same time (i.e., when x distinct coded packets are received). Thus, each packet of a coding group experiences the same delivery delay defined above.

Procedure 2 Source-to-relay transmission:

1. S randomly selects a node as relay node R within its transmission range;
2. **if** R is an unutilized relay node **then**
3. S transmits a copy of head-of-line coded packet P_h in its local-queue to R;
4. **if** f copies of P_h have already been delivered out **then**
5. S puts P_h to the end of its backup-queue, and then moves ahead remaining coded packets in its local-queue;
6. **end if**
7. **else**
8. S keeps idle at this time slot;
9. **end if**

Procedure 3 Relay-to-destination transmission:

1. S randomly selects a node as destination node V within its transmission range;
2. S initiates a handshake to check which coded packets of the coding group that V is requesting have been received by V.
3. **if** there exists a new coded packet of the coding group in its relay-queue specified for V **then**
4. S transmits the coded packet to V;
5. **else**
6. S keeps idle at this time slot;
7. **end if**

S deletes all non-new coded packets destined for V from its relay-queue;

4.2 Markov Chain Model

To depict the packet delivery process under the considered routing algorithm, we adopt a three-tuple (i, j, k) to denote general transient state for coded packets of a coding group, where source S is delivering the j_{th} $(1 \leq j \leq f)$ copy of the i_{th} $(1 \leq i \leq \tau \cdot x)$ coded packet of the group, and destination D has received k $(0 \leq k < x, k \leq i)$ of $\tau \cdot x$ coded packets. We further use to $(*, *, k)$ to denote the transient state that S has already finished dispatching all copies of $\tau \cdot x$ coded packets while D has only received k $(0 \leq k < x)$ distinct coded packets of them. Suppose that current transient state is (i, j, k), based on this considered routing algorithm we can see that only one of the following four transmission cases will happen in the next time slot.

- SR case: Source-to-relay transmission, i.e., S successfully delivers the j_{th} copy of the i_{th} coded packet to an unutilized relay node. As shown in Fig. 4-3(a), under the SR case, the state (i, j, k) can transit to any of its three neighboring

states depending on indexes i and j.

- RD case: Relay-to-destination transmission, i.e., a helping-node successfully delivers a new coded packet to D. As shown in Fig. 4-3(b), under the RD case, the state (i, j, k) can only transit to state $(i, j, k + 1)$.

- SR+RD case: Both source-to-relay transmission and relay-to-destination transmission happen simultaneously. As shown in Fig. 4-3(c), under the $SR + RD$ case, the state (i, j, k) can transit to any state of $(i, j+1, k+1)$, $(i+1, 1, k+1)$ and $(*, *, k + 1)$.

- SD case: Source-to-destination transmission, i.e., S successfully delivers a new coded packet to D. As shown in Fig. 4-3(d), under the SD case, the state (i, j, k) can transit to any of states $(i+1, 1, k+1)$, $(i+2, 1, k+1)$ and $(*, *, k+1)$, depending on indexes i and k.

Notice that the source S always delivers out coded packet sequentially, thus a coded packet delivered out earlier from its source S will be likely received early at its destination D. To simplify the analysis, under the SD case we assume that for the transient state (i, j, k) with $k < i < \tau \cdot x$, S is delivering the i_{th} coded packet but less than i distinct coded packets have been received by D. Thus, under the SD case in Fig.4-3(d), the transient state (i, j, k) will always transit to the state $(i + 1, 1, k + 1)$ when $k < i < \tau \cdot x$.

Based on the transient states in Fig.4-3, the packet delivery process under the considered routing algorithm can be depicted by a discrete time multi-dimensional Markov chain model shown in Fig.4-4, where A denotes the absorbing state that destination D has received x distinct coded packets of the specified coding group.

As illustrated in Fig.4-4, we denote by β the total number of transient states in the Markov chain model, then β is determined as

$$\beta = (2\tau x^2 - x^2 + 3x - 2) \cdot f/2 + 1, \tag{4.4}$$

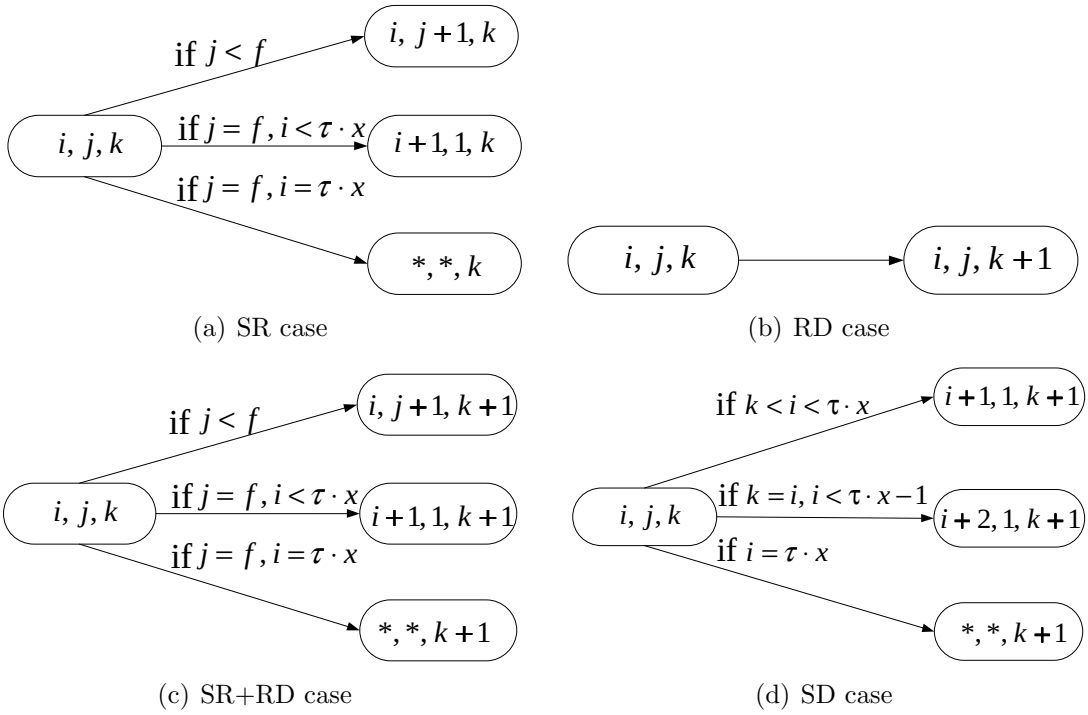

(a) SR case (b) RD case

(c) SR+RD case (d) SD case

Figure 4-3: The transition diagrams of the state $(i,\ j,\ k)$, where $1 \leq i \leq \tau \cdot x$, $1 \leq j \leq f$, and $0 \leq k < x, k \leq i$.

where all β transient states are arranged into x columns. We number these transient states sequentially as $1, 2, 3\ , \ldots, \beta$, and number the absorbing state A as $\beta + 1$, in a top-to-down and left-to-right way. Thus, the number of transient states c_k in the k_{th} column $(0 \leq k \leq x - 1)$ can be determined as

$$c_k = \begin{cases} \tau x \cdot f + 1 & if\ k = 0, \\ (\tau x + 1 - k) \cdot f & if\ 1 \leq k \leq x - 1. \end{cases} \tag{4.5}$$

For the l_{th} transient state of the k_{th} column in Fig.4-4, $l \in [1, c_k]$, $k \in [0, x - 1]$, the number of utilized relay nodes u_h and the number of unutilized relay nodes u_c can be determined as:

- When $k = 0$

$$u_h = l - 1, \tag{4.6}$$

$$u_c = n - l - 1. \tag{4.7}$$

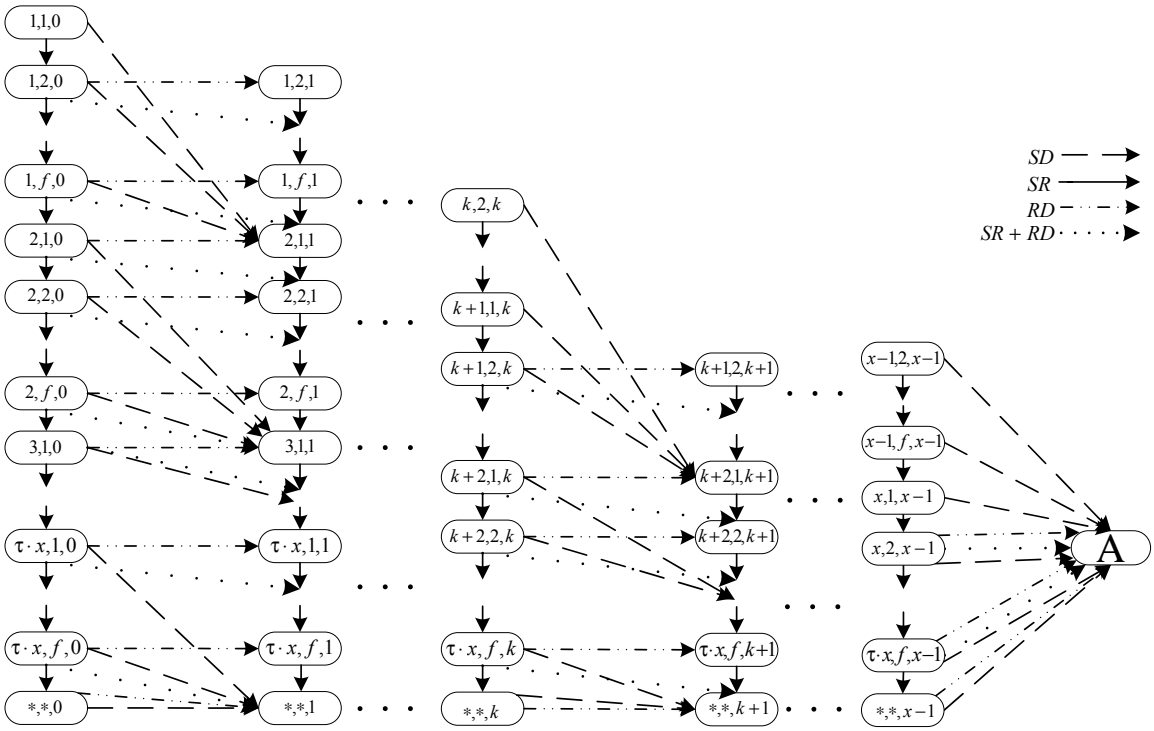

Figure 4-4: Absorbing Markov chain for the considered routing algorithm. For simplicity, the transition back to each transition state itself is not shown.

- When $k \in [1, x-1]$

$$u_h \approx \begin{cases} 0 & if\ l < f, \\ l - f & if\ l \geq f, \end{cases} \tag{4.8}$$

$$u_c \approx \begin{cases} n-2 & if\ l < f, \\ n-2-l+f & if\ l \geq f, \end{cases} \tag{4.9}$$

4.3 Packet Delivery Delay Modeling

Based on the Markov chain model in Fig.4-4, we proceed to analyze the packet delivery delay and related delay variance under the considered routing algorithm.

4.3.1 Expected Packet Delivery Delay and Delay Variance

For the Markov chain model in Fig.4-4, we use random variable t_k to denote the time it takes for the chain to reach the absorbing state A starting from the k_{th} transient

state ($1 \leq k \leq \beta$). Thus, the expected value $E\{t_1\}$ of t_1 just corresponds to the expected packet delivery delay under the considered routing algorithm.

To derive $E\{t_1\}$, we first need to determine the values of vector $\mathbf{t} = (E\{t_1\}, E\{t_2\}, \ldots, E\{t_\beta\})^T$. Using the first step analysis, we have

$$E\{t_k\} = \sum_{l=1}^{\beta+1} q_{kl}(1 + E\{t_l\}) = 1 + \sum_{l=1}^{\beta} q_{kl}E\{t_l\} \tag{4.10}$$

where q_{ij} denotes the transition probability from the i_{th} state to the j_{th} state. Notice that $E\{t_l\} = 0$ when $l = \beta + 1$.

We define a matrix $\mathbf{P} = (q_{ij})_{(\beta+1)\times(\beta+1)}$ and a submatrix $\mathbf{Q}$ consisting of rows 1 through β and columns 1 through β of matrix $\mathbf{P}$. Then, we can rewrite (4.10) as

$$\mathbf{t} = (1, 1, \cdots, 1)^T + \mathbf{Q}\mathbf{t}. \tag{4.11}$$

Thus, we have

$$\mathbf{t} = (\mathbf{I} - \mathbf{Q})^{-1} \cdot (1, 1, \cdots, 1)^T, \tag{4.12}$$

where $\mathbf{I}$ denotes a β-by-β identity matrix.

Let $\mathbf{N}$ denote the fundamental matrix of the Markov chain in Fig.4-4. According to Markov chain theory [65], we have

$$\mathbf{N} = (\mathbf{I} - \mathbf{Q})^{-1}. \tag{4.13}$$

By substituting (4.13) into (4.12), we have

$$E\{t_1\} = \sum_{i=1}^{\beta} \mathbf{N}(1, i), \tag{4.14}$$

where $\mathbf{N}(1, i)$ denotes the $(1, i)$-entry of $\mathbf{N}$.

We proceed to derive variance $Var\{t_1\}$ of packet delivery delay. Since

$$Var\{t_1\} = E\{t_1^2\} - (E\{t_1\})^2, \tag{4.15}$$

we need to determine $E\{t_1^2\}$ to obtain $Var\{t_1\}$. Notice that

$$E\{t_i^2\} = \sum_{l=1}^{\beta+1} q_{il} E\{(1+t_l)^2\} = \sum_{l=1}^{\beta} q_{il} E\{t_l^2\} + 2\sum_{l=1}^{\beta} q_{il} E\{t_l\} + 1. \tag{4.16}$$

We define $\mathbf{t}_{sq} = (E\{t_1^2\}, E\{t_2^2\}, \ldots, E\{t_\beta^2\})^T$, then we can rewrite (4.16) as

$$\mathbf{t}_{sq} = \mathbf{Q} \cdot \mathbf{t}_{sq} + 2\mathbf{Q} \cdot \mathbf{t} + (1, 1, \cdots, 1)^T. \tag{4.17}$$

Combining (4.12), (4.13) and (4.17), we obtain

$$\mathbf{t}_{sq} = \mathbf{N}(2\mathbf{Q} \cdot \mathbf{N} + \mathbf{I})\mathbf{b}, \tag{4.18}$$

where $\mathbf{b} = (1, 1, \cdots, 1)^T$. Thus, $E\{t_1^2\}$ can be evaluated based on (4.18).

We can see from (4.14), (4.15) and (4.18) that we need to determine $\mathbf{Q}$ and $\mathbf{N}$ for the evaluation of $E\{t_1\}$ and $Var\{t_1\}$.

4.3.2 Derivation of Matrix Q

To simplify the calculation, we arrange $\mathbf{Q}$ as the following partitioned matrices

$$\mathbf{Q} = \begin{bmatrix} \mathbf{Q}_0 & \mathbf{Q}'_0 & & & & & & \\ & \mathbf{Q}_1 & \mathbf{Q}'_1 & & & & & \\ & & \ddots & \ddots & & & & \\ & & & & \mathbf{Q}_k & \mathbf{Q}'_k & & \\ & & & & & \ddots & \ddots & \\ & & & & & & \mathbf{Q}_{x-2} & \mathbf{Q}'_{x-2} \\ & & & & & & & \mathbf{Q}_{x-1} \end{bmatrix}, \tag{4.19}$$

where $\{\mathbf{Q}_k\}$ and $\{\mathbf{Q}'_k\}$ denote the main diagonal and upper diagonal blocks (sub-matrices) of $\mathbf{Q}$, and all other blocks are zero matrices and thus are omitted here. The block $\mathbf{Q}_k$ of size $c_k \times c_k$ defines the transition probabilities among the transient states of the k_{th} column in the Markov chain model, while the block $\mathbf{Q}'_k$ of size $c_k \times c_{k+1}$ defines the transition probabilities from the transient states of the k_{th} column to that of the $(k+1)_{th}$ column in the Markov chain model.

We first establish the following lemmas regarding some basic probabilities in the Markov chain model of Fig.4-4, which will help us to derive the matrix $\mathbf{Q}$.

Lemma 1. *For a time slot and a given S-D pair, let p_0 denote the probability that S is scheduled to conduct SD transmission, and let p_1 denote the probability that S is scheduled to conduct SR transmission or RD transmission. Then we have*

$$p_0 = \frac{1}{\alpha^2}\left(\frac{9n-m^2}{n(n-1)} - \left(1-\frac{1}{m^2}\right)^{n-1}\frac{8n+1-m^2}{n(n-1)}\right), \tag{4.20}$$

$$p_1 = \frac{1}{\alpha^2}\left(\frac{m^2-9}{n-1}\left(1-\left(1-\frac{1}{m^2}\right)^{n-1}\right) - \left(1-\frac{9}{m^2}\right)^{n-1}\right). \tag{4.21}$$

Lemma 2. *For a given S-D pair, suppose that at current time slot there are h utilized relay nodes and c unutilized relay nodes. For the next time slot, we use $p_{rev}(h)$, $p_{dev}(c)$ and $p_{sim}(h,c)$ to denote the probability that destination D will receive a new coded packet, the probability that S will successfully deliver out a coded packet to an unutilized relay node and the probability of simultaneous SR and RD transmissions, respectively. Then we have*

$$p_{rev}(h) = p_0 + \frac{h}{2(n-2)}p_1, \tag{4.22}$$

$$p_{dev}(c) = \frac{c}{2(n-2)}p_1, \tag{4.23}$$

$$\begin{aligned} p_{sim}(h,c) = {} & \frac{hc(m^2-\alpha^2)}{4m^2\alpha^4}\sum_{k=0}^{n-5}\binom{n-5}{k}\psi(k) \\ & \cdot\left\{\sum_{t=0}^{n-k-4}\binom{n-k-4}{t}\psi(t)\left(1-\frac{18}{m^2}\right)^{n-k-t-4}\right\}, \end{aligned} \tag{4.24}$$

where

$$\psi(\theta) = \frac{9(\frac{9}{m^2})^{\theta+1} - 8(\frac{8}{m^2})^{\theta+1}}{(\theta+1)(\theta+2)}. \tag{4.25}$$

The proof of lemma 1 and lemma 2 is similar to that in [22], so we omit it here. Based on the results of above lemmas, we can determine matrix $\mathbf{Q}$ as follows.

- When $k = 0$, the non-zero entries of $\mathbf{Q}_0$ and $\mathbf{Q}'_0$ can be determined as

$$\mathbf{Q}_0(i,i) = \begin{cases} 1 - p_{rev}(\tau x \cdot f) & \text{if } i = c_0, \\ 1 - p_{dev}(u_c) - p_{rev}(u_h) & \\ +p_{sim}(u_h, u_c) & \text{if } i \in [1, c_0), \end{cases} \tag{4.26}$$

$$\mathbf{Q}_0(i,i+1) = p_{dev}(u_c) - p_{sim}(u_h, u_c) \quad \text{if } i \in [1, c_0), \tag{4.27}$$

$$\mathbf{Q}'_0(i,i) = p_{sim}(u_h, u_c) \qquad \text{if } i \in [2, c_0), \tag{4.28}$$

$$\mathbf{Q}'_0(i,i-1) = \begin{cases} p_{rev}(\tau x \cdot f) & \text{if } i = c_0, \\ p_{rev}(u_h) - p_0 & \\ -p_{sim}(u_h, u_c) & \text{if } i \in [2, c_0), \end{cases} \tag{4.29}$$

$$\mathbf{Q}'_0(i, f \cdot \left\lceil \frac{i}{f} \right\rceil) = p_0 \qquad \text{if } i \in [1, c_0). \tag{4.30}$$

- When $k \in [1, x-1]$, the non-zero entries of $\mathbf{Q}_k$ can be determined as

$$\mathbf{Q}_k(i,i) = \begin{cases} 1 - p_0 - p_{dev}(u_c) & \text{if } i \in [1, f], \\ 1 - p_{dev}(u_c) - p_{rev}(u_h) & \\ +p_{sim}(u_h, u_c) & \text{if } i \in [f+1, c_k), \\ 1 - p_{rev}(u_h) & \text{if } i = c_k, \end{cases} \tag{4.31}$$

$$\mathbf{Q}_k(i,i+1) = \begin{cases} p_{dev}(u_c) & \text{if } i \in [1, f], \\ p_{dev}(u_c) - p_{sim}(u_h, u_c) & \text{if } i \in [f+1, c_k). \end{cases} \tag{4.32}$$

- When $k \in [1, x-2]$, the non-zero entries of $\mathbf{Q}'_k$ can be determined as

$$\mathbf{Q}'_k(i, i-f+1) = p_{sim}(u_h, u_c) \qquad \text{if } i \in [f+1, c_k), \tag{4.33}$$

$$\mathbf{Q}'_k(i, i-f) = \begin{cases} p_{rev}(u_h) & \text{if } i = c_k, \\ p_{rev}(u_h) - p_0 & \\ -p_{sim}(u_h, u_c) & \text{if } i \in [f+1, c_k), \end{cases} \tag{4.34}$$

$$\mathbf{Q}'_k(i, f) = p_0 \qquad \text{if } i \in [1, f], \tag{4.35}$$

$$\mathbf{Q}'_k(i, f \cdot \left\lfloor \frac{i}{f} \right\rfloor) = p_0 \qquad \text{if } i \in [f+1, c_k). \tag{4.36}$$

4.3.3 Derivation of the Matrix N

For the Markov chain model in Fig.4-4, we can actually partition the fundamental matrix $\mathbf{N}$ into x-by-x blocks $\mathbf{N} = (\mathbf{N}_{ij})_{x \times x}$, where the block $\mathbf{N}_{ij}$ corresponds to the expected number of times in the transient states of the $(j-1)_{th}$ column of the Markov chain model given that Markov chain starts from the transient states of the $(i-1)_{th}$ column. We define a matrix $\mathbf{H} = \mathbf{I} - \mathbf{Q}$, so we obtain $\mathbf{H}^{-1} = \mathbf{N}$. Since $\mathbf{H}$ can also be defined in block structure, we use $\{\mathbf{H}_k\}$ and $\{\mathbf{H}'_k\}$ to denote the main diagonal and upper diagonal blocks of $\mathbf{H}$, respectively. Then we have

$$\mathbf{H}_k^{'}(i,j) = -\mathbf{Q}_k^{'}(i,j), \tag{4.37}$$

$$\mathbf{H}_k(i,j) = \begin{cases} 1 - \mathbf{Q}_k(i,j) & \text{if } i = j, \\ -\mathbf{Q}_k(i,j) & \text{otherwise.} \end{cases} \tag{4.38}$$

Based on the definition of $\mathbf{Q}_k$, we know that $0 < \mathbf{Q}_k(i,i) < 1$, $\mathbf{Q}_k(i,i+1) > 0$, so $0 < \mathbf{H}_k(i,i) < 1$, $\mathbf{H}_k(i,i+1) < 0$, and all other entries of $\mathbf{H}_k$ are zero. It is easy to see that $\mid \mathbf{H}_k \mid \neq 0$, so $\mathbf{H}_k$ is an invertible matrix.

To derive $\mathbf{N} = \mathbf{H}^{-1}$ based on elementary row operations, we first construct a combined matrix $[\mathbf{H} \mid \mathbf{I}]$ consisting of matrix $\mathbf{H}$ and the identity matrix $\mathbf{I}$ of the same size. By applying elementary row operations to the combined matrix, we get $[\mathbf{I} \mid \mathbf{N}]$, so we have

$$\mathbf{N} = \begin{bmatrix} \mathbf{H}_0^{-1} & \cdots & \cdots & \cdots & \mathbf{N}_{1j} & \cdots \\ & \ddots & \cdots & \cdots & \cdots & \cdots \\ & & \mathbf{H}_i^{-1} & \cdots & \mathbf{N}_{ij} & \cdots \\ & & & \ddots & \cdots & \cdots \\ & & & & \ddots & \cdots \\ & & & & & \mathbf{H}_{x-1}^{-1} \end{bmatrix}. \tag{4.39}$$

Notice that $\mathbf{N}$ is an upper triangle matrix, the (i,j)-entry $\mathbf{N}_{ij}$ of $\mathbf{N}$ is then determined as

$$\mathbf{N}_{ij} = (-1)^{j-i} \Big(\prod_{k=i-1}^{j-2} \mathbf{H}_k^{-1} \mathbf{H}_k' \Big) \mathbf{H}_{j-1}^{-1}, \tag{4.40}$$

where $i \in [1,x]$, $j \in (i,x]$.

The (4.39) and (4.40) indicate that inverse matrix $\mathbf{H}_k^{-1}$ needs to be derived. Based on elementary row operations, we have

$$\mathbf{H}_k^{-1} = \begin{bmatrix} \frac{1}{\mathbf{H}_k(1,1)} & \cdots & \cdots & \cdots & \mathbf{H}_k^{-1}(1,j) & \cdots \\ & \ddots & \cdots & \cdots & \cdots & \cdots \\ & & \frac{1}{\mathbf{H}_k(i,i)} & \cdots & \mathbf{H}_k^{-1}(i,j) & \cdots \\ & & & \ddots & \cdots & \cdots \\ & & & & \ddots & \cdots \\ & & & & & \frac{1}{\mathbf{H}_k(c_k,c_k)} \end{bmatrix}. \tag{4.41}$$

We can see that matrix $\mathbf{H}_k^{-1}$ is also an upper triangle matrix, and its (i,j)-entry $\mathbf{H}_k^{-1}(i,j)$ can be evaluated as

$$\mathbf{H}_k^{-1}(i,j) = (-1)^{j-i}\left(\prod_{z=i}^{j-1}\frac{\mathbf{H}_k(z,z+1)}{\mathbf{H}_k(z,z)}\right)\frac{1}{\mathbf{H}_k(j,j)} \tag{4.42}$$

where $k \in [0, x-1]$, $i \in [1, c_k]$, and $j \in (i, c_k]$.

4.4 Numerical Results

In this section, we first validate our theoretical models on expected packet delivery delay and delay variance, and then apply these models to illustrate how system parameters will affect the delay performance.

4.4.1 Model Validation

A network simulator in C++ was developed to simulate the packet delivery process under the considered routing algorithm and i.i.d. mobility model, where transmission group with guard factor $\Delta = 1$ is adopted for transmission scheduling. For comparison, another two realistic mobility models, random walk model [66] and random waypoint model [35], were also implemented in the simulator. Based on the simulator, extensive simulations have been conducted for a network with $n = 100$, $m = 16$, $x = 2$ and $f = 3$. Under different setting of replication factor τ, the corresponding

theoretical and simulation results on expected value $E\{t_1\}$ and normalized standard deviation $\delta = \sqrt{Var\{t_1\}}/E\{t_1\}$ of packet delivery delay are summarized in Fig. 4-5.

We can see from Fig. 4-5 that our theoretical models on expected packet delivery delay and delay variance are very efficient in capturing the delay behavior under the i.i.d. mobility and the considered routing algorithm. It is interesting to notice in Fig. 4-5 that with the considered routing algorithm, the delay behaviors under the i.i.d. mobility and random waypoint are very similar each other, while the delay under the random walk exhibits a different behavior. Thus, our theoretical models, although was developed under the i.i.d. mobility model, can be used to predict the delay behavior under the random waypoint mobility model as well. The results in Fig. 4-5 also imply that in general both expected delay $E\{t_1\}$ and standard deviation δ monotonically decrease as replication factor τ increases.

4.4.2 Performance Analysis

We now explore how the packet delivery delay performance (δ, $E\{t_1\}$) of the considered routing algorithm varies with various parameters. With $n = \{100, 200, 300\}$, $m = 16$, $\tau = 2$ and $f = 3$, we examine in Fig. 4-6 how $E\{t_1\}$ and δ vary with coding group size x. One can observe from Fig. 4-6 that as x increases, $E\{t_1\}$ monotonically increases while corresponding δ monotonically decreases. For example, for the setting of $n = 100$, the $E\{t_1\}$ (resp. δ) at $x = 3$ is 3317.71 (resp. 0.429), which is almost 0.61 (resp. 1.62) times that of $x = 6$. The results in Fig. 4-6 indicate through a proper control of coding group size x, a trade-off between $E\{t_1\}$ and δ can be initialized according different delay (and variance) requirements of various applications.

For the scenarios of $n = \{100, 200, 300\}$, $m = 16$, $\tau = 2$ and $x = 3$, Fig. 4-7 illustrates how $E\{t_1\}$ and δ vary with packet redundancy f. It is easy to see from Fig. 4-7 that for given scenario, as f increases, the $E\{t_1\}$ (resp.δ) first decreases and then increases, and there exists an optimum setting of f to achieve the minimum $E\{t_1\}$ (resp.δ). For example, for the case $n = 100$ in Fig. 4-7, a minimal $E\{t_1\}$ (resp. δ) of 3310.21 (resp. 0.384) is achieved at $f = 4$ (resp. $f = 6$). An increase in packet redundancy f has two-fold effects on delay performance: on one hand, it increases

the speed at which the destination receives a coded packet and thus decreases packet delay; on the other hand, it decreases the speed at which the source distributes copies of a coded packet and thus increases packet delay. When the first effect dominates the second one, $E\{t_1\}$ decreases as f increases; when the second effect dominates the first one, $E\{t_1\}$ increases as f further increases.

Finally, for the given setting of $m = \{24, 32, 40\}$, $\tau = 8$, $x = 3$ and $f = 3$, we show in Fig. 4-8 how $E\{t_1\}$ and δ vary with network size n. One can see from Fig. 4-8 that for a given setting of m, we can find a most suitable network size n^* (and thus most suitable average node density n/m^2) to achieve the minimum $E\{t_1\}$ (resp. δ). For example, for the setting of $m = 24, 32$ and 40, the most suitable network size is 100, 150 and 250 (resp. 150, 200 and 200) for a minimum $E\{t_1\}$ (resp. δ). Actually, an increase in network size n has two-fold effects on delay performance: on one hand, it increases the speed at which a coded packet is distributed and thus decreases packet delay; on the other hand, it decreases the speed at which the destination receives a coded packet due to the negative effects of interference and medium contention issues and thus increases packet delay. When the network is sparse, the first effect dominates the second one, and thus $E\{t_1\}$ decreases as n increases; when the network users become relatively densely distributed, the second effect dominates the first one, and thus $E\{t_1\}$ increases as n further increases.

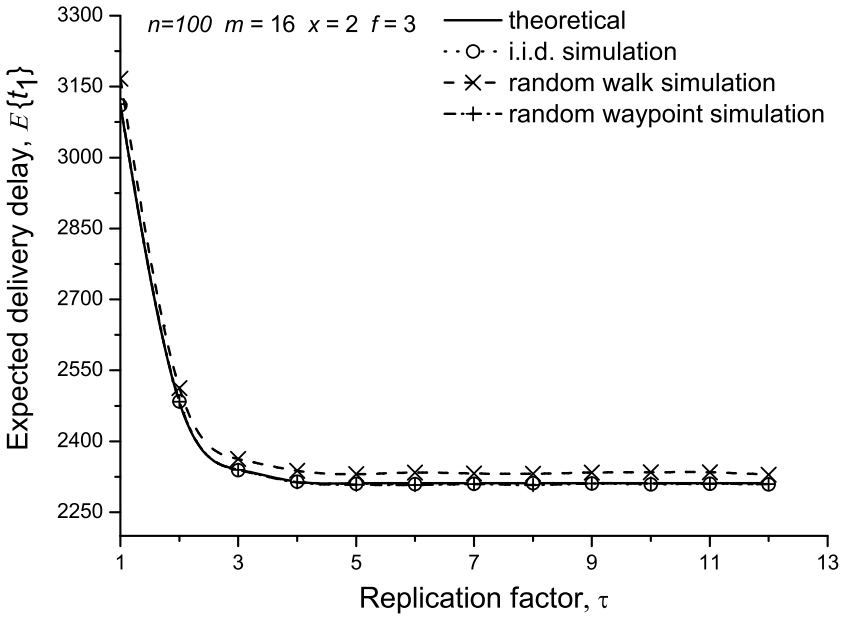

(a) $E\{t_1\}$ vs. τ

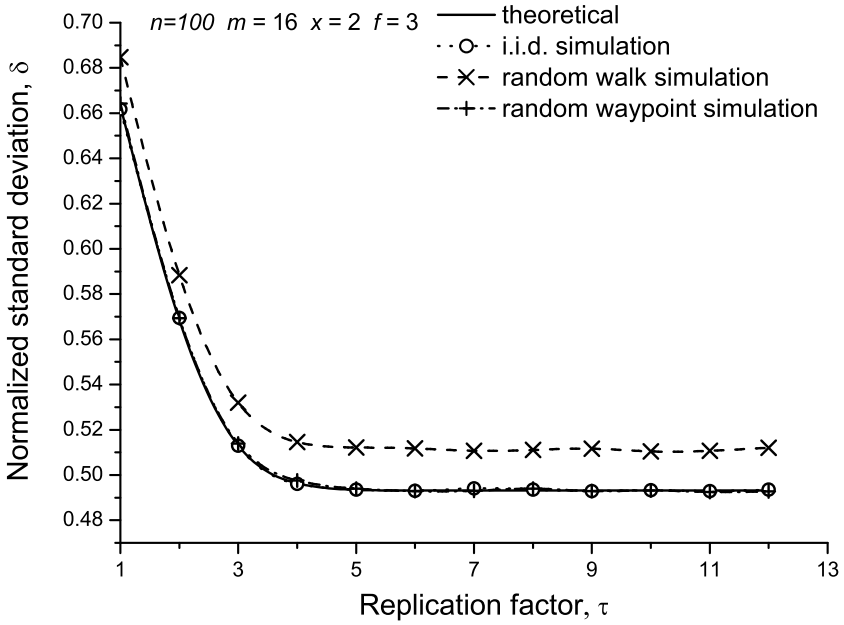

(b) δ vs. τ

Figure 4-5: Theoretical and simulation results for model validation.

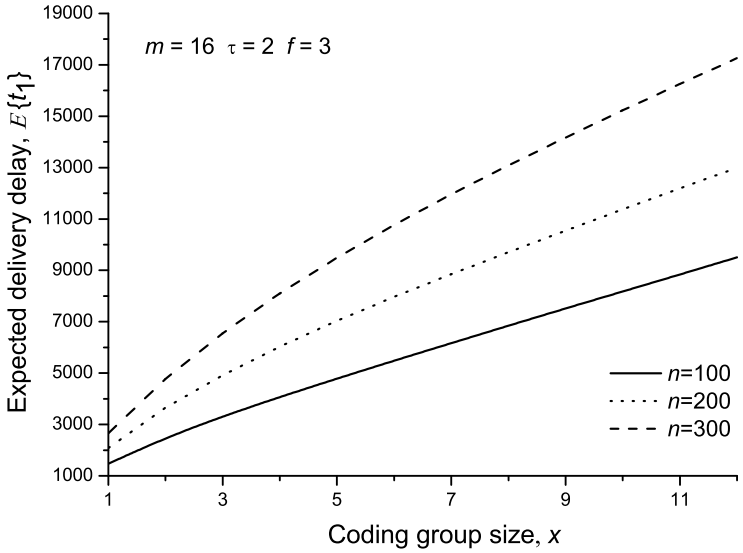

(a) $E\{t_1\}$ vs. coding group size x

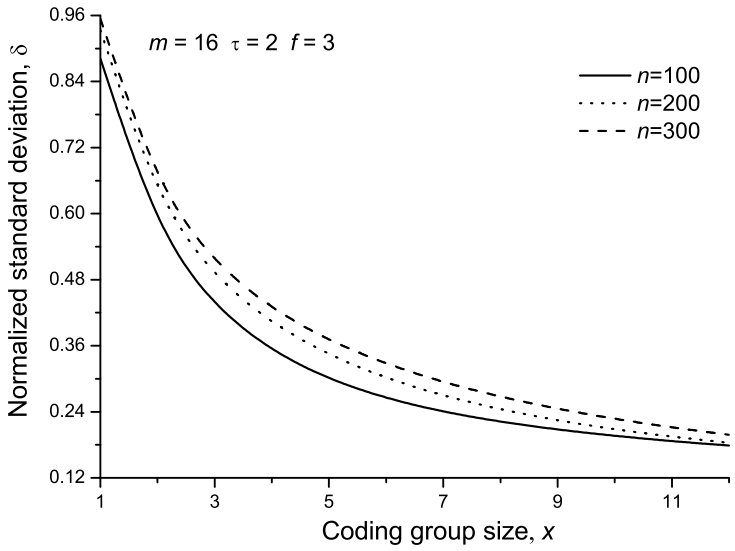

(b) δ vs. coding group size x

Figure 4-6: Delay performance vs. coding group size x.

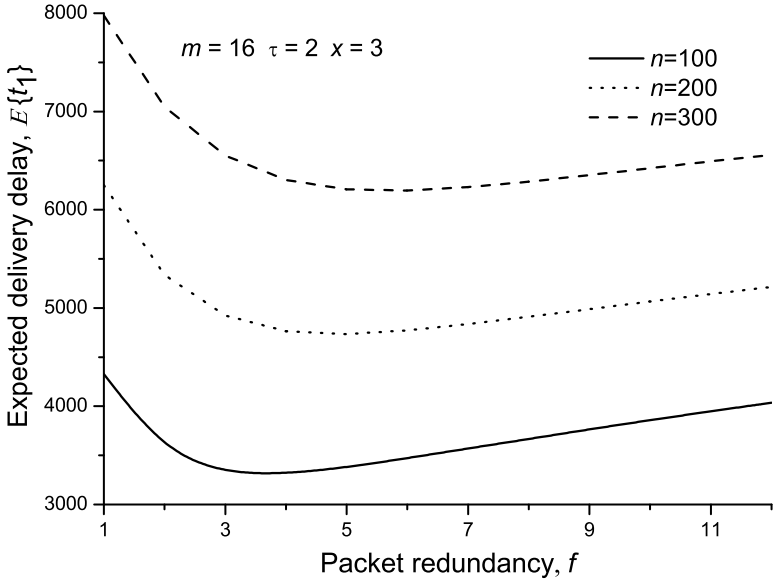

(a) $E\{t_1\}$ vs. packet redundancy f

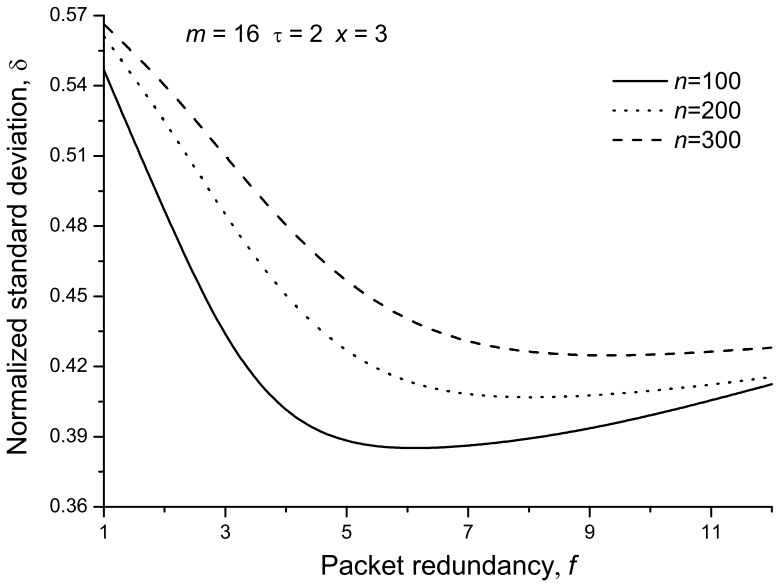

(b) δ vs. packet redundancy f

Figure 4-7: Delay performance vs. packet redundancy f.

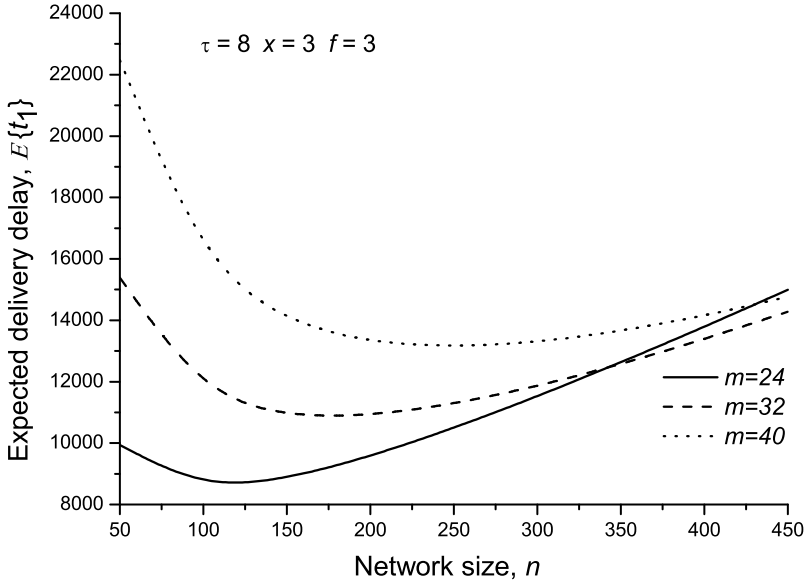

(a) $E\{t_1\}$ vs. network size n

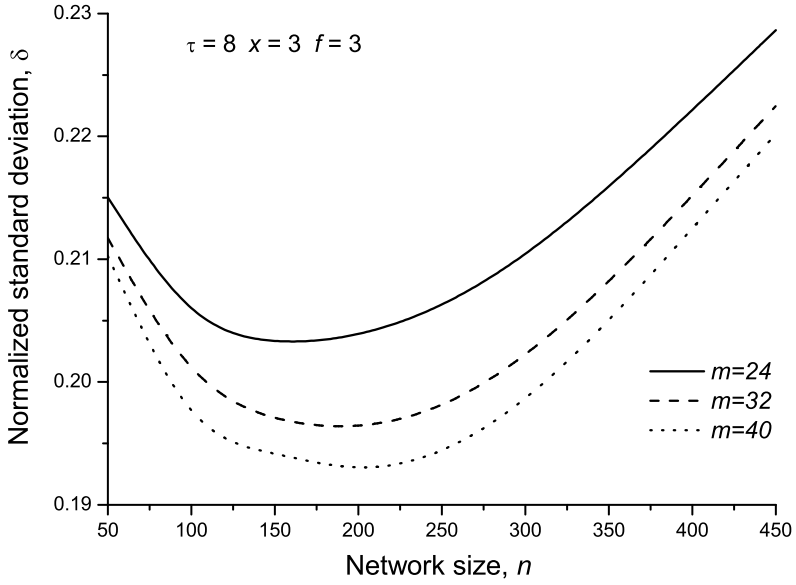

(b) δ vs. network size n

Figure 4-8: Delay performance vs. network size n.

4.5 Summary

To study the delay performance in MANETs, this chapter adopts a general routing algorithm by combining erasure coding and packet redundancy techniques. Theoretical models were further developed to reveal the delay performance under the considered routing algorithm. Numerical results indicate a flexible trade-off between expected delivery delay and delay variance can be obtained through a proper setting of coding group size x, replication factor τ and packet redundancy f. It is expected that the delay performance study can facilitate various applications with different requirements on delay and delay variance in future MANETs.

Chapter 5

Throughput Capacity Study for MANETs with Erasure Coding and f-cast Relay

Throughput capacity is of great importance for the design and performance optimization of MANETs. This chapter studies the exact throughput capacity of MANETs under the routing algorithm introduced in chapter 4. Under this routing algorithm, a source node first encodes a group of x packets into g ($g \geq x$) distinct coded packets, and then replicates each of the coded packets to at most f distinct relay nodes which help to forward them to destination node. All original packets can be recovered once the destination node receives any x distinct coded packets of the group. To study the throughput capacity of MANETs, we first construct two absorbing Markov chain models to depict the fastest packet distributing process at source and the fastest packet receiving process at destination. Based on these two Markov chain models, an analytical expression of the throughput capacity is further derived.

5.1 System Assumptions and Performance Metric

In this section, we first introduce the traffic pattern, and then define the throughput capacity involved in our study.

5.1.1 Traffic Pattern

We consider the random derangement traffic pattern [62]. Under this traffic pattern, if we let $\phi(i)$ denote the destination node of the traffic flow originated from node i, $i = 1, 2, \cdots, n$, the source-destination pairs are matched at random such that the sequence $(\phi(1), \phi(2), \cdots, \phi(n))$ is just a derangement of the set of nodes $\{1, 2, \cdots, n\}$, e.g., $\phi(1) = 2$, $\phi(2) = 3$, $\cdots$, $\phi(n) = 1$ and $\phi(1) = 2$, $\phi(2) = 1$, $\cdots$, $\phi(n-1) = n$, $\phi(n) = n - 1$. Accordingly, there are a total of n unicast traffic flows in the network. Each node has one originating flow and one incoming flow and there is no overlapping source or destination. Besides its own originating and incoming flows, each node also serves as a relay node to help to forward the coded packets for the other $n - 2$ traffic flows. We assume that the traffic flow originated at each node has an average input rate λ (packets/slot). We further assume that there are no constraints of nodes buffer size and packet loss.

5.1.2 Performance Metric

Throughput capacity: For a MANET with the considered routing algorithm, the network is called stable under the packet input rate λ (packets/slot) to each node if the queue length at each node will not grow to infinity as the time goes to infinity. The per node throughput capacity (throughput capacity for brevity) is then defined as the maximum value of λ that the network can stably support.

5.2 Markov Chain Models and Throughput Capacity

In this section, we first construct two absorbing Markov chain models to depict the packet delivery process under the considered routing algorithm. With the help of the Markov chain models, we then derive the exact throughput capacity.

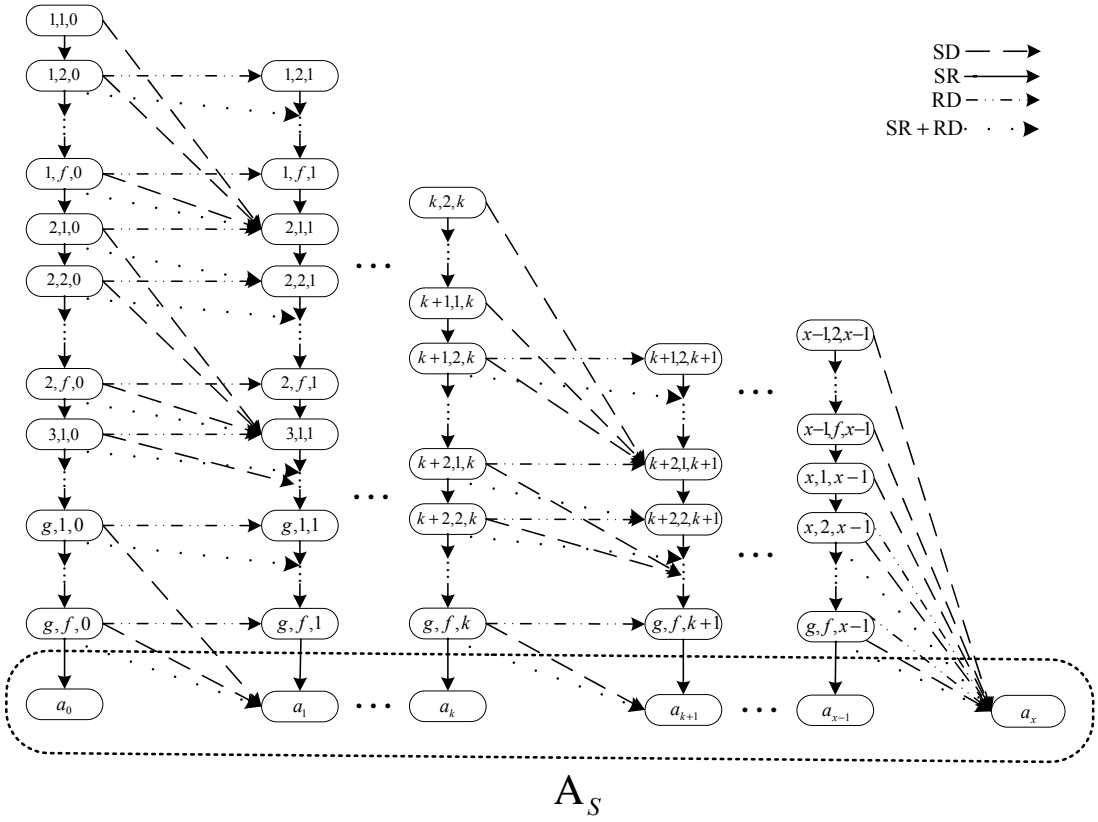

(a) Absorbing Markov chain for the fastest packet distributing process at source S.

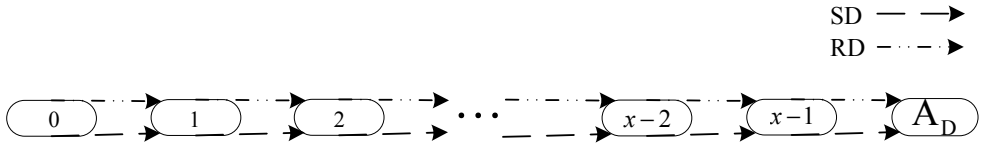

(b) Absorbing Markov chain for the fastest packet receiving process at destination D.

Figure 5-1: Two absorbing Markov chains. For each state, the transition back to itself is not plotted for simplicity.

5.2.1 Markov Chain Models

For the specific traffic flow and a given coding group, under the considered routing algorithm, we model two discrete-time absorbing Markov chain models illustrated in Figs. 5-1(a) and 5-1(b) to depict the fastest packet distributing process at source S and the fastest packet receiving process at destination D, respectively. The fastest packet distributing process corresponds to the process from the beginning (that S starts to distribute the first coded packet of the group and D also starts to request for the group at the same time slot) to the end (that S finishes distributing coded

packets of the group), while the fastest packet receiving process corresponds to the process from the beginning (that D starts to request for coded packets of the group and S has already distributed out all g coded packets of the group at the same time slot) to the end (that D has received x distinct coded packets of the group).

As shown in Fig. 5-1(b), any transient state i represents that S has distributed out all $g \cdot f$ copies of g coded packets for a given coding group, while D has already received any i $(0 \leq i < g)$ distinct coded packets of them; the absorbing state A_D indicates that D finishes the fastest packet receiving process, i.e., it has already received x distinct coded packets of the group. For the Markov chain in Fig. 5-1(b), in each time slot, only one of the following two transmissions will happen: a transmission from source to destination and another transmission from relay to destination.

As shown in Fig. 5-1(a), any transient state (i, j, k) represents that S is distributing the j-th $(1 \leq j \leq f)$ copy of the i-th $(1 \leq i \leq g)$ coded packet, while D has already received k $(0 \leq k < x, k \leq i)$ distinct coded packets of the group; the absorbing state set $A_S = \{a_0, a_1, ..., a_x\}$ indicates that S terminates the fastest packet distributing process, i.e., it finishes copy transmission for coded packets of the group. Notice that an absorbing state a_t $(0 \leq t \leq x)$ in the set represents that D has already received t distinct coded packets of the group.

In some time slot, suppose that the current state of the Markov chain in Fig. 5-1(a) is (i, j, k), then in the next time slot, only one of the following four transmissions will happen.

- Transmission from source to relay: S transmits the j-th copy of the i-th coded packet to an unutilized relay node. Under this transmission, the state (i, j, k) may transit to one of the states $(i, j+1, k)$, $(i+1, 1, k)$ and a_k. If the states can be reached, they should satisfy the following conditions: 1)$j < f$, 2)$j = f$ and $i < g$, and 3) $j = f$ and $i = x$, respectively.

- Transmission from relay to destination: A utilized relay node transmits a new coded packet to D. Under this transmission, the state (i, j, k) may transit to the state $(i, j, k+1)$.

- Concurrent transmissions: Both the transmission from source to relay and the transmission from relay to destination happen concurrently. Under these transmissions, the state (i, j, k) may transit to one of the states $(i, j+1, k+1)$, $(i+1, 1, k+1)$ and a_{k+1}. If the states can be reached, they should satisfy the following conditions: 1)$j < f$, 2)$j = f$ and $i < g$, and 3) $j = f$ and $i = g$, respectively.

- Transmission from source to destination: S transmits a new coded packet directly to D. Under this transmission, the state (i, j, k) may transit to one of the states $(i+1, 1, k+1)$, $(i+2, 1, k+1)$ and a_{k+1}. If the states can be reached, they should satisfy the following conditions: 1) $k < i < g$, 2) $k = i$ and $i < g-1$, and 3) $i = g$, respectively.

For the case of transmission from source to destination, we assume that if $k < i < g$, the current state (i, j, k) will transit to the state $(i+1, 1, k+1)$. Under the current state, regarding the ith $(i > 1)$ coded packet, the other $i-1$ coded packets that are delivered out earlier by S will be probably received earlier by D, and the transmission opportunities from source to destination is negligible in comparison with that from source to relay or relay to destination in a large MANET, thus for this transmission case, we can assume that the ith coded packet is not received by D before S conducts this transmission from source to destination. Based on this assumption, the current state will transit to the state $(i+1, 1, k+1)$ under the transmission, when $k < i < g$.

We further observe from Fig. 5-1(a) that all transient states are arranged into x columns along a direction from left to right in the Markov chain. Denoting L_k as the number of transient states in the kth column $(0 \leq k \leq x-1)$, and it is determined as

$$L_k = \begin{cases} gf & \text{if } k = 0, \\ (g+1-k)f - 1 & \text{if } 1 \leq k \leq x-1. \end{cases} \tag{5.1}$$

Denoting β as the total number of transient states, and we have

$$\beta = \frac{1}{2}(x-1)(2f - fx - 2) + xgf. \tag{5.2}$$

5.2.2 Throughput Capacity

We denote by $\mu(g, x, f)$ per node throughput capacity under the considered routing algorithm in a MANET, and then based on the Markov chain models, the per node throughput capacity $\mu(g, x, f)$ is derived in the following Theorem:

Theorem 1. *For the considered MANET, if its per node throughput capacity is denoted by $\mu(g, x, f)$, i.e., the network can stably support any packet input rate $\lambda \leq \mu(g, x, f)$ under the considered routing algorithm, then we have*

$$\mu(g, x, f) = min\left\{ \frac{x}{\boldsymbol{e}_1 \cdot \boldsymbol{N} \cdot \boldsymbol{e}_2}, \frac{x}{\sum_{i=0}^{x-1} \frac{1}{p_0 + \frac{(g-i)f}{2(n-2)} p_1}} \right\}, \tag{5.3}$$

where $\boldsymbol{N}$ denotes the fundamental matrix of the Markov chain in Fig. 5-1(a), $\boldsymbol{e}_1 = (1, 0, \cdots, 0)$, $\boldsymbol{e}_2 = (1, 1, \cdots, 1)^T$, p_0 denotes the probability that a node conducts a transmission from source to destination and p_1 denotes the probability that a node conducts a transmission from relay to destination, for each traffic flow.

Proof. For the considered traffic flow, we denote by IR_S and IR_D the long-term average packet distributing rate at source S and the long-term average packet receiving rate at destination D, respectively. They can be determined as

$$IR_S = \lim_{t \to \infty} \frac{\text{the number of distributed packets at } S \text{ in } (0, t]}{t}, \tag{5.4}$$

$$IR_D = \lim_{t \to \infty} \frac{\text{the number of received packets at } D \text{ in } (0, t]}{t}. \tag{5.5}$$

If the network is stable (i.e., the queue length at each node will not grow to infinity as the time goes to infinity) under the packet input rate λ, then we have

$$\lambda = IR_S = IR_D. \tag{5.6}$$

due to the fact that in a stable network, the long-term average rate of the packet input is equal to that of the packet output.

We denote by t_S and t_D the shortest service time at source S (i.e., the shortest

time S takes to distribute coded packets of a given coding group before it finishes distributing them) and the shortest service time at destination D (i.e., the shortest time D takes to receive x distinct coded packets of the coding group), respectively. $E\{t_S\}$ and $E\{t_D\}$ represent their corresponding expected values, then we have

$$IR_S \leq \frac{x}{E\{t_S\}}, \tag{5.7}$$

$$IR_D \leq \frac{x}{E\{t_D\}}, \tag{5.8}$$

since $\frac{x}{E\{t_S\}}$ represents that the maximum packet distributing rate at S and $\frac{x}{E\{t_D\}}$ represents the maximum packet receiving rate at D.

Based on (5.6), (5.7) and (5.8), we have

$$\lambda \leq \min\left\{\frac{x}{E\{t_S\}}, \frac{x}{E\{t_D\}}\right\}. \tag{5.9}$$

Since $\mu(g, x, f)$ is defined as the maximum value of λ that the network can stably support under the routing algorithm, the $\mu(g, x, f)$ is given by

$$\mu(g, x, f) = \min\left\{\frac{x}{E\{t_S\}}, \frac{x}{E\{t_D\}}\right\}. \tag{5.10}$$

Now, we only need to calculate $E\{t_S\}$ and $E\{t_D\}$. Notice that the Markov chain models in Figs. 5-1(a) and 5-1(b) depict that the fastest packet distributing process at S and that the fastest packet receiving process at D, respectively. Thus, $\mathbb{E}\{t_S\}$ is the expected time the Markov chain in Fig. 5-1(a) takes to become absorbed starting from the initial state $(1, 1, 0)$, and $E\{t_D\}$ is the expected time the Markov chain in Fig. 5-1(b) takes to get absorbed starting from the initial state 0.

We first derive the $E\{t_S\}$. There are β transient states in Fig. 5-1(a), and they are indexed sequentially as $0, 1, 2, \cdots, \beta - 1$ in a top-to-down and left-to-right way. According to Markov chain theory, the fundamental matrix $\mathbf{N}$ of the Markov chain

in Fig. 5-1(a) is given by

$$\mathbf{N} = (\mathbf{I} - \mathbf{Q})^{-1}, \tag{5.11}$$

where $\mathbf{I}$ is a β-by-β identity matrix, matrix $\mathbf{Q} = (q_{i,j})_{\beta \times \beta}$ represents the transition probabilities among all transient states of the Markov chain, and the ij-entry $q_{i,j}$ denotes the transition probability from the ith transient state to the jth transient state.

Since the ij-entry of matrix $\mathbf{N}$ represents the expected number of times in the jth transient state until absorption given that the chain starts from the ith transient state, we have

$$E\{t_S\} = \mathbf{e}_1 \cdot \mathbf{N} \cdot \mathbf{e}_2, \tag{5.12}$$

where $\mathbf{e}_1 = (1, 0, \cdots, 0)$ and $\mathbf{e}_2 = (1, 1, \cdots, 1)^T$.

We now proceed to derive $E\{t_D\}$. All states of the Markov chain in Fig. 5-1(b) are indexed sequentially as $0, 1, 2, \cdots, x$ in a left-to-right way. We denote by X_i the time it takes for the Markov chain in Fig. 5-1(b) to reach the absorbing state A_D given that the chain starts from the ith state ($0 \leq i \leq x$), and $E\{X_i\}$ is the expected value of X_i. We notice that $E\{t_D\} = E\{X_0\}$, we only need to derive $E\{X_0\}$. Based on the first step analysis in Markov chain theory, we have

$$E\{X_i\} = \sum_{j=0}^{x} q'_{i,j}(1 + E\{X_j\}) = 1 + \sum_{j=0}^{x} q'_{i,j} E\{X_j\}, \tag{5.13}$$

where $q'_{i,j}$ denotes the transition probability from the ith state to the jth state.

Since except transiting back to itself, the ith transient state can only transit to its next state (i.e., the $(i+1)$th state), we have $q'_{i,i+1} \neq 0$, and $q'_{i,j} = 0$ when $j \neq i$ and $j \neq i + 1$. We also know that $q'_{i,i+1} = 1 - q'_{i,i}$, thus $E\{X_i\}$ is further determined

as

$$E\{X_i\} = 1 + q'_{i,i}E\{X_i\} + q'_{i,i+1}E\{X_{i+1}\} = \frac{1}{q'_{i,i+1}} + E\{X_{i+1}\}. \tag{5.14}$$

Notice that $E\{X_x\} = 0$ for the xth state, i.e., absorbing state A_D. By iterating the formula (5.14), we obtain

$$E\{X_0\} = \sum_{i=0}^{x-1} \frac{1}{q'_{i,i+1}}. \tag{5.15}$$

Recall that the ith transient state in the Markov chain of Fig. 5-1(b) represents that the source node S has distributed out all $g \cdot f$ copies of x code packets for the group while the destination node D has received any i distinct coded packets of them. In current time slot, if the chain is in the ith transient state, there are $(g-i)f$ utilized relay nodes each carrying a new coded packet for the group. Then in the next time slot, the Markov chain will transit to the next state (i.e., the $(i+1)$th state) if D receives a new coded packet either from S or one of the $(g-i)f$ utilized relay nodes. Notice that these $(g-i)f+1$ events are mutually exclusive. Since the probabilities that D receives a new coded packet from S and from a utilized relay node are p_0 and $\frac{p_1}{2(n-2)}$, respectively, $q'_{i,i+1}$ can be obtained by summing over the probabilities of these $(g-i)f+1$ events and substituting it into (5.15) yields:

$$E\{X_0\} = \sum_{i=0}^{x-1} \frac{1}{p_0 + \frac{(g-i)f}{2(n-2)}p_1}, \tag{5.16}$$

so $E\{t_D\}$ is derived.

This finishes the proof of Theorem 1. □

We can see from formulas (5.3), (5.11) that the per node throughput capacity can be calculated based on the transition matrix $\mathbf{Q}$ derived in chapter 4.

5.3 Numerical Results

In this section, we first provide simulation results to validate the efficiency of our theoretical expression on throughput capacity, and then apply it to investigate how system parameters will affect the throughput capacity under the considered routing algorithm.

5.3.1 Validation of Throughput Capacity

We develop a simulator to simulate the packet delivery process of the considered routing algorithm in the considered MANETs. Here, the parameter in scheduling is determined as α=min$\{8, m\}$ with the setting of the guard zone $\Delta = 1$. In addition to the i.i.d. mobility model, the random walk model [50] and random waypoint model [35], are also implemented in the simulator, which are defined as follows:

- **Random Walk Model**: At the beginning of each time slot, with probability 1/9 each node moves from its current cell to one of its eight neighboring cells or stays at the current cell.

- **Random Waypoint Model**: At the beginning of each time slot, each node first generates a 2-tuple (y_1, y_2), where the value of each element is uniformly selected from $[1/m, 3/m]$, and then moves a distance of y_1 along the horizontal direction, and a distance of y_2 along the vertical direction.

Based on the simulator, extensive simulations were conducted to verify the theoretical expression on throughput capacity under two network scenarios of $n = 64, m = 8, x = 3, g = 6, f = 3$ and $n = 200, m = 16, x = 4, g = 8, f = 4$. The simulation results on throughput under different system loads ρ ($\rho = \lambda/\mu(g, x, f)$) are summarized in Fig. 5-2, where the throughput is measured as the time average of number of packets that are successfully delivered from a source node to its destination node. As shown in Fig. 5-2, each simulation result on throughput is averaged over 10^9 time slots for each given system load ρ, and the dots represent the simulated throughput

and the dashed lines are the corresponding theoretical throughput capacity $\mu(g, x, f)$, calculated by Theorem 1.

Figs. 5-2(a) and 5-2(b) show that for both the two network scenarios here, the per node throughput first increases linearly with ρ and as ρ further increases to the value no less than 1 (i.e., the input rate λ increases to the value no less than the theoretical throughput capacity $\mu(g, x, f)$), the per node throughput will achieve theoretical throughput capacity $\mu(g, x, f)$ of 1.59×10^{-3} and 6.79×10^{-4} in Figs. 5-2(a) and 5-2(b), respectively. This is an expected phenomenon since when $\rho < 1$, the queuing system in the network is under-loaded and as ρ approaches 1 and beyond, the queuing system saturates. This phenomenon indicates clearly that our theoretical expression can nicely capture the throughput capacity of the considered MANETs, and the theoretical throughput capacity is also achieved by adopting the routing algorithm in the networks.

Another observation from Fig. 5-2 is that the throughput under the random walk or random waypoint model also achieves the throughput capacity developed based on the i.i.d. mobility model. It suggests that our throughput capacity result can also be used to estimate the throughput capacity for these mobility models. This observation agrees with the Corollary 5 of [67], which implies that the throughput capacity depends only on the steady-state distribution of nodes locations. Since both of these mobility models lead to a uniform distribution of nodes locations in steady state, they lead to an identical throughput capacity to that of the i.i.d. mobility model.

5.3.2 Impact of System Parameters on Throughput Capacity

To explore the impact of system parameters on the throughput capacity, we now summarize in Fig. 5-3 how the per node throughput capacity $\mu(g, x, f)$ varies with the number of coded packets g and packet redundancy f under the network settings of $n = 150$, $m = 16$, $f = 3$, $x = \{2, 4, 6\}$, and $n = 250$, $m = 16$, $x = 4$, $g = \{4, 6, 8\}$, respectively.

We can observe from Fig. 5-3(a) that for a given x, the throughput capacity

first increases with the number of coded packets g, and there exists some threshold value of x, at which the throughput capacity achieves maximum and remains almost unchanged as g further increases. Actually, such behavior can be interpreted as follows: when g is relatively small, increasing g can increase the number of relay nodes each carrying a coded packet of a given coding group and thus increases the speed at which coded packets are delivered to their destination node, and also improves the throughput capacity performance; when g continues to increase up, all g coded packets of the group at source node can not be distributed out while the destination node has received x distinct coded packets of the group, and thus increasing g can not further improve the throughput capacity performance.

From Fig. 5-3(b) we can see that for each setting of g, the throughput capacity first increases and then decreases as f increases and there always exists an optimal f to maximize throughput capacity. This is due to the following reasons: increase of f has a two-fold effect on the throughput capacity. On the one hand, when f is small, increasing f can increase the speed at which the destination receives a coded packet and thus increases throughput capacity; on the other hand, when f becomes larger, increasing f can decrease the speed at which the source distributes out copies of a coded packet and thus decreases throughput capacity. We further compare the throughput capacity performance of the routing algorithm and two-hop relay routing routing with pure erasure coding [28, 29] (i.e., the special case of the considered routing algorithm at $f = 1$) to show the efficiency of the considered routing algorithm. It is easy to see from Fig. 5-3(b) that in comparison with the pure erasure coding based routing algorithm, distributing copies of coded packets could improve the throughput capacity performance.

To examine the impact of g on the maximum throughput capacity, we illustrate in Fig. 5-4 how the $\mu^* = \max_f\{\mu\{g, x, f\}\}$ and the corresponding optimum setting of f (as observed in Fig. 5-3(b)) vary with g for a network setting of $n = 250$, $m = 16$ and $x = \{2, 3, 4\}$. As can be seen from Fig. 5-4(a), for a given x, the maximum throughput capacity μ^* increases with g, and at last it is nearly unchanged as g continues to increase. This is due to the fact that the destination node has received

x distinct coded packets of the group before the source node finishes distributing copies of g coded packets, and thus a larger g leads to little throughput capacity gain. Fig 5-4(b) shows that for each setting of x there, the corresponding optimum setting of f is a piecewise decreasing function of g.

Finally, we explore in Fig. 5-5 how the throughput capacity varies with the number of nodes n, given that $m = 16$, $x = 4$, $g = 9$ and $f = \{3, 5, 7\}$. We can observe from Fig. 5-5 that for each setting of f, as n increases, the throughput capacity first increases and then decreases. This can be explained as follows: on one hand, when the network is sparse (thus n is relatively small), increasing n will result in more opportunities for source or relays to execute transmissions and thus increases throughput capacity; however, on the other hand, a larger n will cause more significant interferences and medium contentions among nodes and thus results in a decrease of transmission opportunities for each node, and incurs the decrease of throughput capacity.

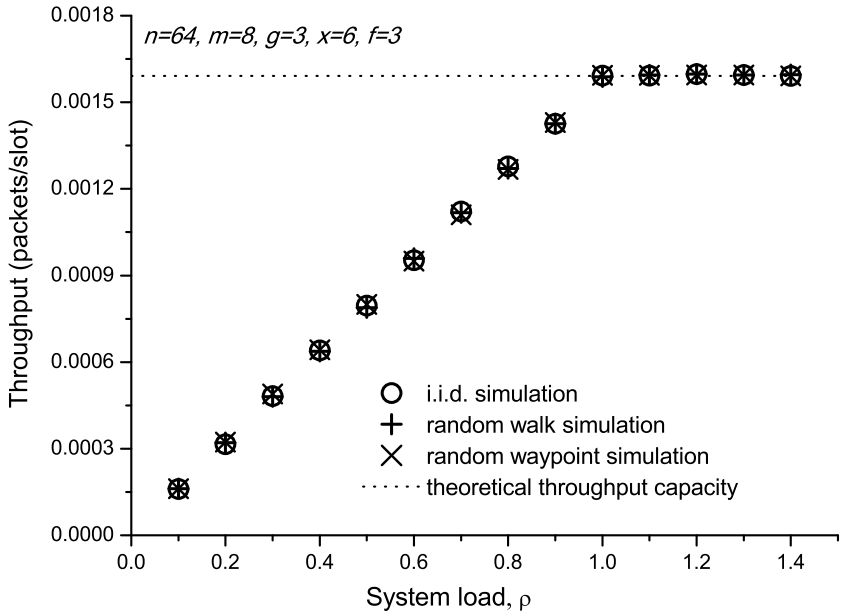

(a) The per node throughput for network scenario ($n = 64, m = 8, x = 3, g = 6, f = 3$)

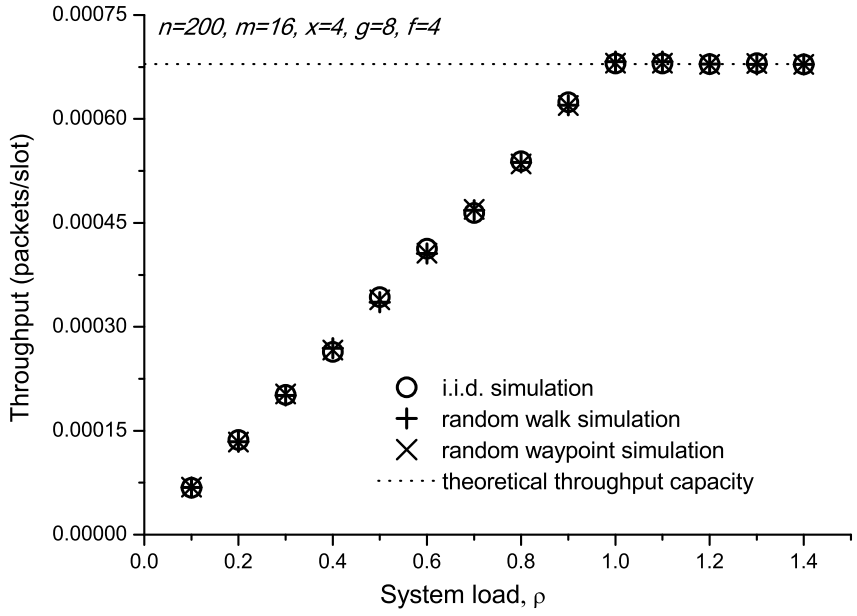

(b) The per node throughput for network scenario ($n = 200, m = 16, x = 4, g = 8, f = 4$)

Figure 5-2: Comparisons between simulation results and theoretical ones for validation of theoretical throughput capacity.

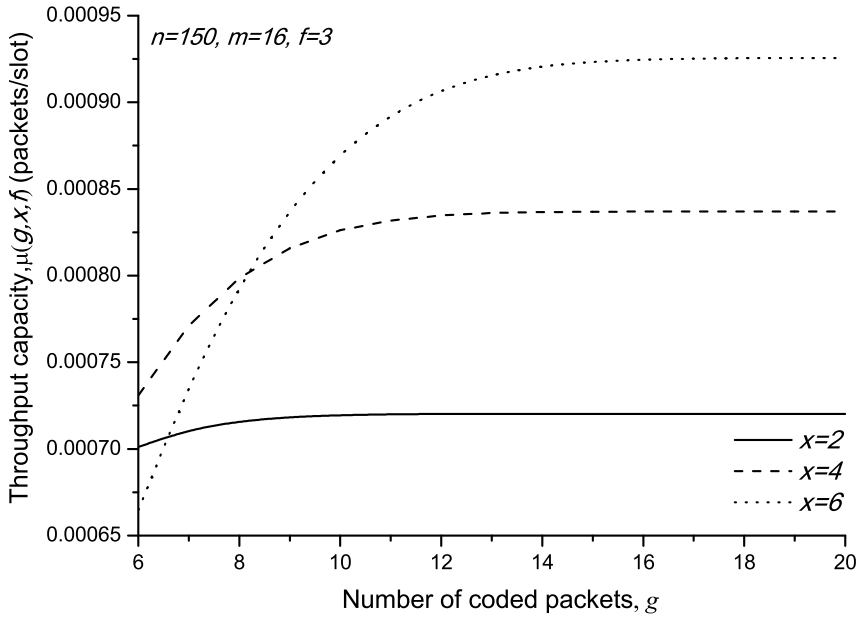

(a) $\mu(g, x, f)$ vs. g

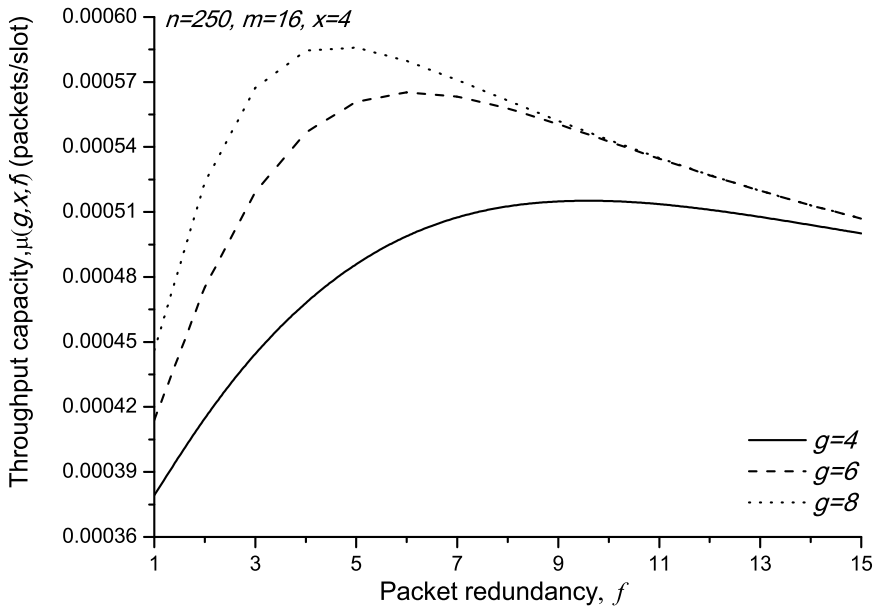

(b) $\mu(g, x, f)$ vs. f

Figure 5-3: Throughput capacity $\mu(g, x, f)$ versus number of coded packets g and packet redundancy f.

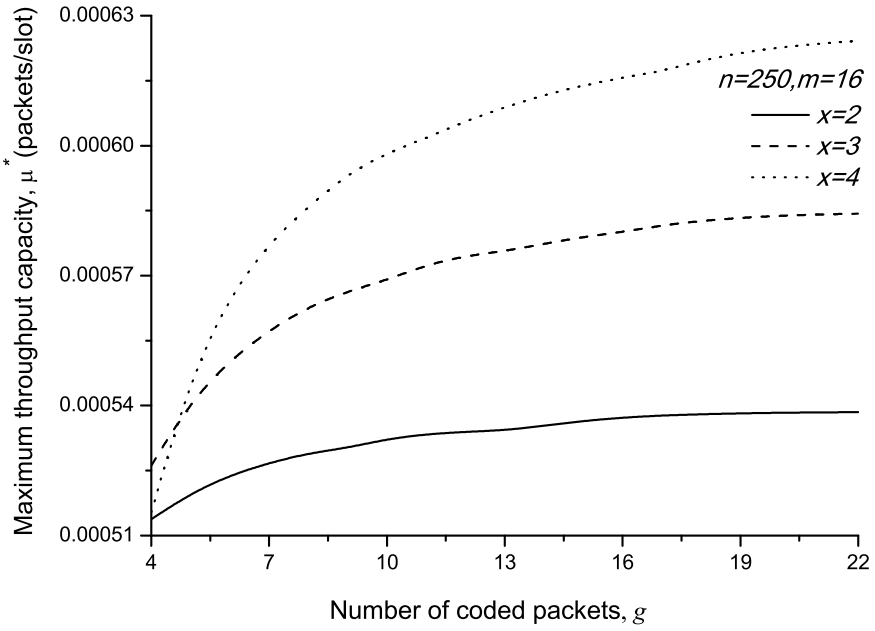

(a) The maximum throughput capacity μ^* vs. x

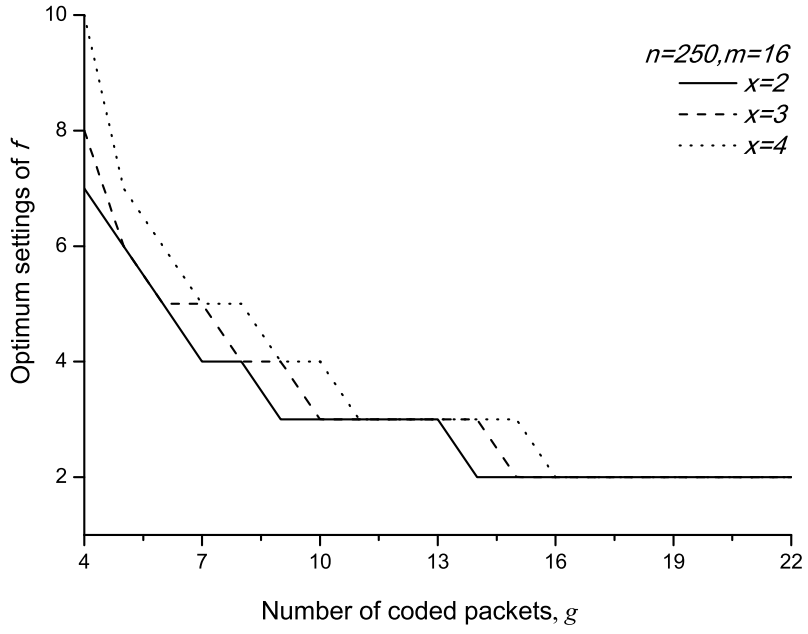

(b) The optimum setting of f vs. x

Figure 5-4: The maximum throughput capacity μ^* and the corresponding optimum setting of f.

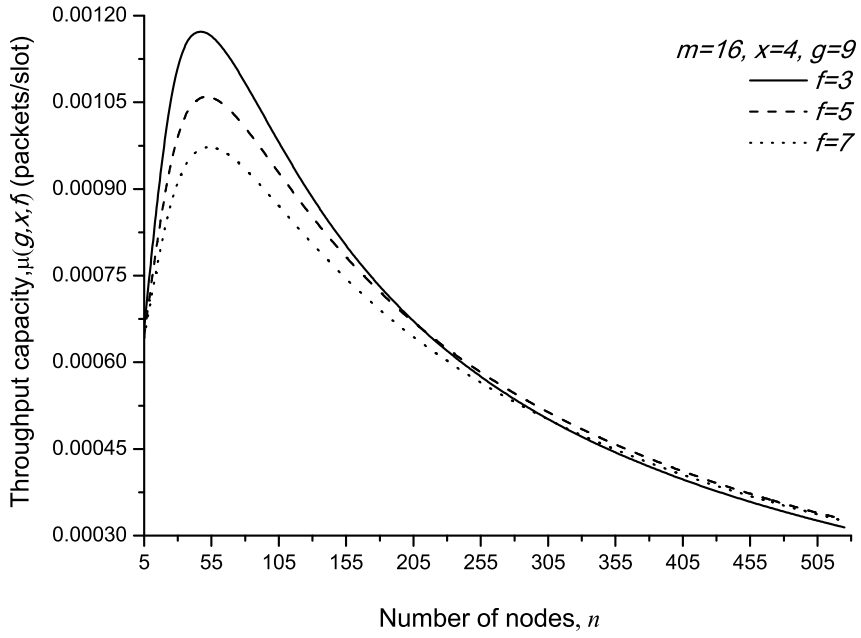

Figure 5-5: Throughput capacity $\mu(g, x, f)$ versus number of nodes n.

5.4 Summary

In this chapter, we investigated the per node throughput capacity of MANETs under the considered routing algorithm that combines erasure coding and packet redundancy techniques. Two absorbing Markov chain models were constructed to depict the fastest packet distributing/receiving processes at source and destination, respectively. With the help of the Markov chain models, an analytical expression of throughput capacity was derived. Extensive simulation illustrates that the analytical expression can accurately capture the throughput capacity under the routing routing. Numerical results show that for a given parameter g, we always find an optimal setting of packet redundancy f to maximize the throughput capacity. This phenomenon demonstrates that it can improve the throughput capacity by distributing proper copies of coded packets.

THIS PAGE INTENTIONALLY LEFT BLANK

Chapter 6

Multicast Delivery Delay Study for MANETs with f-cast Relay

The study of multicast delay performance in MANETs is critical for supporting future multicast-intensive applications in such networks. This chapter explores the exact multicast delay achievable in MANETs under a general multicast two-hop relay routing algorithm with packet redundancy f and multicast fanout z. In such an algorithm, each packet can be replicated up to f distinct relay nodes and it should be delivered to its z destination nodes through either its source node or these relay nodes. This chapter first develops a Markov chain-based theoretical framework to model the complicated packet delivery process under the multicast routing algorithm and then determines some basic probabilities related to packet delivery process. With the help of the theoretical framework and related basic packet delivery probabilities, the analytical models are further derived for both the mean value and variance of exact multicast delay.

6.1 System Assumptions and Performance Metric

In this section, we first introduce the traffic pattern, then present the considered multicast routing algorithm with packet redundancy technique and finally provide the definition of packet multicast delay involved in our study.

6.1.1 Traffic Pattern

We consider a multicast traffic pattern similar to that of [40, 68], where all nodes in the network are divided into different multicast groups, each of which consists of $z+1$ nodes [1] and in a specific muticast group, each node is a source node that transmits its packets to other z destination nodes within this multicast group, and is also a relay node that helps to forward packets from other multicast groups. We called a source node and its z destination nodes as a multicast session. Therefore, there are $z+1$ multicast sessions in a multicast group and n multicast sessions in the network. We assume that there are no constraints of nodes' buffer size and packet loss.

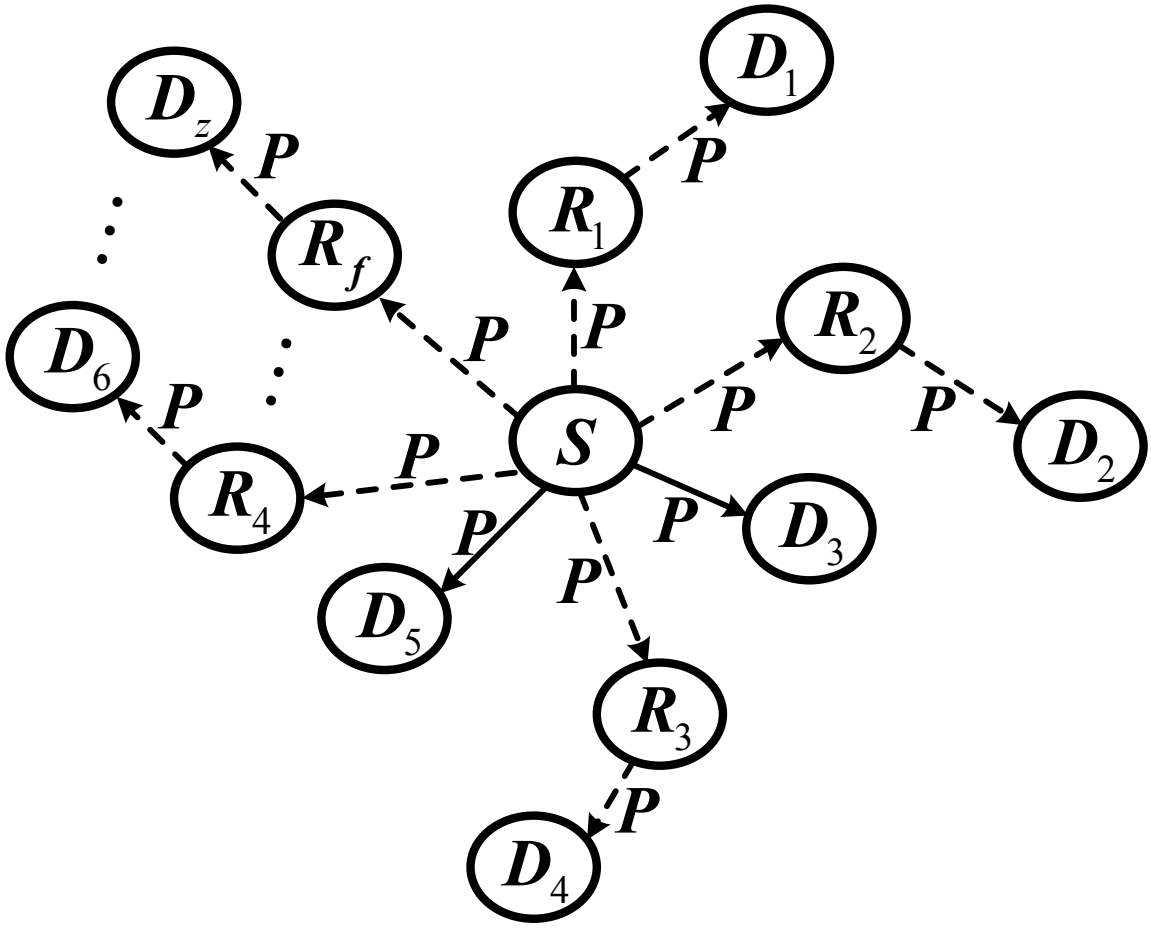

Figure 6-1: Illustration of the multicast routing algorithm.

[1] The number of nodes in the network is approximately equal to some integer multiple of $z+1$.

6.1.2 Performance Metric

Multicast Delay: For a packet at a source node, the multicast delay of the packet is defined as the time duration from the time slot when the source node starts to transmit the first copy of the packet to the time slot when all the z destination nodes have received the packet.

6.1.3 Multicast Routing Algorithm

Without loss of generality, we focus on a tagged multicast session of a multicast group and denote its source node and destination nodes as S and D_1, D_2,$\cdots$, D_z, respectively. As illustrated in Fig. 6-1, under the considered multicast routing algorithm, the source node will replicate a packet P to at most f distinct relay nodes (i.e., R_1, R_2,$\cdots$, R_f). Each of the destination nodes may receive the packet from either the source node or one of the relay nodes that carry this packet.

Notice that each node can be a potential relay for the $n-(z+1)$ multicast sessions of other multicast groups (except the mulitcast group including itself). To support the operation of the multicast routing algorithm, we assume that each node has $n-z+1$ individual queues in its buffer: One local-queue to store the locally generated packets waiting for their copies to be transmitted, one already-transmitted queue to store the packets whose f copies have already been transmitted to distinct relay nodes but this node has not confirmed that its z destination nodes have received the packet, and $n-(z+1)$ relay-queues to store the packets for the multicast sessions of other multicast groups (one queue per multicast session).

In each multicast session, each node, e.g., S, labels each packet in its local-queue with a *transmit number* and let $TN(S)$ denote the *transmit number* of the head-of-line packet. Similarly, each destination node, e.g., D_i $(1 \leq i \leq z)$, also holds a *request number* $RN(D_i)$ equal to the *transmit number* of the packet it is currently requesting, so that each packet will be received in order at the destination node D_i and D_i has already received all packets with *transmit numbers* less than $RN(D_i)$.

When S obtains a transmission opportunity via the transmission scheduling scheme,

it will perform the operation of the considered multicast routing algorithm summarized in Algorithm 4.

Algorithm 4 Multicast routing algorithm:

if there exists destination node(s) in the transmission range of S **then**
2. S conducts *source-to-destination* transmission (see Procedure 1);
else
4. S randomly selects a node R_i $(1 \leq i \leq n - (z + 1))$ from the nodes in its transmission range;
S flips a fair coin (i.e., the probability of head or tail is 1/2);
6. **if** it is the head **then**
S conducts *source-to-relay* transmission (see Procedure 2);
8. **else**
S conducts *relay-to-destination* transmission (see Procedure 3);
10. **end if**
end if

Procedure 1 Source-to-destination transmission:

S randomly selects a node D_i over all possible destination nodes in its transmission range;
2. S initiates a handshake with D_i to obtain the $RN(D_i)$;
if $TN(S) == RN(D_i)$ **then**
4. S transmits a copy of the packet with $TN(S)$ to D_i from its local-queue;
else if $TN(S) > RN(D_i)$ **then**
6. S transmits a copy of the packet with $RN(D_i)$ to D_i from its already-transmitted queue;
else
8. S transmits a copy of the packet with $RN(D_i)$ to D_i from its local-queue;
end if

Procedure 2 Source-to-relay transmission:

if R_i (as a relay) does not carry a copy of the head-of-line (HOL) packet in the local-queue of S **then**
2. S transmits a copy of the HOL packet to R_i;
if f copies of the HOL packet have been transmitted to distinct relay nodes **then**
4. S removes the HOL packet from its local-queue and then inserts it into the end of its already-transmitted queue;
end if
6. **else**
S remains idle;
8. **end if**

Procedure 3 Relay-to-destination transmission:

S initiates a handshake with R_i to obtain the $RN(R_i)$;
if there exists a packet with $RN(R_i)$ in its relay-queue **then**
    S transmits a copy of the packet to R_i;
else
    S remains idle;
end if

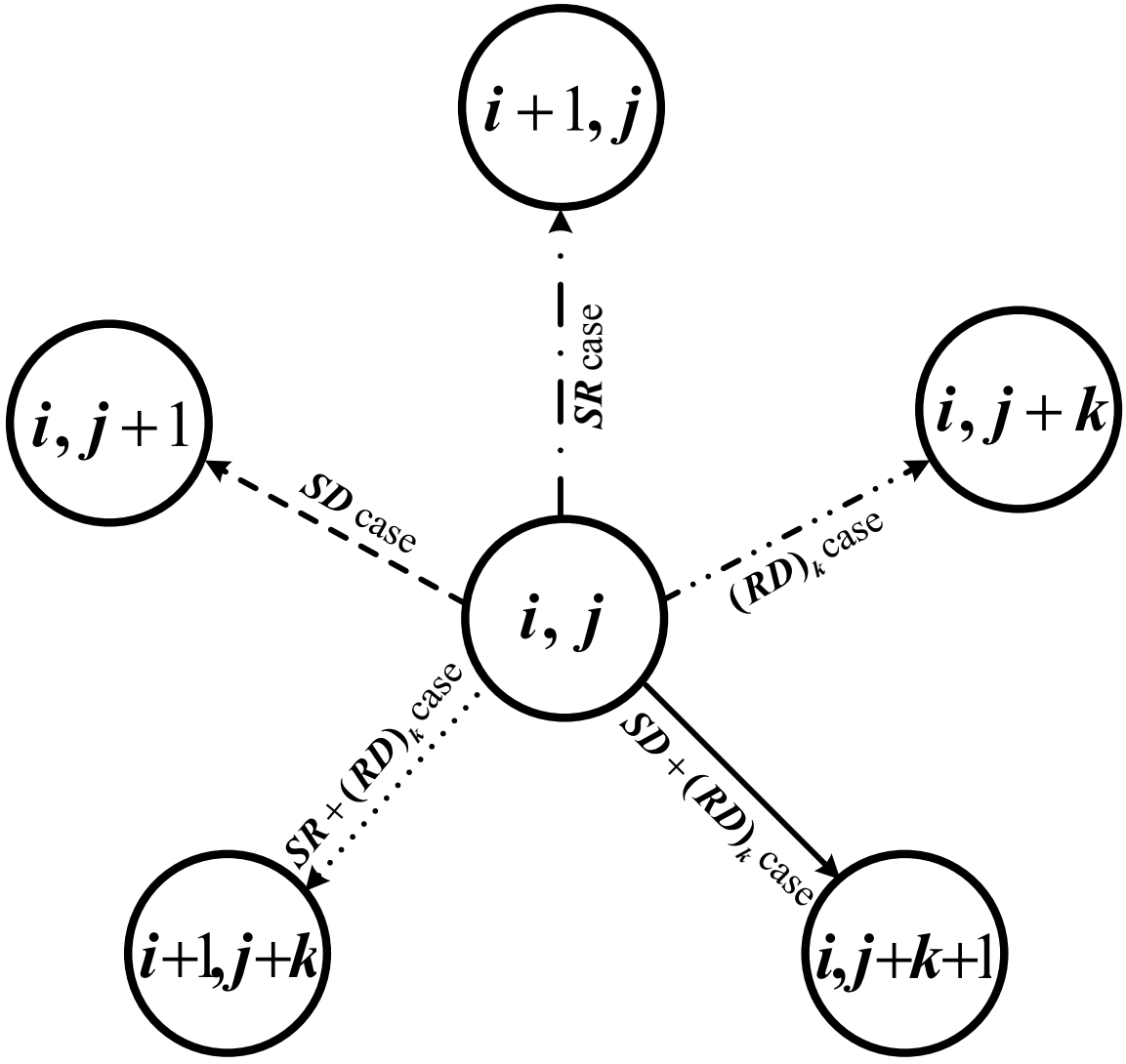

Figure 6-2: The transition diagram of a general transient state (i, j).

6.2 Markov Chain model

For a given packet associated with the tagged multicast session, we use a 2-tuple (i, j) to denote a general transient state during the packet delivery process, where the i $(0 \leq i \leq f)$ and j $(0 \leq j \leq z)$ denote the number of relay nodes that carry a copy of the packet and the number of destination nodes that have received the packet at current time slot, respectively.

According to the multicast routing algorithm, as illustrated in Fig. 6-2, when the considered multicast session is in state (i, j) at the current time slot, one of the following transition cases will happen:

- SD case: source-to-destination transmission only, i.e., S successfully transmits the packet to some destination node that does not receive it, while none of relay nodes transmits the packet to any of destination nodes. Under such a transition case, the state (i, j) will transit to $(i, j + 1)$.

- SR case: source-to-relay transmission only, i.e., S successfully transmits a copy to some relay node that does not carry it, while none of relay nodes transmits the packet to any of destination nodes. The state (i, j) will transit to $(i + 1, j)$ under the SR case.

- $(RD)_k$ case: k relay-to-destination transmissions only, i.e., k relay-to-destination transmissions happen simultaneously where each transmission represents that a relay node successfully transmits the packet to some destination node that does not receive it, while other transition cases such as SD and SR do not happen. Under the $(RD)_k$ case, the state (i, j) will transit to one element of state set $\{(i, j + k)$: $1 \leq k \leq i$ and $j + k \leq z\}$.

- SD+$(RD)_k$ case: a source-to-destination transmission and k relay-to-destination transmissions only, i.e., these $k + 1$ transmissions happen simultaneously, while the SR case does not happen. Under this transition case, the state (i, j) will transit to one element of state set $\{(i, j + k + 1)$: $1 \leq k \leq i$ and $j + k + 1 \leq z\}$.

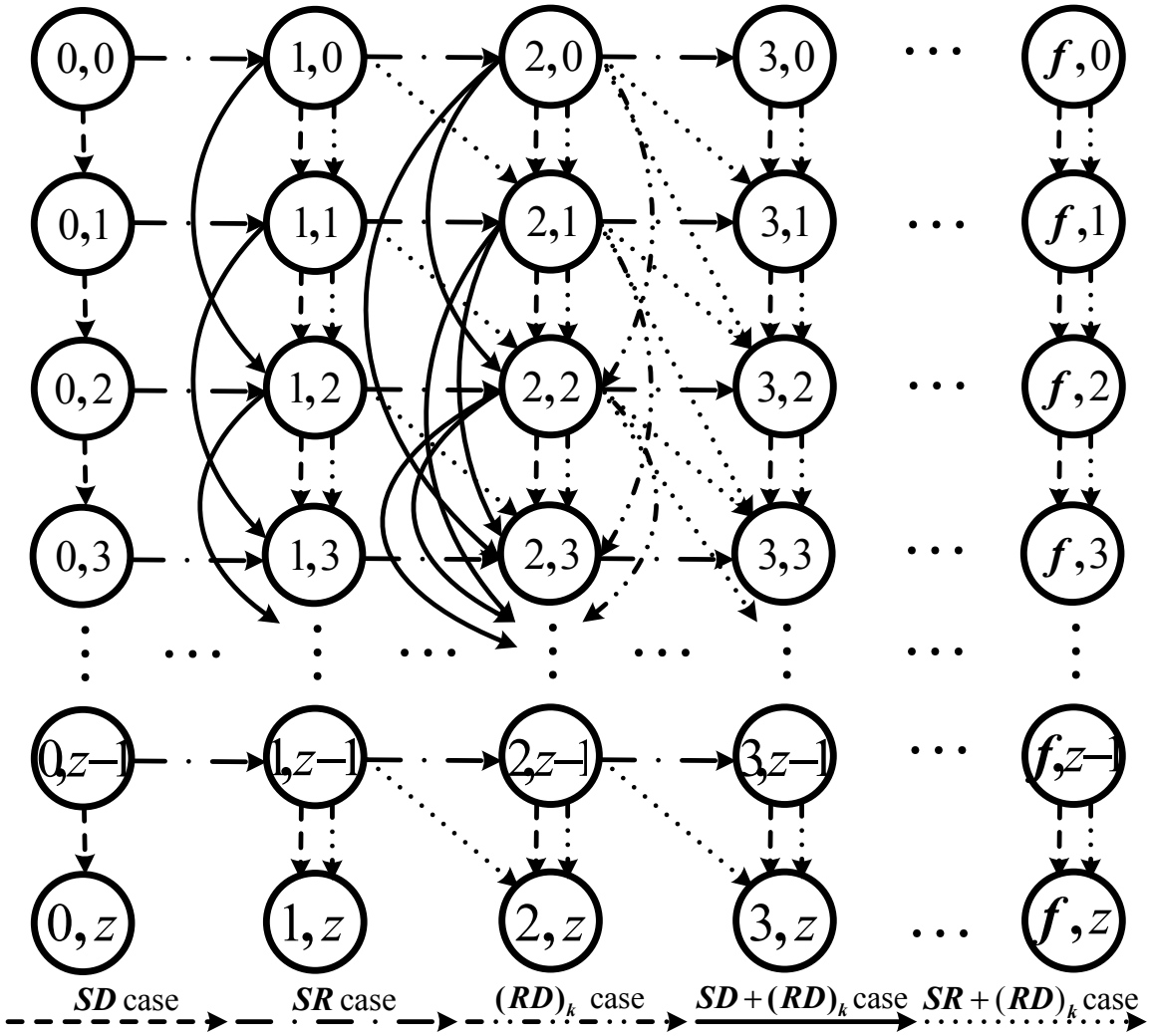

Figure 6-3: Absorbing Markov chain for the multicast routing algorithm. For simplicity, the transition back to itself is not shown for each transient state.

- $SR + (RD)_k$ case: a source-to-relay transmission and k relay-to-destination transmissions only, i.e., these $k+1$ transmissions happen simultaneously, while the SD case does not happen. Under such a transition case, the target state is one element of state set $\{(i+1, j+k)$: $1 \leq k \leq i$ and $j+k \leq z\}$.

If we use (i, z) to denote an absorbing state that each of the z destination nodes has received the packet when there are i relay nodes carrying a copy of the packet, then the transition diagram in Fig. 6-2 indicates that we can develop a discrete-time finite-state absorbing Markov chain illustrated in Fig. 6-3 to model the packet delivery process. The transitions of SD, SR, $(RD)_k$, $SD + (RD)_k$ and $SR + (RD)_k$ cases in

Fig. 6-3 correspond to the transmissions of source-to-destination, source-to-relay, k relay-to-destination, source-to-destination and k relay-to-destination, and source-to-relay and k relay-to-destination, respectively.

6.2.1 Basic Results

Based on the Markov chain framework in Fig. 6-3, we have the following results.

Lemma 3. *For a time slot and a tagged multicast session with source node S and z destination nodes, if we denote by p_2 the probability that S conducts a source-to-destination transmission, and denote by p_3 the probability that S conducts a source-to-relay transmission, then we have*

$$p_2 = \frac{1}{\alpha^2}\left(\sum_{k=1}^{z}\binom{z}{k}\left(\frac{1}{m^2}\right)^k\left(1-\frac{1}{m^2}\right)^{z-k}\cdot\sum_{i=0}^{n-z-1}\varphi(i)\right.$$
$$\left.\frac{1}{k+i+1}+\sum_{k=1}^{z}\binom{z}{k}\left(\frac{8}{m^2}\right)^k\left(1-\frac{9}{m^2}\right)^{z-k}\cdot\sum_{i=0}^{n-z-1}\varphi(i)\frac{1}{i+1}\right), \quad (6.1)$$

$$p_3 = \frac{1}{\alpha^2}\left(1-\frac{9}{m^2}\right)^z\left(\sum_{i=1}^{n-z-1}\binom{n-z-1}{i}\left(\frac{1}{m^2}\right)^i\right.$$
$$\left.\left(1-\frac{1}{m^2}\right)^{n-z-1-i}\frac{1}{i+1}+\sum_{i=1}^{n-z-1}\binom{n-z-1}{i}\left(\frac{8}{m^2}\right)^i\left(1-\frac{9}{m^2}\right)^{n-z-1-i}\right), \quad (6.2)$$

where $\varphi(i) = \binom{n-z-1}{i}(\frac{1}{m^2})^i(1-\frac{1}{m^2})^{n-z-1-i}$.

Lemma 4. *For a transient state (i,j) of the Markov chain framework in Fig. 6-3 $(0 \le i \le f,\ 0 \le j \le z-1)$ and a given packet, we use μ_1 to denote the number of destination nodes that do not receive the packet, use μ_2 to denote the number of relay nodes that carry a copy of the packet, and use μ_3 to denote the number of relay nodes*

that do not carry a copy of the packet under the transient state. Then we have

$$\mu_1 = z - j, \tag{6.3}$$

$$\mu_2 = i, \tag{6.4}$$

$$\mu_3 = n - z - 1 - i. \tag{6.5}$$

In current time slot, suppose that the Markov chain in Fig. 6-3 is in the transient state (i, j), then we establish the following Lemmas.

Lemma 5. *For the next time slot, we use $P_{SD}(\mu_1)$ to denote the probability that S will successfully deliver a copy of the packet to a destination node (i.e., a successful source-to-destination transmission), use $P_{SR}(\mu_3)$ to denote the probability that S will successfully deliver a copy of the packet to a relay node (i.e., a successful relay-to-destination transmission). Then we have*

$$P_{SD}(\mu_1) = \frac{\mu_1}{z} p_2, \tag{6.6}$$

$$P_{SR}(\mu_3) = \frac{\mu_3}{2(n-z-1)} p_3. \tag{6.7}$$

Lemma 6. *For a tagged multicast session and a given packet, we use $P_{RD}(x, \mu_1, \mu_2)$ to denote the probability that x successful relay-to-destination transmissions will occur simultaneously in the next time slot, where $1 \leq x \leq \min\{\mu_1, \mu_2\}$. The probability $P_{RD}(x, \mu_1, \mu_2)$ can be determined as*

$$P_{RD}(x, \mu_1, \mu_2) = \binom{\mu_2}{x} \frac{\binom{\mu_1}{x}}{\binom{z}{x}} \lambda_1 \lambda_2 \cdots \lambda_i \cdots \lambda_x, \tag{6.8}$$

where

$$\lambda_i = \begin{cases} \frac{m^2 - \alpha^2(i-1)}{2\alpha^2 m^2} \sum\limits_{k_i=0}^{l_i} \binom{l_i}{k_i} \sum\limits_{h_i=1}^{w_i} \binom{w_i}{h_i} \psi(k_i, h_i), & \text{if } 1 \leq i \leq x-1, \\ \frac{m^2 - \alpha^2(i-1)}{2\alpha^2 m^2} \sum\limits_{k_i=0}^{l_i} \binom{l_i}{k_i} \sum\limits_{h_i=1}^{w_i} \binom{w_i}{h_i} \psi(k_i, h_i)(1 - \frac{9x}{m^2})^{\nu}, & \text{if } i = x. \end{cases} \tag{6.9}$$

Here, $l_i = n-2z-x-\sum_{j=1}^{i} k_{j-1}$, $k_0 = 0$, $w_i = z-\sum_{j=1}^{i} h_{j-1}$, $h_0 = 0$, $\nu = n-x-\sum_{j=1}^{x}(k_j+h_j)$ *and* $\psi(k_i,h_i) = \sum_{k=0}^{k_i}\binom{k_i}{k}\sum_{h=0}^{h_i}\binom{h_i}{h}(\frac{1}{m^2})^{k+h}(\frac{8}{m^2})^{k_i+h_i-k-h}\frac{1}{k+h+1}\frac{h_i}{k_i+h_i}$.

Lemma 7. *For a tagged multicast session and a given packet, we use* $P_{SD,RD}\,(x,\mu_1,\mu_2)$ *to denote the probability that a successful source-to-destination transmission and* x *successful relay-to-destination transmissions will occur simultaneously in the next time slot, where* $1 \le x \le \min\{\mu_1-1,\mu_2\}$. *Then we have*

$$P_{SD,RD}(x,\mu_1,\mu_2) = \binom{\mu_2}{x}\frac{\binom{\mu_1}{x+1}}{\binom{z}{x+1}}\rho_1\rho_2\cdots\rho_i\cdots\rho_{x+1}, \tag{6.10}$$

where

$$\rho_i = \begin{cases} \frac{m^2-\alpha^2(i-1)}{2\alpha^2m^2}\sum_{k_i=0}^{l_i-1}\binom{l_i-1}{k_i}\sum_{h_i=1}^{w_i}\binom{w_i}{h_i}\psi(k_i,h_i), & \text{if } 1\le i\le x,\\ \frac{m^2-\alpha^2(i-1)}{\alpha^2m^2}\sum_{k_i=0}^{l_i+z-1}\binom{l_i+z-1}{k_i}\sum_{h_i=1}^{w_i-h_{i-1}}\binom{w_i-h_{i-1}}{h_i}\psi(k_i,h_i) & \\ \cdot\frac{k_i+h_i}{h_i}(1-\frac{9(x+1)}{m^2})^{\nu-k_i-h_i-1}, & \text{if } i=x+1. \end{cases} \tag{6.11}$$

Here, l_i, w_i z *and* $\psi(k_i,h_i)$ *are defined after* (6.9).

Lemma 8. *For a tagged multicast session and a given packet, we use* $P_{SR,RD}\,(x,\mu_1,\mu_2,\mu_3)$ *to denote the probability that a successful source-to-relay transmission and* x *successful relay-to-destination transmissions will occur simultaneously in the next time slot, where* $1 \le x \le \min\{\mu_1,\mu_2\}$. *Then we have*

$$P_{SR,RD}(x,\mu_1,\mu_2,\mu_3) = \binom{\mu_2}{x}\frac{\mu_3\binom{\mu_1}{x}}{\binom{z}{x}}\theta_1\theta_2\cdots\theta_i\cdots\theta_{x+1}, \tag{6.12}$$

where

$$\theta_i = \begin{cases} \frac{m^2-\alpha^2(i-1)}{2\alpha^2m^2}\sum_{k_i=0}^{l_i-2}\binom{l_i-2}{k_i}\sum_{h_i=1}^{w_i}\binom{w_i}{h_i}\psi(k_i,h_i), & \text{if } 1\le i\le x,\\ \frac{m^2-\alpha^2(i-1)}{2\alpha^2m^2}\sum_{k_i=0}^{l_i+z-2}\binom{l_i+z-2}{k_i}\sum_{k=0}^{k_i}\binom{k_i}{k}\sum_{r=0}^{1}\binom{1}{r}(\frac{1}{m^2})^{k+r}(\frac{8}{m^2})^{k_i+1-k-r} & \\ \cdot\frac{1}{k+r+1}\frac{1}{k_i+1}(1-\frac{9(x+1)}{m^2})^{\nu-k_i-2}, & \text{if } i=x+1. \end{cases} \tag{6.13}$$

Here, l_i, w_i z *and* $\psi(k_i,h_i)$ *are defined after* (6.9).

The basic idea of the proof of Lemma 6 is summarized as follows. For x relay nodes carrying a copy of the packet of the tagged multicast session, we first show how the probability $P_{RD}(x,\, \mu_1, \mu_2)$ is related to the probability that these x relay nodes conduct x relay-to-destination transmissions simultaneously. Then the probability is derived as the product of the probabilities that one of these x relay nodes conducts a relay-to-destination transmission, which is determined based on the probabilities of its sub-events. Finally, by summarizing these results, $P_{RD}(x,\, \mu_1, \mu_2)$ can be derived. The derivations of Lemmas 7 and 8 are similar to that of Lemma 6. The detailed proofs of these Lemmas can be found in Appendix A.

6.3 Packet Multicast Delay Modeling

In this section, we analyze both expected value and variance of packet multicast delay under the multicast algorithm.

6.3.1 Expected Packet Multicast Delay

For the Markov chain in Fig. 6-3, we use β to denote the total number of transient states, which can be determined as $\beta = z(f+1)$. These β transient states are arranged into z rows and indexed as 1, 2, $\cdots$, β in a left-to-right and top-to-down fashion. Similarly, the $f+1$ absorbing states are indexed as $\beta+1$, $\beta+2$, $\cdots$, $\beta+f+1$ in a left-to-right fashion.

Let t_i denote the time that the Markov chain in Fig. 6-3 takes to arrive at an absorbing state given that the chain starts from the ith transient state ($1 \leq i \leq \beta$). It is notable that the 1st transient state $(0, 0)$ indicates that the source node starts to transmit the first copy of the packet, and an absorbing state corresponds to that all the z destination nodes have received the packet. Thus, the expectation $E[t_1]$ just corresponds to the expected packet multicast delay under the multicast routing algorithm.

To derive $E[t_1]$, we first determine the vector $\mathbf{t} = (E[t_1], E[t_2], \cdots, E[t_\beta])^T$. We define a matrix $\mathbf{P} = (q_{i,j})_{(\beta+f+1)\times(\beta+f+1)}$ and its submatrix $\mathbf{Q}$ which consists of rows

1 through β and columns 1 through β of $\mathbf{P}$, where the ij-entry $q_{i,j}$ of $\mathbf{P}$ denotes the transition probability from the ith state to the jth state in Fig. 6-3 ($1 \leq i, j \leq \beta + f + 1$). Based on the definition of t_i, we have

$$E[t_i] = \sum_{j=1}^{\beta+f+1} q_{i,j}(1 + E[t_j]) = 1 + \sum_{j=1}^{\beta} q_{ij} E[t_j]. \tag{6.14}$$

Notice that since the jth state is an absorbing state when $\beta + 1 \leq j \leq \beta + f + 1$, we have $E[t_j] = 0$.

Then, (6.14) can be expressed as

$$\mathbf{t} = \mathbf{b} + \mathbf{Q} \cdot \mathbf{t} \tag{6.15}$$

where $\mathbf{b}$ is the $\beta \times 1$ column vector with all entries being 1, i.e., $\mathbf{b} = \{1, 1, \cdots, 1\}^T$. Thus, we have

$$\mathbf{t} = \mathbf{(I\text{-}Q)}^{-1} \cdot \mathbf{b} \tag{6.16}$$

where $\mathbf{I}$ is a $\beta \times \beta$ identity matrix.

We use $\mathbf{N} = (\mathbf{N}_{i,j})_{\beta \times \beta}$ to denote the fundamental matrix of the Markov chain in Fig. 6-3 ($1 \leq i, j \leq \beta$). According to the Markov chain theory [65], we have

$$\mathbf{N} = \mathbf{(I\text{-}Q)}^{-1}. \tag{6.17}$$

By substituting (6.17) into (6.16), we have

$$\mathbf{t} = \mathbf{N} \cdot \mathbf{b}. \tag{6.18}$$

From (6.18), the expected packet multicast delay $E[t_1]$ is determined as

$$E[t_1] = \sum_{j=1}^{\beta} N_{1,j}. \tag{6.19}$$

6.3.2 Delay Variance

The variance $\mathrm{Var}[t_1]$ of packet multicast delay is given by

$$\mathrm{Var}[t_1] = E[t_1^2] - (E[t_1])^2. \tag{6.20}$$

Since the $E[t_1]$ can be determined by (6.19), we only need to derived the $E[t_1^2]$ here. Based on the definition of t_i, we have

$$E[t_i^2] = \sum_{j=1}^{\beta+f+1} q_{i,j} E[(1+t_j)^2] = \sum_{j=1}^{\beta} q_{i,j} E[t_j^2] + 2\sum_{j=1}^{\beta} q_{i,j} E[t_j] + 1 \tag{6.21}$$

Since the jth state is an absorbing state when $\beta+1 \leq j \leq \beta+f+1$, we have $E[t_j] = 0$ and $E[t_j^2] = 0$.

Let $\mathbf{t}^* = (t_1^2, t_2^2, \cdots, t_\beta^2)^T$, then we can rewritten (6.21) as

$$\mathbf{t}^* = \mathbf{Q} \cdot \mathbf{t}^* + 2\mathbf{Q} \cdot \mathbf{t} + \mathbf{b}. \tag{6.22}$$

Substituting (6.18) into (6.22), we have

$$\mathbf{t}^* = \mathbf{N}(2\mathbf{Q} \cdot \mathbf{N} + \mathbf{I})\mathbf{b}. \tag{6.23}$$

Then $E[t_1^2]$ can be determined as

$$E[t_1^2] = \mathbf{e} \cdot \mathbf{t}^*. \tag{6.24}$$

where $\mathbf{e} = (1, 0, \cdots, 0)$.

To calculate the values of both $E[t_1]$ and $\mathrm{Var}[t_1]$, we only need to derive the matrix $\mathbf{Q}$.

6.3.3 Derivation of Matrix Q

Recall that the entry $q_{c,d}$ of $\mathbf{Q}$ represents the transition probability from the cth transient state to the dth transient state in the Markov chain of Fig. 6-3 ($1 \leq c, d \leq \beta$). Suppose that the cth transient state is the transient state (i, j), where $0 \leq i \leq f$ and $0 \leq j \leq z$. Based on the Markov chain structure and some related basic results derived in Subsection 6.2.1, we can calculate non-zero $q_{c,d}$ as follows.

When (i, j) transits to $(i + 1, j)$,

$$q_{c,c+1} = P_{SR}(\mu_3), \text{ if } c \bmod (f+1) \neq 0 \text{ (i.e., } i \,!= \, f). \tag{6.25}$$

When (i, j) transits to $(i, j + 1)$,

$$q_{c,c+f+1} = \begin{cases} P_{SD}(\mu_1), \text{ if } c - (f+1)\lfloor \frac{c}{f+1} \rfloor = 1 \text{ (i.e., } i \, = \, 0), \\ P_{SD}(\mu_1) + P_{RD}(1, \mu_1, \mu_2), \text{ otherwise,} \end{cases} \tag{6.26}$$

where $\lfloor \theta \rfloor$ is the largest integer not greater than θ.

When (i, j) transits to $(i, j + k)$,

$$\begin{aligned} &q_{c,c+k(f+1)} = P_{SD,RD}(k-1, \mu_1, \mu_2) + P_{RD}(k, \mu_1, \mu_2), \\ &\text{if } 2 \leq k \leq \min\{\mu_1, \mu_2\} \text{ and } c - (f+1)\lfloor \frac{c}{f+1} \rfloor \neq 1. \end{aligned} \tag{6.27}$$

When (i, j) transits to $(i + 1, j + k)$,

$$\begin{aligned} &q_{c,c+1+k(f+1)} = P_{SR,RD}(k, \mu_1, \mu_2, \mu_3), \text{ if } 1 \leq k \leq \min\{\mu_1, \mu_2\}, \\ &c - (f+1)\lfloor \frac{c}{f+1} \rfloor \neq 1 \text{ and } c \bmod (f+1) \neq 0. \end{aligned} \tag{6.28}$$

When (i, j) transits to itself,

$$q_{c,c} = \begin{cases} 1 - P_{SD}(\mu_1) - P_{SR}(\mu_3), & \text{if } c - (f+1)\left\lfloor \frac{c}{f+1} \right\rfloor = 1, \\ 1 - P_{SD}(\mu_1) - \sum_{k=1}^{\min\{\mu_1,\mu_2\}} P_{RD}(k, \mu_1, \mu_2) & \\ - \sum_{k=1}^{\min\{\mu_1-1,\mu_2\}} P_{SD,RD}(k, \mu_1, \mu_2), & \text{if } c \bmod (f+1) = 0, \\ 1 - P_{SD}(\mu_1) - P_{SR}(\mu_3) - \sum_{k=1}^{\min\{\mu_1,\mu_2\}} P_{RD}(k, \mu_1, \mu_2) & \\ - \sum_{k=1}^{\min\{\mu_1-1,\mu_2\}} P_{SD,RD}(k, \mu_1, \mu_2) - \sum_{k=1}^{\min\{\mu_1,\mu_2\}} P_{SR,RD}(k, \mu_1, \mu_2, \mu_3), & \text{otherwise.} \end{cases} \tag{6.29}$$

6.4 Numerical Results

In this section, we first provide simulation results to validate the accuracy of the analytical multicast delay models, and then apply the theoretical results to explore how the system parameters would affect the packet multicast delay performance in the considered MANETs.

6.4.1 Simulator Setting

A simulator was developed to simulate the packet delivery process under the multicast routing algorithm and the system models considered in this chapter. In addition to the i.i.d mobility model, we also implemented the random walk model [50] and random waypoint model [35].

We denote $\bar{y}$ as the expected multicast delay obtained from simulation, where is calculated as the average value of 10^7 random and independent simulation results. We denote s as the related sample standard deviation, which is calculated as

$$s = \sqrt{\frac{1}{10^7 - 1} \sum_{i=1}^{10^7} (y_i - \bar{y})^2}, \tag{6.30}$$

where y_i is the multicast delay in the ith simulation.

The simulated relative standard deviation δ is then obtained according to the following formula:

$$\delta = \frac{s}{\bar{y}}. \tag{6.31}$$

6.4.2 Model Validation

To validate the accuracy of multicast delay analysis, we conduct simulations for a network scenario with $n = 100$, $m = 16$, $f = 4$, $\Delta = 1$ and different values of z [2]. The corresponding simulation results and the theoretical ones are summarized in Fig. 6-4, where each simulation result of relative standard deviation δ is obtained from (6.31) and each theoretical one of δ is calculated as

$$\delta = \frac{\sqrt{Var[t_1]}}{E[t_1]}. \tag{6.32}$$

Fig. 6-4 indicates clearly that the simulation results under the i.i.d mobility model agree very well with the theoretical ones, indicating that our theoretical results can accurately capture the multicast delay performance under the M2HR-(f, z) algorithm. Notice that these results of $z = 1$ are the same as those under unicast traffic pattern. We can also see from Fig. 6-4(a) that as the number of destination nodes z increases, the multicast delay $E[t_1]$ will increase. This is because for the network scenario there, the time that all z destination nodes take to receive an identical packet, will increase with z, so the multicast delay of the packet will increase. On the other hand, we can see that the increase of z leads to the decrease of the corresponding relative standard deviation δ in Fig. 6-4(b).

It is notable that in Figs. 6-4(a) and 6-4(b), the simulation results under the random walk model show very similar multicast delay behaviors with the theoretical results under the i.i.d. mobility model. While those under the random waypoint model are slightly different from those under the i.i.d. mobility model, but they well

[2]Since Δ is set as 1, the transmission-group parameter α is determined as $\alpha = \min\{8, m\}$ according to the following formula defined in (3.3): $\alpha = \min\{\lceil (1+\Delta)\sqrt{8} \rceil + 2, m\}$.

approximate the general trends of $E[t_1]$ and δ.

6.4.3 Performance Analysis

Based on our theoretical results, we first explore the impact of f on the performance $(E[t_1], \delta)$. For the network scenarios of $n = \{50, 300, 600\}$ and setting of $m = 16$, $z = 4$ and $\Delta = 1$, we summarize in Fig. 6-5 how $E[t_1]$ and δ vary with f. It can be observed from Fig. 6-5 that as f increases, both $E[t_1]$ and δ monotonously decrease. This is mainly due to that the number of relay nodes that carry a copy of an identical packet increases with f, which leads to more opportunities that the destination nodes receive the packet from the relay nodes, and thus a lower multicast delay. The result in Fig. 6-5 indicates that the packet redundancy technique could efficiently support these important applications with stringent multicast delay/variance requirements in future MANETs, such as military communication, emergency disaster relief, real-time monitoring and video streaming.

To understand the impact of n on the performance $(E[t_1], \delta)$, we summarize in Fig. 6-6 how $E[t_1]$ and δ vary with network setting of $m = \{16, 24, 32\}$, $f = 5$, $z = 4$ and $\Delta = 1$. We can see from Fig. 6-6 that as n increases, both $E[t_1]$ and δ first decrease and then increase, and there exists an optimal value of n to achieve the minimum $E[t_1]$ or δ. This is because the effects of n on the performance are two folds. On one hand, when the network is sparse, a bigger n will result in a higher packet delivery speed at which a packet is distributed, and thus a lower multicast delay. On the other hand, when the network becomes relatively crowded, a bigger n will result in a lower packet delivery speed due to the negative effects of wireless interference and medium access contention issues, and thus a higher multicast delay. Another observation from Fig. 6-6 is for each fixed setting of n, a larger value of m leads to a higher $E[t_1]$. This observation can be explained as follows. Recall that in our study, the considered network area is evenly divided into $m \times m$ cells of equal size. Under the same setting of n, a larger value of m leads to a lower node density (i.e., n/m^2) and thus a more sparse network. Since the packet delivery speed becomes lower in a more sparse network, the multicast delay becomes higher for a larger m.

The results in Fig. 6-7 summarize how $E[t_1]$ and δ vary with Δ. We can see from Fig. 6-7(a) that for each setting of z there, $E[t_1]$ is a piecewise function of Δ, and as Δ increases, $E[t_1]$ monotonically increases and there exists a threshold value of Δ, beyond which $E[t_1]$ will converge to a constant value. This can be explained as follows. When Δ is relatively small, we can see from the formula (3.3) that increasing Δ will increase the number of transmission-groups (i.e., α^2) and will also decrease the number of cells (i.e., m^2/α^2) in each transmission-group. This will lead to a decrease in the transmission opportunity of each node and thus a higher multicast delay. A careful observation from the formula (3.3) that both the numbers of transmission-groups and cells in each transmission-group remain unchanged for a small range of Δ, which will lead to a constant value of $E[t_1]$ in the small range of Δ. Thus, $E[t_1]$ is a piecewise function of Δ. When Δ further increases such that $\alpha^2 = m^2$, the number of cells in each transmission-group achieves a minimal value 1 and remains unchanged, thus $E[t_1]$ converges to a maximal constant value. Interestingly, Fig. 6-7(b) illustrates that for each setting of z, δ remains unchanged as Δ increases.

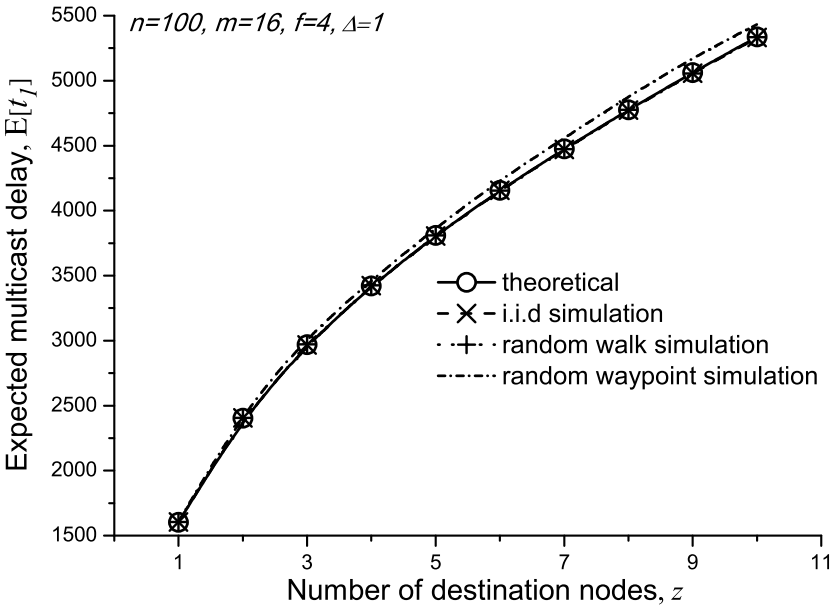

(a) Expected multicast delay $E[t_1]$ vs. number of destination nodes z

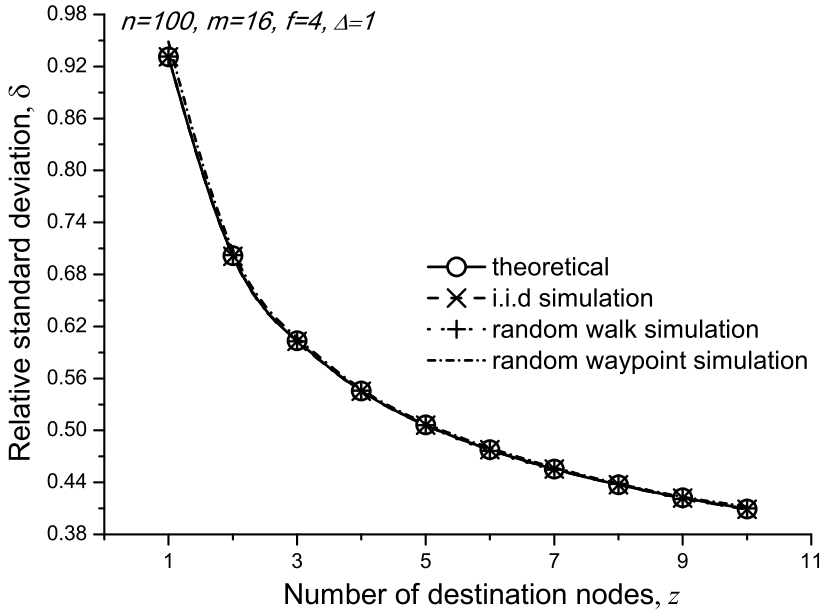

(b) Relative standard deviation δ vs. number of destination nodes z

Figure 6-4: Model validation through comparison between theoretical and simulation results

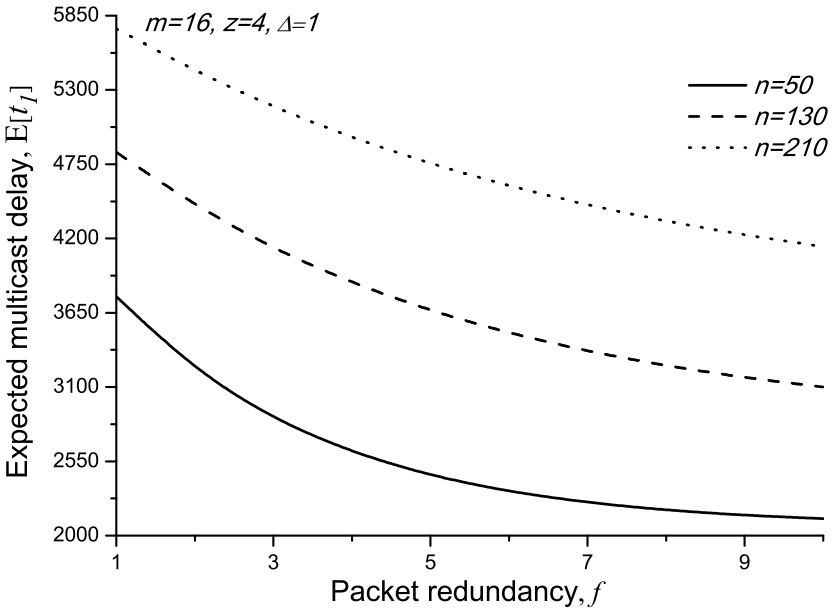

(a) $E[t_1]$ vs. f

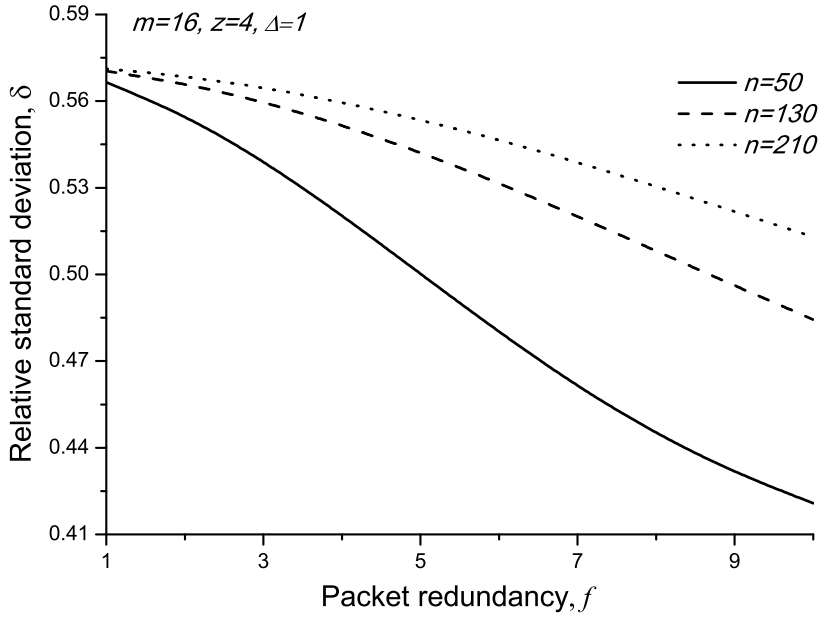

(b) δ vs. f

Figure 6-5: Multicast delay vs. packet redundancy f

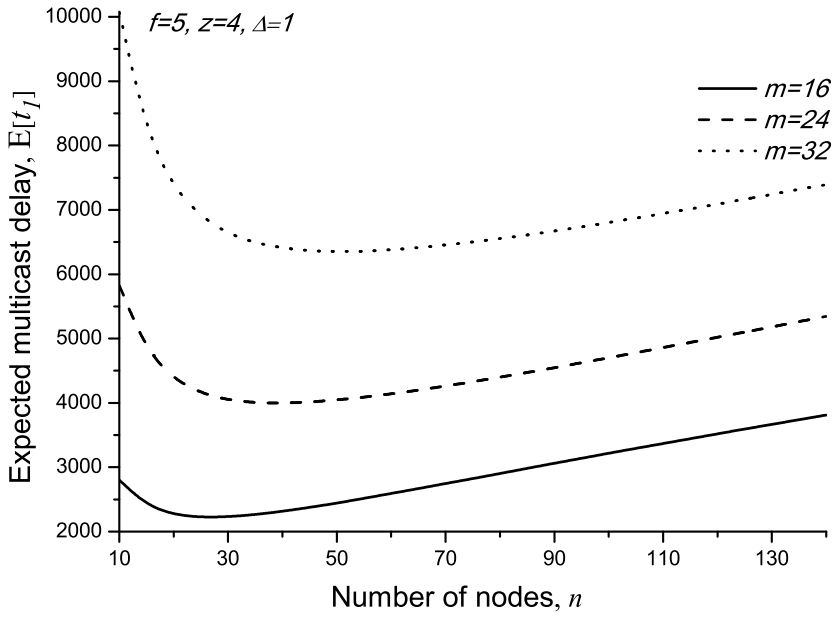

(a) $E[t_1]$ vs. n

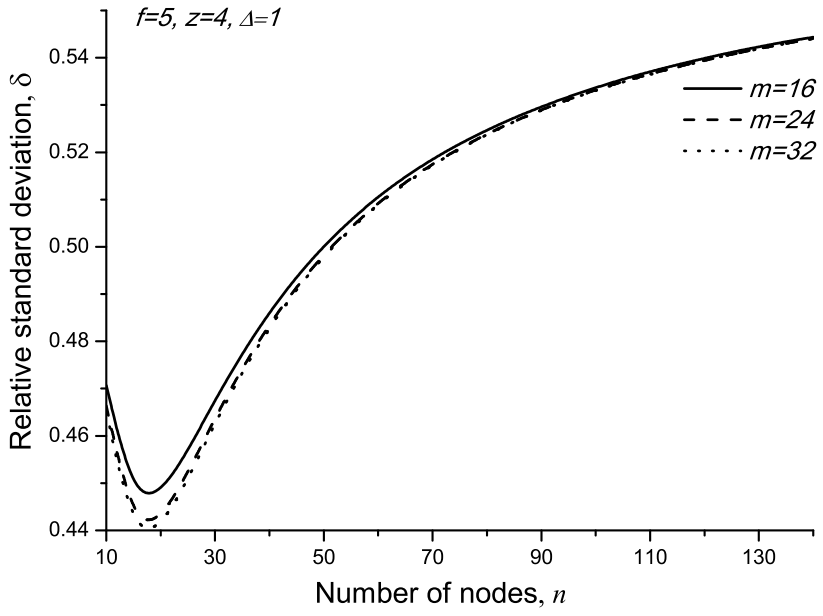

(b) δ vs. n

Figure 6-6: Multicast delay vs. number of nodes n

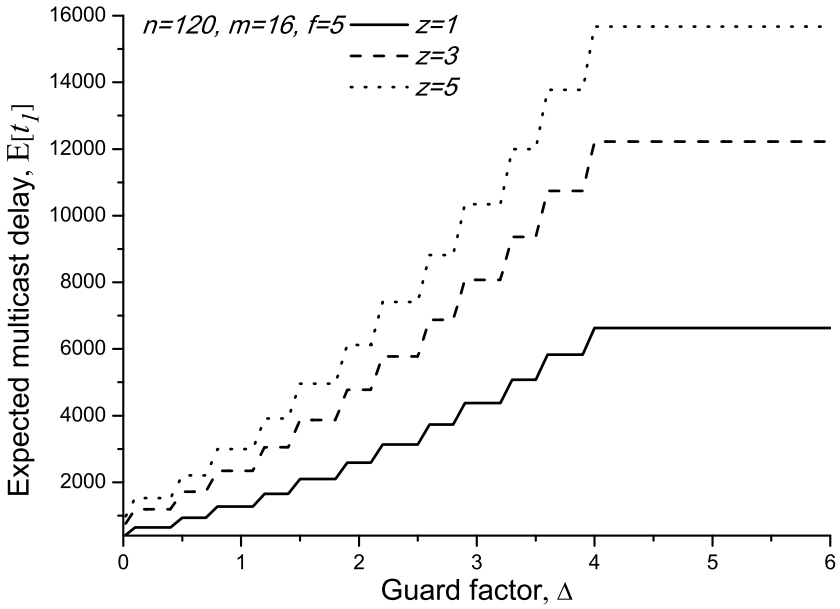

(a) $E[t_1]$ vs. Δ

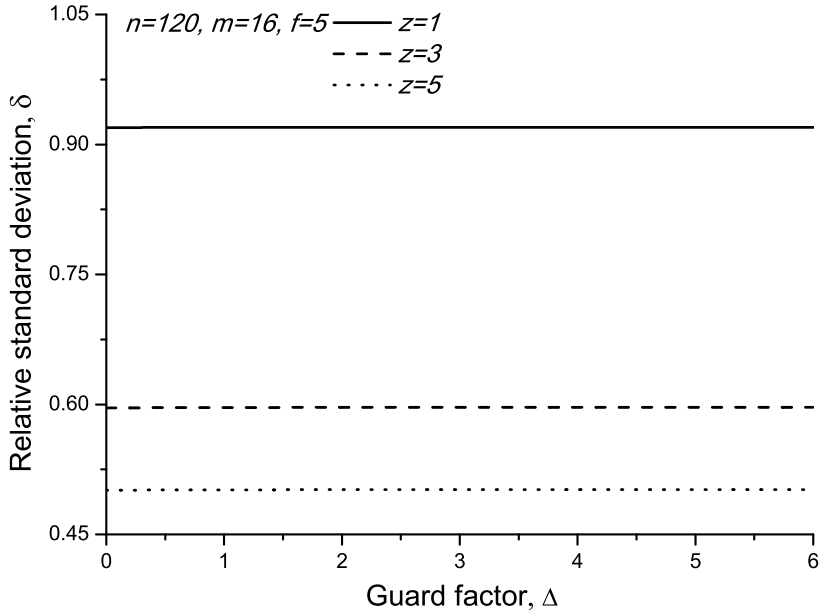

(b) δ vs. Δ

Figure 6-7: Multicast delay vs. guard factor Δ

6.5 Summary

In this chapter, we derived the analytical models for both the mean and variance of the exact multicast delay in a general MANET where the interference and medium access control are taken into account. Extensive simulations show that our theoretical framework can efficiently capture the packet delivery process and thus accurately predicts the packet multicast delay/variance performance. Our results indicate that packet redundancy technique can remarkably decrease packet multicast delay and variance, which provides an efficient support for these critical applications with stringent multicast delay/variance requirements in future MANETs. It is expected that our study will help network designers to determine a suitable network size, so as to minimize the packet multicast delay and variance while simultaneously meet a given multicast delay/variance performance requirement.

THIS PAGE INTENTIONALLY LEFT BLANK

Chapter 7

Conclusion

This chapter summarizes our contributions and points out future research directions.

7.1 Summary of the Thesis

This work focuses on the performance studies of an important class of MANETs with erasure coding and packet redundancy. The main contributions are summarized as follows.

- By combining erasure coding and packet redundancy techniques, we first introduced a general two-hop relay routing algorithm for the study of packet delivery delay performance in MANETs under unicast traffic pattern. We then developed a Markov chain-based theoretical framework to model packet delivery process under the routing algorithm. With the help of the theoretical framework, we further derived the analytical expressions for the mean and variance of packet delivery delay. Based on the packet delivery delay models, we finally demonstrated that a flexible trade-off between expected delivery delay and delay variance can be obtained through a proper setting of coding group size x, replication factor τ and packet redundancy f. It is expected that our delay performance study can facilitate various applications with different delay/delay variance requirements in future MANETs.

- We next investigated the throughput capacity of MANETs under the above routing algorithm with unicast traffic pattern. We developed two absorbing Markov chain models to depict the fastest packet distributing/receiving processes at source and destination, respectively. Based on these two Markov chain models, we further derived an analytical expression for throughput capacity. Theoretical results of throughput capacity showed that for each fixed setting of coded packet group size g, we always find an optimal setting of packet redundancy f to maximize the throughput capacity. This phenomenon demonstrates that the throughput capacity performance can be increased by distributing proper copies of coded packets.

- We finally studied packet delivery delay performance in MANETs under a two-hop relay routing algorithm with multicast traffic pattern. We developed a Markov chain-based theoretical framework to model packet delivery process under the routing algorithm, based on which we then derived the analytical expressions for both the mean and variance of multicast delay in MANETs where the interference and medium access control are taken into account. Theoretical results indicated that packet redundancy technique can remarkably decrease packet multicast delay and delay variance. It is expected that our study can provide an efficient support for these critical applications with stringent multicast delay/variance requirements in future MANETs.

7.2 Future Work

We summarize the future interesting directions as follows.

- In this thesis, we consider a simple scenario, where each relay node randomly selects a node as its receiver from its neighbor nodes, which may cause a waste of the transmission opportunity if the relay node does not carry coded packet for the receiver. Therefore, one interesting future direction is to further explore the performance of MANETs under a more flexible scenario, where each relay

node can select its receiver from the neighbor nodes for which it carries coded packets.

- We developed Markov chain-based theoretical frameworks to explore packet delivery performance in cell-partitioned MANETs, and it will be interesting direction to study how to evaluate the performance under our theoretical frameworks in other network scenarios, such as delay tolerant networks (DTNs) [28] and ALOHA networks [69].

- It is notable that our studies in this thesis focused on two-hop relay mobile ad hoc networks. Another interesting direction is to further extend the developed theoretical models to analyze packet delivery performance in multi-hop relay mobile ad hoc networks. It is also interesting to explore the packet delivery performance with constraints of nodes buffer size and packet loss in our future research.

THIS PAGE INTENTIONALLY LEFT BLANK

Appendix A

Proofs of the Lemmas 3-8

Proof of Lemma 3: We first derive p_2. For the tagged multicast session with source node S and z destination nodes, at a time slot, S can conduct a source-to-destination transmission iff the following four events occur: 1) S is in an active cell; 2) There are k ($k \geq 1$) destination nodes in the same active cell as S or in its eight neighbor cells; 3) There are i ($0 \leq i \leq n-z-1$) other nodes in the active cell (except S and its z destination nodes); 4) S is selected as a transmitter.

We use E_1, E_2, E_3 and E_4 to denote these four events, respectively. Note that E_2 consists of two mutually exclusive sub-events denoted by $E_{2'}$ and $E_{2''}$, where $E_{2'}$ represents that these k destination nodes are in the same active cell as S and $E_{2''}$ represents that they are in the eight neighbor cells of the active cell. For the former sub-event, the probability that S is selected as a transmitter is $\frac{1}{k+i+1}$, then the joint probability $P(E_1, E_{2'}, E_3, E_4)$ can be determined as

$$\begin{aligned} &P(E_1, E_{2'}, E_3, E_4) = P(E_1)P(E_{2'} \mid E_1)P(E_3 \mid E_1, E_{2'})P(E_4 \mid E_1, E_{2'}, E_3) \\ &= \frac{\frac{m^2}{\alpha^2}}{m^2} \sum_{k=1}^{z} \binom{z}{k} \left(\frac{1}{m^2}\right)^k \left(1 - \frac{1}{m^2}\right)^{z-k} \cdot \sum_{i=0}^{n-z-1} \varphi(i) \frac{1}{k+i+1} \end{aligned} \tag{A.1}$$

where $\varphi(i) = \binom{n-z-1}{i}(\frac{1}{m^2})^i(1-\frac{1}{m^2})^{n-z-1-i}$. For the latter sub-event, the probability that S is selected as a transmitter is $\frac{1}{i+1}$, then the joint probability $P(E_1, E_{2''}, E_3, E_4)$

can be determined as

$$P(E_1, E_{2''}, E_3, E_4) = P(E_1)P(E_{2''} \mid E_1)P(E_3 \mid E_1, E_{2''})P(E_4 \mid E_1, E_{2''}, E_3)$$
$$= \frac{\frac{m^2}{\alpha^2}}{m^2} \sum_{k=1}^{z} \binom{z}{k} \left(\frac{8}{m^2}\right)^k \left(1 - \frac{9}{m^2}\right)^{z-k} \cdot \sum_{i=0}^{n-z-1} \varphi(i) \frac{1}{i+1} \quad \text{(A.2)}$$

where $\varphi(i)$ is the same as that of (A.1). Then p_2 follows by summing over these two probabilities of (A.1) and (A.2).

We proceed to derive p_3. S can conduct a source-to-relay transmission at a time slot iff the following four events occur: 1) S is in an active cell; 2) None of the z destination nodes is in the same active cell as S or its eight neighbor cell; 3) There are i ($1 \leq i \leq n - z - 1$) other nodes in the active cell or in its eight neighbor cell (except S); 4) S is selected as a transmitter. We note that the 3rd event consists of two mutually exclusive sub-events: these i other nodes are either in the active cell or in its eight neighbor cells. For the former one, the probability that S is selected as a transmitter is $\frac{1}{i+1}$. For the latter one, the probability is 1. By summing over the joint probability of these events under the former one and that under the latter one, p_3 then follows.

Proof of Lemma 4: Under the transient state (i, j) in the Markov chain of Fig. 6-3, we can see that the number of destination nodes that have received the packet is j, and a multicast session has z destination nodes, thus (6.3) follows. Since all the i relay nodes carry a copy of the packet under the transient state, (6.4) follows. For each multicast session, all the $n - z - 1$ relay nodes help to forward copies of the packet to destination nodes. Since $\mu_2 + \mu_3 = n - z - 1$, (6.5) then follows.

Proof of Lemma 5: Given μ_1 destination nodes that have not received the packet in current time slot, the source node S may deliver a copy of the packet to one of the μ_1 destination nodes in the next time slot. Note that these μ_1 events are mutually exclusive. The probability that S will deliver a copy to a single destination

node is $\frac{p_2}{z}$. By summing over the probabilities of these μ_1 events, we have

$$P_{SD}(\mu_1) = \frac{\mu_1}{z} p_2. \tag{A.3}$$

We now derive $P_{SR}(\mu_3)$. Similarly, given μ_3 relay nodes that do not carry a copy of the packet in current time slot, S may deliver a copy of the packet to one of μ_3 relay nodes in the next time slot. Note that these μ_3 events are mutually exclusive. The probability that S will deliver a copy to a single relay node is $\frac{p_3}{2(n-z-1)}$. By summing over the probabilities of these μ_3 events, we have

$$P_{SR}(\mu_3) = \frac{\mu_3}{2(n-z-1)} p_3. \tag{A.4}$$

Proof of Lemma 6: To derive $P_{RD}(x, \mu_1, \mu_2)$, we first consider x relay nodes carrying a copy of the packet of the tagged multicast session, and use $P(F_1, F_2, \cdots, F_x)$ to denote the probability that x relay-to-destination transmissions will be performed simultaneously from these x relay nodes to any x destination nodes of the tagged multicast session in the next time slot, where F_i $(1 \leq i \leq x)$ denotes the ith relay-to-destination transmission. Since the number of x-combinations of the μ_2 relay nodes carrying a copy of the packet is $\binom{\mu_2}{x}$, these relay nodes in each x-combination may conduct x successful relay-to-destination transmissions simultaneously. Under successful relay-to-destination transmissions, these relay nodes in each x-combination successfully deliver copies of the packet to distinct destination nodes (one copy per destination node). Notice that these $\binom{\mu_2}{x}$ events are mutually exclusive. Given that there are μ_1 destination nodes that do not receive the packet, the probability of such an event is $\frac{\binom{\mu_1}{x}}{\binom{z}{x}} P(F_1, F_2, \cdots, F_x)$. By summing over the probabilities of these $\binom{\mu_2}{x}$ events, we then have

$$P_{RD}(x, \mu_1, \mu_2) = \binom{\mu_2}{x} \frac{\binom{\mu_1}{x}}{\binom{z}{x}} P(F_1, F_2, \cdots, F_x). \tag{A.5}$$

To derive $P(F_1, F_2, \cdots, F_x)$, we apply the multiplication rule to obtain that

$$P(F_1, F_2, \cdots, F_x) = P(F_1^*)P(F_2^*)\cdots P(F_i^*)\cdots P(F_x^*) \tag{A.6}$$

where F_1^* denotes F_1 and F_i^* denotes $F_i|F_1F_2\cdots F_{i-1}$ $(2 \le i \le x)$.

Now we need to determine those probabilities in $(A.6)$. First, we derive F_i^* when $1 \le i \le x-1$. For the event F_i^* that represents a transmission from a given relay node (e.g.,R_i) to any destination node, it will occur in the next time slot iff the following five sub-events occur: 1) R_i is in an active cell; 2) There are k_i $(0 \le k_i \le n - 2z - x - \sum_{j=1}^{i} k_{j-1})$ other nodes in the same cell as R_i and its eight neighbor cells (except the z destination nodes of the source node S, the considered x relay nodes, the z destination nodes of R_i serving as a source node for another multicast session) and those $\sum_{j=1}^{i} k_{j-1}$ other nodes residing in the same cells as the considered x relay nodes and their neighbor cells), and among these k_i other nodes, k nodes are in the same cell as R_i and the other $k_i - k$ nodes are in the eight neighbor cells; 3) There are h_i $(1 \le h_i \le z - \sum_{j=1}^{i} h_{j-1})$ destination nodes in the same cell as R_i and its eight neighbor cells, and among them, h nodes are in the same cell and the other $h_i - h$ nodes are in the eight neighbor cells; 4) R_i and one destination node are selected as a transmitter and a receiver; 5) R_i selects to conduct relay-to-destination transmission.

The probabilities of these sub-events can be determined as $\frac{m^2-\alpha^2(i-1)}{\alpha^2 m^2}$, $\sum_{k_i=0}^{l_i} \binom{l_i}{k_i} \sum_{k=0}^{k_i} \binom{k_i}{k}$ $(\frac{1}{m^2})^k(\frac{8}{m^2})^{k_i-k}$, $\sum_{h_i=1}^{w_i} \binom{w_i}{h_i} \sum_{h=0}^{h_i} \binom{h_i}{h}(\frac{1}{m^2})^h(\frac{8}{m^2})^{h_i-h}$, $\frac{1}{k+h+1}\frac{h_i}{k_i+h_i}$, and $\frac{1}{2}$, respectively. Here, $l_i = n - 2z - x - \sum_{j=1}^{i} k_{j-1}$ and $w_i = z - \sum_{j=1}^{i} h_{j-1}$. Multiplying the probabilities of these sub-events, we can get the probabilities of the event F_i^* $(1 \le i \le x-1)$.

We proceed to derive $P(F_x^*)$. For the event F_x^*, it can be divided into six sub-events consisting of above five sub-events and a new sub-event. The new sub-event is that all remaining nodes are in the other $m^2 - 9x$ cells except those cells where the considered x relay nodes reside and their neighbor cells. The probability of the new sub-event is $(\frac{m^2-9x}{m^2})^z$, where $z = n - x - \sum_{j=1}^{x}(k_j + h_j)$. Multiplying the probabilities of these six sub-events, we then get the probabilities of the event F_x^*.

By multiplying the probabilities of these events $\{F_1^*, F_2^*, \cdots, F_x^*\}$, $(A.6)$ then follows. (6.8) follows by substituting $(A.6)$ into $(A.5)$.

Proof of Lemma 7:

To derive $P_{SD,RD}(x, \mu_1, \mu_2)$, we first consider the source node S and x relay nodes carrying a copy of the packet of the tagged multicast session, and use $P(A, F_1, F_2, \cdots, F_x)$ to denote the probability that a source-to-destination transmission from S to any destination node and x relay-to-destination transmissions from the considered x relay nodes to any x destination nodes will be performed simultaneously in the next time slot, where A and F_i $(1 \leq i \leq x)$ denote the source-to-destination transmission and the ith relay-to-destination transmission, respectively. Since the number of x-combinations of the μ_2 relay nodes carrying a copy of the packet is $\binom{\mu_2}{x}$, these relay nodes in each x-combination may conduct x successful relay-to-destination transmissions simultaneously. Under a successful source-to-destination transmission and x successful relay-to-destination transmissions, S successfully delivers the packet to a destination node and these relay nodes in each x-combination successfully deliver copies of the packet to distinct destination nodes (one copy per destination node). Notice that these $\binom{\mu_2}{x}$ events are mutually exclusive. Given that there are μ_1 destination nodes that do not receive the packet, the probability of such an event is $\frac{\binom{\mu_1}{x+1}}{\binom{z}{x+1}} P(A, F_1, F_2, \cdots, F_x)$. By summing over the probabilities of these $\binom{\mu_2}{x}$ events, we then have

$$P_{SD,RD}(x, \mu_1, \mu_2) = \binom{\mu_2}{x} \frac{\binom{\mu_1}{x+1}}{\binom{z}{x+1}} P(A, F_1, F_2, \cdots, F_x). \tag{A.7}$$

To derive $P(A, F_1, F_2, \cdots, F_x)$, we use the multiplication rule to obtain that

$$P(A, F_1, F_2, \cdots, F_x) = P(F_1)P(F_2|F_1)\cdots P(F_x|F_1F_2\cdots F_{x-1})P(A|F_1F_2\cdots F_x). \tag{A.8}$$

Now we need to determine those probabilities in $(A.8)$. Similar to the derivation process of $P(F_1, F_2, \cdots, F_x)$ in $(A.6)$, we can get the probabilities of these events $\{F_1, F_2, \cdots, F_x\}$. We proceed to derive $P(A|F_1F_2\cdots F_x)$. For the event A given

$F_1F_2\cdots F_x$, it can be divided into five sub-events: 1) S is in an active cell; 2) There are k_{x+1} $(0 \le k_{x+1} \le n-z-x-\sum_{j=1}^{x+1} k_{j-1}-1)$ other nodes in the same cell as S and its eight neighbor cells (except S, the z destination nodes of S, the considered x relay nodes and those $\sum_{j=1}^{x+1} k_{j-1}$ other nodes residing in the same cells as the considered x relay nodes and their neighbor cells), and among these k_{x+1} other nodes, k nodes are in the same cell as S and the other $k_{x+1}-k$ nodes are in the eight neighbor cells; 3) There are h_{x+1} $(1 \le h_{x+1} \le w_x - h_x)$ destination nodes in the same cell as S and its eight neighbor cells, and among them, h nodes are in the same cell; 4) S is selected as a transmitter; 5) All remaining nodes are in the other $m^2-9(x+1)$ cells except those cells where the considered x relay nodes and S reside and their neighbor cells.

The probabilities of these sub-events can be determined as $\frac{m^2-\alpha^2(i-1)}{\alpha^2 m^2}$, $\sum_{k_{x+1}=0}^{l_x+z-k_x-1} \binom{l_x+z-k_x-1}{k_{x+1}} \sum_{k=0}^{k_{x+1}} \binom{k_{x+1}}{k} (\frac{1}{m^2})^k (\frac{8}{m^2})^{k_{x+1}-k}$, $\sum_{h_{x+1}=1}^{w_x-h_x} \binom{w_x-h_x}{h_{x+1}} \sum_{h=0}^{h_{x+1}} \binom{h_{x+1}}{h} (\frac{1}{m^2})^h \cdot (\frac{8}{m^2})^{h_{x+1}-h}$, $\frac{1}{k+h+1}$ and $(\frac{m^2-9(x+1)}{m^2})^{\nu-k_{x+1}-h_{x+1}-1}$, respectively. Multiplying the probabilities of these sub-events, we can get the probabilities of the event A given $F_1F_2\cdots F_x$.

By multiplying the probabilities of these events $\{F_1, F_2|F_1, \ldots, A|F_1F_2\cdots\ F_x\}$, (A.8) then follows. (6.10) follows by substituting (A.8) into (A.7).

Proof of Lemma 8: To derive $P_{SR,RD}(x, \mu_1, \mu_2, \mu_3)$, we first consider the source node S, x relay nodes carrying a copy of the packet of the tagged multicast session and a relay node (e.g., R) that does not carry its copy, and use $P(B, F_1, F_2, \cdots, F_x)$ to denote the probability that a source-to-relay transmission from S to R and relay-to-destination transmissions from the considered x relay nodes to any x destination nodes will be performed simultaneously in the next time slot, where B and F_i $(1 \le i \le x)$ denote the source-to-relay transmission and the ith relay-to-destination transmission, respectively. Since the number of x-combinations of the u_2 relay nodes carrying a copy of the packet is $\binom{\mu_2}{x}$, these relay nodes in each x-combination may conduct x successful relay-to-destination transmissions simultaneously. Similarly, S may conduct a successful source-to-relay transmission from it to one of u_3 relay nodes that

do not carry a copy of the packet. Thus, $P_{SR,RD}(x, \mu_1, \mu_2, \mu_3)$ can be determined as

$$P_{SR,RD}(x, \mu_1, \mu_2, \mu_3) = \binom{\mu_2}{x} \frac{u_3 \binom{\mu_1}{x}}{\binom{z}{x}} P(B, F_1, F_2, \cdots, F_x). \tag{A.9}$$

To derive $P(B, F_1, F_2, \cdots, F_x)$, we use the multiplication rule to obtain that

$$P(B, F_1, F_2, \cdots, F_x) = P(F_1)P(F_2|F_1)\cdots P(F_x|F_1F_2\cdots F_{x-1})P(B|F_1F_2\cdots F_x). \tag{A.10}$$

Now we need to determine those probabilities in $(A.10)$. Similar to the derivation process of $P(F_1, F_2, \cdots, F_x)$ in $(A.6)$, we can get the probabilities of these events $\{F_1, F_2, \cdots, F_x\}$. We proceed to derive $P(B|F_1F_2\cdots F_x)$. For the event B given $F_1F_2\cdots F_x$, it can be divided into five sub-events: 1)S is in an active cell; 2) There are k_{x+1} $(0 \leq k_{x+1} \leq n-z-x-\sum_{j=1}^{x+1} k_{j-1}-2)$ other nodes in the same cell as S and its eight neighbor cells (except S, the z destination nodes of S, R, the considered x relay nodes and those $\sum_{j=1}^{x+1} k_{j-1}$ other nodes residing in the same cells as the considered x relay nodes and their neighbor cells), and among these k_{x+1} other nodes, k nodes are in the same cell as S and the other $k_{x+1}-k$ nodes are in the eight neighbor cells; 3)R is either in the same cell as S or in the eight neighbor cells; 4) S and R are selected as a transmitter and a receiver; 5) All remaining nodes are in the other $m^2-9(x+1)$ cells except those cells where the considered x relay nodes and S reside and their neighbor cells.

The probabilities of these sub-events can be determined as $\frac{m^2-\alpha^2 x}{\alpha^2 m^2}$, $\sum_{k_{x+1}=0}^{l_x+z-k_x-2} \binom{l_x+z-k_x-2}{k_{x+1}} \sum_{k=0}^{k_{x+1}} \binom{k_{x+1}}{k} (\frac{1}{m^2})^k (\frac{8}{m^2})^{k_{x+1}-k}$, $\sum_{r=0}^{1} \binom{1}{r} (\frac{1}{m^2})^r (\frac{8}{m^2})^{1-r}$, $\frac{1}{k+r+1} \cdot \frac{1}{k_{x+1}+1}$, and $(\frac{m^2-9(x+1)}{m^2})^{\nu-k_{x+1}-2}$, respectively. Multiplying the probabilities of these sub-events, we can get the probabilities of the event B given $F_1F_2\cdots F_x$.

By multiplying the probabilities of these events $\{F_1, F_2|F_1, \ldots, B|F_1F_2\cdots\ F_x\}$, $(A.10)$ then follows. (6.12) follows by substituting $(A.10)$ into $(A.9)$.

□

Bibliography

[1] J. Andrews, S. Shakkottai, R. Heath, N. Jindal, M. Haenggi, R. Berry, D. Guo, M. Neely, S. Weber, S. Jafar, and A. Yener. Rethinking information theory for mobile ad hoc networks. *IEEE Commun. Mag.*, 46(12):94–101, Dec. 2008.

[2] Y. Wang, S. Jain, M. Martonosi, and K. Fall. Erasure-coding based routing for opportunistic networks. In *WDTN*, 2005.

[3] Y. Liao, K. Tan, Z. Zhang, and L. Gao. Estimation based erasure coding routing in delay tolerant networks. In *IWCMC*, 2006.

[4] L.-J. Chen, C.-H. Yu, T. Sun, Y.-C. Chen, and H. Hua Chu. A hybrid routing approach for opportunistic networks. In *ACM SIGCOMM.*, 2006.

[5] A. A. Hanbali, A. A. Kherani, and P. Nain. Simple models for the performance evaluation of a class of two-hop relay protocols. In *IFIP Netw.*, 2007.

[6] F. Tsapeli and V. Tsaoussidis. Routing for opportunistic networks based on probabilistic erasure coding. In *WWIC*, 2012.

[7] J. Liu, X. Jiang, H. Nishiyama, and N. Kato. Performance modeling for two-hop relay with erasure coding in MANETs. In *Globecom*, 2011.

[8] M. J. Neely and E. Modiano. Capacity and delay tradeoffs for ad-hoc mobile networks. *IEEE Trans. Inf. Theory*, 51(6):1917–1936, Jun. 2005.

[9] A. Panagakis, A. Vaios, and I. Stavrakakis. Study of two-hop message spreading in DTNs. In *WiOpt*, 2007.

[10] E. Bulut, Z. Wang, and B. K. Szymanski. cost effective multi-period spraying for routing in delay tolerant networks. *IEEE/ACM Trans. Netw.*, 18(5):1530–1543, Oct. 2010.

[11] J. Liu, X. Jiang, H. Nishiyama, and N. Kato. Delay and capacity in ad hoc mobile networks with f-cast relay algorithms. In *ICC*, 2011.

[12] J. Liu, X. Jiang, H. Nishiyama, and N. Kato. Generalized two-hop relay for flexible delay control in MANETs. *IEEE/ACM Trans. Netw.*, 20(6):1950–1963, Dec. 2013.

[13] P. Gupta and P.R. Kumar. The capacity of wireless networks. *IEEE Trans. Inf. Theory*, 46(2):388–404, Mar. 2000.

[14] B. Kannhavong, H. Nakayama, N. Kato, A. Jamalipour, and Y. Nemoto. A study of a routing attack in olsr-based mobile ad hoc networks. *International J. Communication Systems*, 20(11):1245–1261, Nov. 2007.

[15] B. Kannhavong, H. Nakayama, Y. Nemoto, N. Kato, and A. Jamalipour. A survey of routing attacks in mobile ad hoc networks. *IEEE Wirel. Commun. Mag.*, 14(5):85–91, Oct. 2007.

[16] C. Buraagohain, S. Suri, C. Toth, and Y. Zhou. Improved throughput bounds for interference-aware routing in wireless networks. In *COCOON*, 2007.

[17] O. Dousse, M. Franceschetti, and P. Thiran. On the throughput scaling of wireless relay networks. *IEEE Trans. Inf. Theory*, 52(6):2756–2761, Jun. 2006.

[18] M. Franceschetti, O. Dousse, D. N. C. Tse, and P. Thiran. Closing the gap in the capacity of wireless networks via percolation theory. *IEEE Trans. Inf. Theory*, 53(3):1009–1018, Mar. 2007.

[19] X. Lin, G. Sharma, and R. R. Mazumdarand N. B. Shroff. Degenerate delay-capacity tradeoffs in ad-hoc networks with brownian mobility. *IEEE/ACM Trans. Netw.*, 14(SI):2777C–2784, Jun. 2006.

[20] P. Li, Y. Fang, J. Li, and X. Huang. Smooth trade-offs between throughput and delay in mobile ad hoc networks. *IEEE Trans. Mobile Comput.*, 11(3):427–438, Mar. 2012.

[21] Y. Wang, X. Chu, X. Wang, and Y. Cheng. Throughput, delay, and mobility in wireless ad hoc networks. In *INFOCOM*, 2010.

[22] J. Liu, X. Jiang, H. Nishiyama, and N. Kato. Delay and capacity in ad hoc mobile networks with f-cast relay algorithms. *IEEE Trans. Wirel. Commun.*, 10(8):2738–2751, August 2011.

[23] G. Sharma and R. Mazumdar. On achievable delay/capacity trade-offs in mobile ad hoc networks. In *WiOpt*, 2004.

[24] G. Sharma, R. Mazumdar, and N. Shroff. Delay and capacity tradeoffs in mobile ad hoc networks: A global perspective. *IEEE/ACM Transactions on Networking*, 15(5):981–992, October 2007.

[25] R. Groenevelt, P. Nain, and G. Koole. The message delay in mobile ad hoc networks. *Performance Evaluation*, 62(1-4):210–228, Oct. 2005.

[26] A. A. Hanbali, P. Nain, and E. Altman. Performance of ad hoc networks with two-hop relay routing and limited packet lifetime-extended version. *Performance Evaluation*, 65(6-7):463–483, Jun. 2008.

[27] T. Spyropoulos, K. Psounis, and C. S. Raghavendra. Spray and wait: An efficient routing scheme for intermittently connected mobile networks. In *ACM SIGCOMM Workshop*, 2005.

[28] E. Altman and F. D. Pellegrini. Forward correction and fountain codes in delay-tolerant networks. *IEEE/ACM Trans. Netw.*, 19(1):1–13, Feb. 2011.

[29] Z. Kong, E. M. Yeh, and E. Soljanin. Coding improves the throughput-delay tradeoff in mobile wireless networks. *IEEE Trans. Inf. Theory*, 58(11):6894–6906, Nov. 2012.

[30] G. Rodolakis, A. M. Naimi, and A. Laouiti. Multicast overlay spanning tree protocol for ad hoc networks. In *WWIC*, 2007.

[31] J. P. Jeong, T. He, and D. H. C. Du. TMA: Trajectory-based multi-anycast forwarding for efficient multicast data delivery in vehicular networks. *Computer Networks*, 57(13):662–672, September 2013.

[32] X. Xiang, X. Wang, and Y. Yang. Supporting efficient and scalable multicasting over mobile ad hoc networks. *IEEE Trans. Mobile Comput.*, 10(4):544–559, Apr. 2011.

[33] Z. Qian, X. Tian, X. Chen, W. Huang, and X. Wang. Multicast capacity in MANET with infrastructure support. *IEEE Trans. Parall. Distr.*, 25(7):1808–1818, Jul. 2014.

[34] Z. Li, C. Wang, C. Jiang, and X. Li. Multicast capacity scaling for inhomogeneous mobile ad hoc networks. *Ad Hoc Netw.*, 11(1):29–38, Jan. 2013.

[35] S. Zhou and L. Ying. On delay constrained multicast capacity of large-scale mobile ad-hoc networks. In *INFOCOM*, 2010.

[36] S. Shakkottai, X. Liu, and R. Srikant. The multicast capacity of large multihop wireless networks. *IEEE/ACM Trans. Netw.*, 18(5):1691–1700, Oct. 2010.

[37] P. Sakarindr and N. Ansari. Security services in group communications over wireless infrastructure, mobile ad hoc, and wireless sensor networks. *IEEE Wirel. Commun.*, 14(5):8–20, Oct. 2007.

[38] W. Wang and T. Stransky. Stateless key distribution for secure intra and inter-group multicast in mobile wireless network. *Computer Networks*, 51(15):4303–4321, June 2007.

[39] H. L. Nguyen and U. T. Nguyen. A study of different types of attacks on multicast in mobile ad hoc networks. *Ad Hoc Netw.*, 6(1):32–46, Jan. 2008.

[40] X. Wang, W. Huang, S. Wang, J. Zhang, and C. Hu. Delay and capacity tradeoff analysis for motioncast. *IEEE/ACM Trans. Netw.*, 19(5):1354–1367, Oct. 2011.

[41] C. Hu, X. Wang, and F. Wu. Motioncast: On the capacity and delay tradeoffs. In *MobiHoc*, 2009.

[42] X. Wang, Y. Bei, Q. Peng, and L. Fu. Speed improves delay-capacity trade-off in motioncast. *IEEE Trans. Parall. and Distr.*, 22(5):729–741, May 2011.

[43] X. Wang, Q. Peng, and Y. Li. Cooperation achieves optimal multicast capacity-delay scaling in MANET. *IEEE Trans. Commun.*, 60(10):3023–3031, Oct. 2012.

[44] J. Liu, X. Jiang, H. Nishiyama, and N. Kato. Multicast capacity, delay and delay jitter in intermittently connected mobile networks. In *INFOCOM*, 2012.

[45] Y. Li, G. Su, D. Wu, D. Jin, L. Su, and L. Zeng. The impact of node selfishness on multicasting in delay tolerant networks. *IEEE Trans. Veh. Tech.*, 60(5):2224–2238, Jun. 2011.

[46] A. Goldsmith, M. Effros, R. Koetter, M. Medard, A. Ozdaglar, and L. Zheng. Beyond shannon: The quest for fundamental performance limits of wireless ad hoc networks. *IEEE Commun. Magazine*, 49(5):195–205, May 2011.

[47] D. Knuth. *The Art of Computer Programming.* Addison-Wesley, 1998.

[48] M. Grossglauser and D. N. Tse. Mobility increases the capacity of ad hoc wireless networks. In *INFOCOM*, 2001.

[49] A. E. Gamal, J. Mammen, B. Prabhakar, and D. Shah. Throughput delay trade-off in wireless networks. In *INFOCOM*, 2004.

[50] Y. Cai, X. Wang, Z. Li, and Y. Fang. Delay and capacity in MANETs under random walk mobility model. *Wirel. Netw.*, 20(3):525–536, Apr. 2014.

[51] J. Mammen and D. Shah. Throughput and delay in random wireless networks with restricted mobility. *IEEE Trans. Inf. Theory*, 53(3):1108C–1116, Mar. 2007.

[52] R. Urgaonkar and M. J. Neely. Network capacity region and minimum energy function for a delay-tolerant mobile ad hoc network. *IEEE/ACM Trans. Netw.*, 19(4):1137C–1150, Aug. 2011.

[53] J. Gao, J.Liu, X. Jiang, O. Takahashi, and N. Shiratori. Throughput capacity of MANETs with group-based scheduling and general transmission range. *IEICE Trans. Commun.*, E96-B(7):1791–1802, Jul. 2013.

[54] L. Ying, S. Yang, and R. Srikant. Coding achieves the optimal delay-throughput trade-off in mobile ad-hoc networks: two-dimensional i.i.d. mobility model with fast mobiles. In *WiOpt*, 2007.

[55] L. Ying, S. Yang, and R. Srikant. Coding achieves the optimal delay-throughput tradeoff in mobile ad hoc networks: a hybrid random walk model with fast mobiles. In *ITA*, 2007.

[56] E. Altman, F. D. Pellegrini, and L. Sassatelli. Dynamic control of coding in delay tolerant networks. In *INFOCOM*, 2010.

[57] E. Altman, L. Sassatelli, and F. D. Pellegrini. Dynamic control of coding for progressive packet arrivals in DTNs. *IEEE Trans. Wirel. Commun.*, 12(2):725–735, Feb. 2013.

[58] L. Ying, S. Yang, and R. Srikant. Optimal delay-throughput trade-offs in mobile ad-hoc networks. *IEEE Trans. Inf. Theory*, 54(9):4119–4143, Sep. 2008.

[59] C. Zhang, Y. Fang, and X. Zhu. Throughput-delay tradeoffs in large-scale MANETs with network coding. In *INFOCOM*, 2009.

[60] S. R. Kulkarni and P. Viswanath. A deterministic approach to throughput scaling in wireless networks. *IEEE Trans. Inf. Theory*, 50(6):1041C1049, Jun. 2004.

[61] Pan Li, Yuguang Fang, and Jie Li. Throughput, delay, and mobility in wireless ad hoc networks. In *INFOCOM*, 2010.

[62] D. Ciullo, V. Martina, M. Garetto, and E. Leonardi. Impact of correlated mobility on delay-throughput performance in mobile ad-hoc networks. In *INFOCOM*, 2010.

[63] M. Garetto, P. Giaccone, and E. Leonardi. Capacity scaling in ad hoc networks with heterogeneous mobile nodes: The subcritical regime. *IEEE/ACM Trans. Netw.*, 17(6):1888C–1901, Dec. 2009.

[64] L. Rizzo. Effective erasure codes for reliable computer communication protocols. *Computer Communication Review*, 27(2):24C–36, Apr. 1997.

[65] C. M. Grinstead and J. L. Snell. *Introduction to Probability, 2nd ed.* American Mathematical Society, 1997.

[66] A. E. Gamal, J. Mammen, B. Prabhakar, and D. Shah. Optimal throughput-delay scaling in wireless networks-part i: The fluid model. *IEEE Trans. Inf. Theory*, 52(6):2568–2592, Jun. 2006.

[67] M. J. Neely. Dynamic power allocation and routing for satellite and wireless networks with time varying channels. In *Ph.D. dissertation, Massachusetts Institute of Technology*, 2003.

[68] J. Zhang, X. Wang, X. Tian, Y. Wang, X. Chu, and Y. Cheng. Optimal multicast capacity and delay tradeoffs in MANETs. *IEEE Trans. Mob. Comput.*, 13(5):1104–1117, May 2014.

[69] Y. Chen, Y. Shen, X. Jiang, and J. Li. Throughput capacity of ALOHA MANETs. In *ICCC*, 2013.

THIS PAGE INTENTIONALLY LEFT BLANK

Pulications

Journal Articles

[1] Bin Yang, Juntao Gao, Yuezhi Zhou, and Xiaohong Jiang. Delay Control in MANETs with Erasure Coding and f-cast Relay. *Wireless Networks*, 21(8): 2617–2631, November 2014.

[2] Bin Yang, Yin Chen, Ying Cai, and Xiaohong Jiang. Packet Delivery Ratio/Cost in MANETs with Erasure Coding and Packet Replication. *IEEE Transactions on Vehicular Technology*, 64(5): 2062–2070, May 2015.

[3] Bin Yang, Yin Chen, Guilin Chen, and Xiaohong Jiang. Throughput Capacity Study for MANETs with Erasure Coding and Packet Replication. *IEICE Transactions on Communications*, E-98B(8): 1537–1552, August 2015.

[4] Bin Yang, Ying Cai, Yin Chen, and Xiaohong Jiang. On the Exact Multicast Delay in Mobile Ad Hoc Networks with f-cast Relay. *Ad Hoc Networks*, *Accepted*, 2015.

Conference Papers

[5] Bin Yang, Juntao Gao, Yuezhi Zhou, and Xiaohong Jiang. Two-Hop Relay Algorithm with Packet Redundancy and Erasure Coding in MANETs. In *Proc. ICCC*, 2013.

[6] Bin Yang, Yin Chen, Yuezhi Zhou, and Xiaohong Jiang. Packet Delivery Probability in Two-Hop Relay MANETs with Hybrid Routing. In *Proc. CANDAR*, 2013.

[7] Bin Yang, Yin Chen, and Xiaohong Jiang. Multicast Delay of Mobile Ad Hoc Networks. In *Proc. CANDAR*, 2014.